

NASA CR-145194

A COMPUTER PROGRAM FOR CALCULATING THREE-DIMENSIONAL  
COMPRESSIBLE LAMINAR AND TURBULENT BOUNDARY LAYERS  
ON ARBITRARY WINGS

(NASA-CR-145194) A COMPUTER PROGRAM FOR  
CALCULATING THREE-DIMENSIONAL COMPRESSIBLE  
LAMINAR AND TURBULENT BOUNDARY LAYERS ON  
ARBITRARY WINGS (McDonnell-Douglas Corp.)  
64 p HC A04/MF A01

N77-24057

Unclas  
29209

CSCL 01A G3/02

by

Tuncer Cebeci, Kalle Kaups, and Judy A. Ramsey

May 1977

Prepared under Contract No. 12821

By

McDONNELL DOUGLAS CORPORATION

Long Beach, CA 90808

for

**NASA**

National  
Aeronautics and  
Space  
Administration

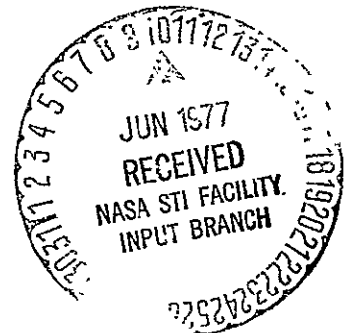


## TABLE OF CONTENTS

	<u>Page</u>
INTRODUCTION . . . . .	1
DESCRIPTION OF THE METHOD . . . . .	3
Governing Equations . . . . .	3
Turbulence Model . . . . .	7
Solution Procedure . . . . .	8
DESCRIPTION OF THE COMPUTER PROGRAM . . . . .	11
Input for the Geometry Program . . . . .	11
Input for the External Velocity Program . . . . .	14
Input for the Boundary-Layer Program . . . . .	18
Output from the Geometry Program . . . . .	22
Output from the Velocity Program . . . . .	24
Output from the Boundary-Layer Program . . . . .	25
Basic Flow Chart of MAIN for Boundary-Layer Program . . . . .	30
SAMPLE CALCULATIONS . . . . .	32
Test Case 1 . . . . .	32
Test Case 2 . . . . .	37
Test Case 3 . . . . .	46
REFERENCES . . . . .	57

## SYMBOLS

A	Van Driest damping length
b	$C(1 + \epsilon_m^+)$ or a constant for scaling the spanwise coordinate y
c	$\rho_e/\rho$ or local chord length
$c_{f_c}$	local skin-friction coefficient based on the Cartesian component of wall shear stress vector in x-coordinate direction
$c_{f_n}$	local skin-friction coefficient based on the Cartesian component of wall shear stress vector normal to the x-y-plane.
C	$\rho\mu/(\rho_e\mu_e)$
$C_p$	pressure coefficient, $2(p - p_\infty)/(\rho_\infty u_\infty^2)$
E	total enthalpy ratio, $H/H_e$
f	transformed vector potential for $\psi$
$f'$	$u/u_e$
g	transformed vector potential for $\phi$
$g'$	$w/u_{ref}$
$h_1$	metric coefficient associated with the x-coordinate
$h_2$	metric coefficient associated with the z-coordinate
H	total enthalpy
i, j, k	unit vectors in $\bar{x}, \bar{y}, \bar{z}$ -directions of the Cartesian coordinate system in which the wing is defined
$K_1 = K_{g1}$ , $K_2 = K_{g2}$	geodesic curvatures
$K_{12}, K_{21}$	geometric parameters
L	modified mixing-length or a scaling constant
$M_\infty$	free-stream Mach number
p	static pressure
Pr	Prandtl number
$R_s$	$u_e s_1/\nu_e$ , Reynolds number

$s_1$	arc length along x-coordinate line
$\vec{t}$	unit tangent vector along (3-D) coordinate line
$T$	temperature
$u$	component of velocity vector in x-coordinate direction
$u_{ref}$	reference velocity
$u_s$	resultant velocity at the edge of boundary layer
$\bar{u}_s$	orthogonal velocity component in $u_s$ direction
$u_t$	total or resultant velocity
$u_x$	derivative $\partial u / \partial x$
$u_\tau$	friction velocity
$u_\infty$	free-stream velocity
$v$	component of velocity vector normal to the surface
$w$	component of velocity vector in z-coordinate direction
$w_z$	$\partial w / \partial z$
$-\rho \overline{u'v'}, -\rho \overline{w'v'},$ $-\rho \overline{v'H'}$	Reynolds stresses
$x$	independent variable in chordwise direction, $x = \phi - \phi_0$
$x'$	chordwise distance measured from airfoil leading edge
$y$	independent variable normal to the surface, is equal to the normal distance
$z$	independent variable in spanwise direction, $z = \bar{y}/b$
$\bar{x}, \bar{y}, \bar{z}$	Cartesian coordinate system used for wing definition
$\alpha$	local geometric angle of attack of wing section chord lines with respect to $\bar{x}$ -axis ( $\alpha(\bar{y})$ expresses wing twist)
$\beta$	flow deflection angle
$\delta_C^*$	displacement thickness based on the Cartesian velocity components in the x-coordinate direction
$\delta_n^*$	displacement thickness based on the Cartesian velocity components normal to the xy-plane
$\epsilon$ (or $\epsilon_m$ ), $\epsilon_H$	eddy viscosity and eddy conductivity, respectively
iv	

$\eta$	transformed coordinate normal to surface
$\theta$	angle in tangent plane between $x$ and $z$ coordinate lines
$\theta_c$	momentum thickness based on the Cartesian velocity components in the $x$ -coordinate direction
$\theta_n$	momentum thickness based on the Cartesian velocity components normal to the $xy$ -plane
$\lambda$	sweep angle
$\mu$	dynamic viscosity
$\nu$	kinematic viscosity
$\rho$	density
$\tau$	shear stress
$\phi$	stretching variable defined by eq. (B5) of reference 1 ( $x$ -coordinate in differential equation is $x = \phi - \phi_0$ )
$\phi, \psi$	two-component vector potential, eq. (32)

#### Subscripts

$e$	outer edge, effective
$g$	geodesic
$i, o$	inner and outer regions for eddy viscosity
$w$	wall
$\infty$	free-stream conditions

bars denote rectangular coordinate system

primes denote differentiation with respect to  $\eta$

A COMPUTER PROGRAM FOR CALCULATING THREE-DIMENSIONAL  
COMPRESSIBLE LAMINAR AND TURBULENT BOUNDARY LAYERS ON ARBITRARY WINGS

by

Tuncer Cebeci, Kalle Kaups, and Judy A. Ramsey  
Douglas Aircraft Company

SUMMARY

This report describes and presents a computer program for calculating three-dimensional compressible laminar and turbulent boundary layers on arbitrary wings. The computer program consists of three separate programs, namely, a geometry program to represent the wing analytically, a velocity program to compute the external velocity components from a given experimental pressure distribution and a finite-difference boundary-layer method to solve the governing equations for compressible flows.

To illustrate the usage of the computer program, three different test cases are presented and the preparation of the input data as well as the computed output data is discussed in some detail.

A COMPUTER PROGRAM FOR CALCULATING THREE-DIMENSIONAL  
COMPRESSIBLE LAMINAR AND TURBULENT BOUNDARY LAYERS ON ARBITRARY WINGS

by

Tuncer Cebeci, Kalle Kaups, and Judy A. Ramsey  
Douglas Aircraft Company

INTRODUCTION

In reference 1, the present authors describe a general method for calculating three-dimensional compressible laminar and turbulent boundary layers on arbitrary wings. The method utilizes a nonorthogonal coordinate system for boundary-layer calculations and includes a geometry program that represents the wing analytically and a velocity program that computes the external velocity components from a given experimental pressure distribution. The boundary-layer method is general, however, and can also be used for an external velocity distribution which is computed theoretically. The boundary-layer method accounts for all the geometric parameters of the coordinate system. The Reynolds stress terms are modeled by the algebraic eddy-diffusivity formulas developed by Cebeci<sup>2</sup>, and the governing equations are solved by the efficient Box method used earlier by Keller and Cebeci for two-dimensional flows<sup>3</sup> and later by Cebeci<sup>2,4</sup> for three-dimensional flows.

In this report we describe and present the computer program for this method. It consists of three separate programs, namely, the geometry program, the external velocity program and the boundary-layer program. The geometry program calculates the coordinate system for a wing defined by streamwise airfoil sections at a number of spanwise stations. These data are stored for use in the external velocity and boundary-layer programs. The program requires that the input data be smooth and treats upper and lower surfaces separately.

The external velocity program computes the components of the free-stream velocity from a given experimental pressure distribution ( $C_p$ ) which is input as a function of fractional chord-location and spanwise stations. This data should also be sufficiently smooth for chordwise and spanwise interpolation. The velocity program could have been incorporated into the boundary-layer

program; however, we found it advantageous to allow the components of the external velocity to be examined before they are used in boundary-layer calculations.

The boundary-layer program requires the specification of the coordinate system, which can be either orthogonal or nonorthogonal, and the external velocity distribution, which can be either experimental or theoretical. The calculations can be performed for either incompressible or compressible laminar and turbulent flows. The location of transition must be input. The calculations are done in the streamwise direction for each spanwise station. When the wall shear becomes negative, the calculations at that streamwise location are stopped and calculations at the next spanwise station are started again in the streamwise direction.

In the next sections we briefly describe the method; we present the governing equations, eddy-diffusivity formulas, similarity transformations, the solution procedure and the marching procedure. We next present the input and output instructions for the three separate computer programs and, to illustrate its use, we present three sample calculations discussed in reference 1.



## DESCRIPTION OF THE METHOD

### Governing Equations

The governing boundary-layer equations for a nonorthogonal coordinate system (see Figure 1) are given in reference 1. They are:

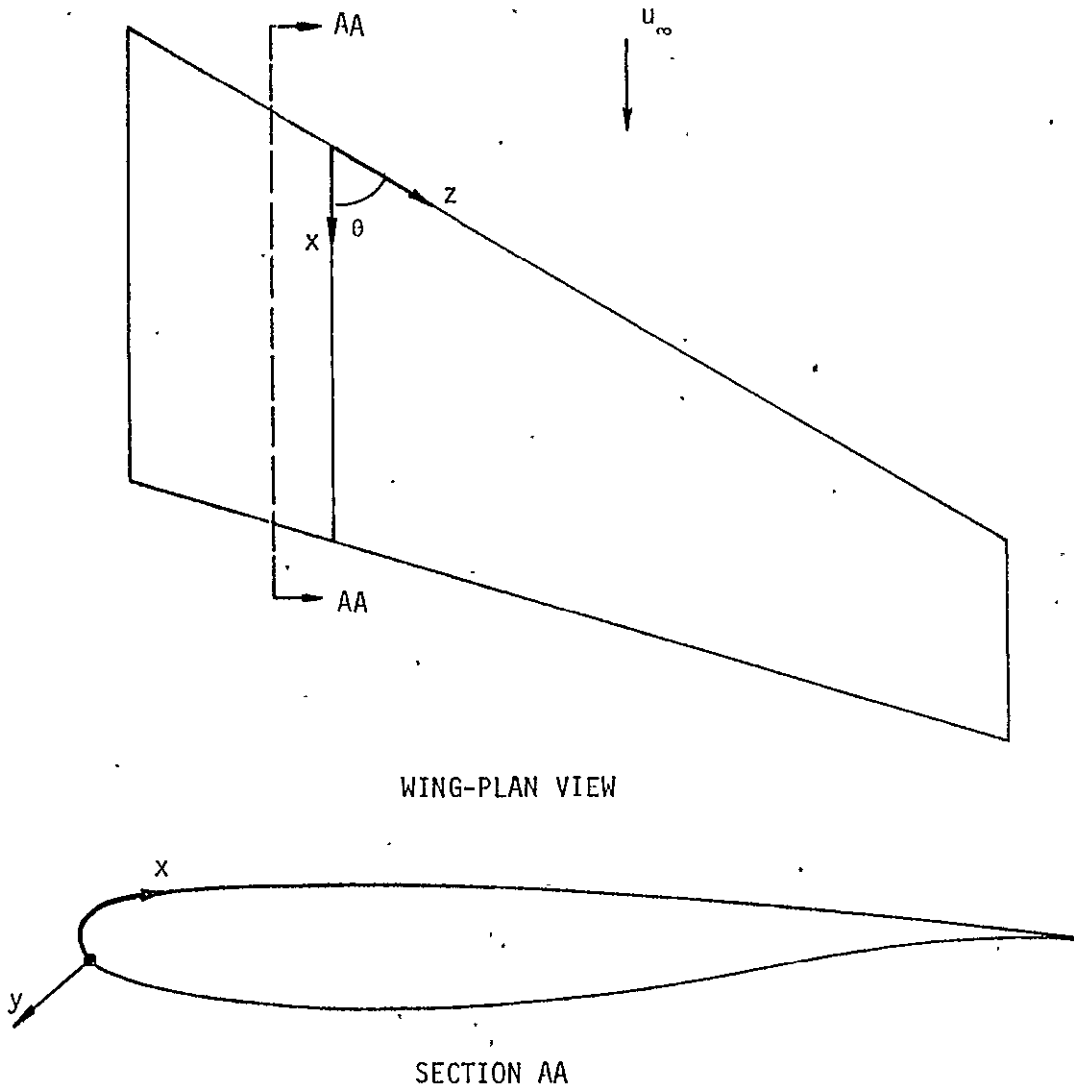


Figure 1. The coordinate system for a swept wing.

Continuity equation

$$\frac{\partial}{\partial x} (\rho u h_2 \sin \theta) + \frac{\partial}{\partial z} (\rho w h_1 \sin \theta) + \frac{\partial}{\partial y} (\rho v h_1 h_2 \sin \theta) = 0 \quad (1)$$

x-Momentum equation

$$\begin{aligned} \rho \frac{u}{h_1} \frac{\partial u}{\partial x} + \rho \frac{w}{h_2} \frac{\partial u}{\partial z} + \bar{\rho v} \frac{\partial u}{\partial y} - \rho \cot \theta K_1 u^2 + \rho \csc \theta K_2 w^2 + \rho K_{12} u w \\ = - \frac{\csc^2 \theta}{h_1} \frac{\partial p}{\partial x} + \frac{\cot \theta \csc \theta}{h_2} \frac{\partial p}{\partial z} + \frac{\partial}{\partial y} \left( \mu \frac{\partial u}{\partial y} - \rho \overline{u'v'} \right) \end{aligned} \quad (2)$$

z-Momentum equation

$$\begin{aligned} \rho \frac{u}{h_1} \frac{\partial w}{\partial x} + \rho \frac{w}{h_2} \frac{\partial w}{\partial z} + \bar{\rho v} \frac{\partial w}{\partial y} - \rho \cot \theta K_2 w^2 + \rho \csc \theta K_1 u^2 + \rho K_{21} u w \\ = \frac{\cot \theta \csc \theta}{h_1} \frac{\partial p}{\partial x} - \frac{\csc^2 \theta}{h_2} \frac{\partial p}{\partial z} + \frac{\partial}{\partial y} \left( \mu \frac{\partial w}{\partial y} - \rho \overline{w'v'} \right) \end{aligned} \quad (3)$$

Energy equation

$$\rho \frac{u}{h_1} \frac{\partial H}{\partial x} + \rho \frac{w}{h_2} \frac{\partial H}{\partial z} + \bar{\rho v} \frac{\partial H}{\partial y} = \frac{\partial}{\partial y} \left[ \frac{\mu}{Pr} \frac{\partial H}{\partial y} + \mu \left( 1 - \frac{1}{Pr} \right) \frac{\partial}{\partial y} \left( \frac{u_t^2}{2} \right) - \rho \overline{v'H'} \right] \quad (4)$$

Here  $\bar{\rho v} = \rho v + \overline{\rho'v'}$ ,  $h_1, h_2$  are metric coefficients and  $K_1$  and  $K_2$  are the geodesic curvatures of the curves  $z = \text{const.}$  and  $x = \text{const.}$ , respectively. The latter are defined by

$$K_1 = \frac{1}{h_1 h_2 \sin \theta} \left[ \frac{\partial}{\partial x} (h_2 \cos \theta) - \frac{\partial h_1}{\partial z} \right], \quad (5)$$

$$K_2 = \frac{1}{h_1 h_2 \sin \theta} \left[ \frac{\partial}{\partial z} (h_1 \cos \theta) - \frac{\partial h_2}{\partial x} \right] \quad (6)$$

The parameters  $K_{12}$  and  $K_{21}$  are defined by

$$K_{12} = \frac{1}{\sin \theta} \left[ - \left( K_1 + \frac{1}{h_1} \frac{\partial \theta}{\partial x} \right) + \cos \theta \left( K_2 + \frac{1}{h_2} \frac{\partial \theta}{\partial z} \right) \right] \quad (7a)$$

$$K_{21} = \frac{1}{\sin \theta} \left[ - \left( K_2 + \frac{1}{h_2} \frac{\partial \theta}{\partial z} \right) + \cos \theta \left( K_1 + \frac{1}{h_1} \frac{\partial \theta}{\partial x} \right) \right] \quad (7b)$$

$u_t$  represents the total velocity within the boundary layer and is given by

$$u_t = (u^2 + w^2 + 2uw \cos \theta)^{1/2} \quad (8)$$

The boundary conditions we consider for (1)-(4) are:

$$y = 0 \quad u, v, w = 0, \quad \left(\frac{\partial H}{\partial y}\right)_w = 0 \quad (9a)$$

$$y = \delta \quad u = u_e(x,z), \quad w = w_e(x,z), \quad H = H_e \quad (9b)$$

The system given by (1) to (4) and (9) requires initial conditions along the stagnation line and initial conditions either along the root or along the tip. For the stagnation-line they are:

Continuity

$$\rho h_2 \sin \theta u_x + \frac{\partial}{\partial z} (\rho w h_1 \sin \theta) + \frac{\partial}{\partial y} (\overline{\rho v} h_1 h_2 \sin \theta) = 0 \quad (10)$$

x-Momentum

$$\rho \frac{u_x^2}{h_1} + \rho \frac{w}{h_2} \frac{\partial u_x}{\partial z} + \overline{\rho v} \frac{\partial u_x}{\partial y} + \rho K_{12} w u_x = \rho_e \left( \frac{u_{xe}^2}{h_1} + \frac{w_e}{h_2} \frac{\partial u_{xe}}{\partial x} + K_{12} w_e u_{xe} \right) + \frac{\partial}{\partial y} \left[ \mu \frac{\partial u_x}{\partial y} - \rho (\overline{u'v'})_x \right] \quad (11)$$

z-Momentum

$$\rho \frac{w}{h_2} \frac{\partial w}{\partial z} + \overline{\rho v} \frac{\partial w}{\partial y} - \rho \cot \theta K_2 w^2 = \rho_e \left( \frac{w_e}{h_2} \frac{\partial w_e}{\partial z} - \cot \theta K_2 w_e^2 \right) + \frac{\partial}{\partial y} \left( \mu \frac{\partial w}{\partial y} - \rho \overline{w'v'} \right) \quad (12)$$

Energy

$$\rho \frac{w}{h_2} \frac{\partial H}{\partial z} + \overline{\rho v} \frac{\partial H}{\partial y} = \frac{\partial}{\partial y} \left[ \frac{\mu}{Pr} \frac{\partial H}{\partial y} + \mu \left( 1 - \frac{1}{Pr} \right) \frac{\partial}{\partial y} \left( \frac{u_t^2}{2} \right) - \rho \overline{v'H'} \right] \quad (13)$$

Here  $u_x = \partial u / \partial x$ ,  $u_{xe} = \partial u_e / \partial x$  and total velocity  $u_t = w$ . These equations are subject to the following boundary conditions

$$y = 0, \quad u_x, v, w = 0, \quad (\partial H / \partial y)_w = 0 \quad (14a)$$

$$y = \delta \quad u_x = u_{xe}(x,z), \quad w = w_e(x,z), \quad H = H_e \quad (14b)$$

For the root region, we have two options: we can use either the line of symmetry equations (chordwise attachment-line equations) or the infinite

swept wing equations. The latter are also used for the tip region. Note that these equations are approximations to the governing equations in those regions. The chordwise attachment-line equations are:

Continuity

$$\frac{\partial}{\partial x} (\rho u h_2 \sin \theta) + \rho h_1 \sin \theta w_z + \frac{\partial}{\partial y} (\overline{\rho v} h_1 h_2 \sin \theta) = 0 \quad (15)$$

x-Momentum

$$\rho \frac{u}{h_1} \frac{\partial u}{\partial x} + \overline{\rho v} \frac{\partial u}{\partial y} - \rho \cot \theta K_1 u^2 = \rho_e \left( \frac{u_e}{h_1} \frac{\partial u_e}{\partial x} - \cot \theta K_1 u_e^2 \right) + \frac{\partial}{\partial y} \left( \mu \frac{\partial u}{\partial y} - \rho \overline{u'v'} \right) \quad (16)$$

z-Momentum

$$\rho \frac{u}{h_1} \frac{\partial w_z}{\partial x} + \frac{\rho}{h_2} w_z^2 + \overline{\rho v} \frac{\partial w_z}{\partial y} + \rho K_{21} u w_z = \rho_e \left( \frac{u_e}{h_1} \frac{\partial w_{ze}}{\partial x} + \frac{w_{ze}^2}{h_2} + K_{21} u_e w_{ze} \right) + \frac{\partial}{\partial y} \left[ \mu \frac{\partial w_z}{\partial y} - \rho \overline{(w'v')}_z \right] \quad (17)$$

Energy

$$\rho \frac{u}{h_1} \frac{\partial H}{\partial x} + \overline{\rho v} \frac{\partial H}{\partial y} = \frac{\partial}{\partial y} \left[ \frac{\mu}{Pr} \frac{\partial H}{\partial y} + \mu \left( 1 - \frac{1}{Pr} \right) \frac{\partial}{\partial y} \left( \frac{u_t^2}{2} \right) - \rho \overline{v'H'} \right] \quad (18)$$

Here  $w_z = \partial w / \partial z$ ,  $w_{ze} = \partial w_e / \partial z$  and total velocity  $u_t = u$ . These equations are subject to the following boundary conditions:

$$y = 0 \quad u = v = 0 \quad w_z = 0 \quad (\partial H / \partial y)_w = 0 \quad (19a)$$

$$y = \delta \quad u = u_e(x, z) \quad w_z = w_{ze} \quad H = H_e \quad (19b)$$

The infinite swept wing equations are:

Continuity

$$\frac{\partial}{\partial x} (\rho u h_2 \sin \theta) + \frac{\partial}{\partial y} (\overline{\rho v} h_1 h_2 \sin \theta) = 0 \quad (20)$$

x-Momentum

$$\begin{aligned} \rho \frac{u}{h_1} \frac{\partial u}{\partial x} + \overline{\rho v} \frac{\partial u}{\partial y} - \rho \cot \theta K_1 u^2 + \rho \csc \theta K_2 w^2 + \rho K_{12} u w \\ = \rho_e \left( \frac{u_e}{h_1} \frac{\partial u_e}{\partial x} - \cot \theta K_1 u_e^2 + \csc \theta K_2 w_e^2 + K_{12} u_e w_e \right) + \frac{\partial}{\partial y} \left( \mu \frac{\partial u}{\partial y} - \overline{\rho u' v'} \right) \end{aligned} \quad (21)$$

z-Momentum

$$\begin{aligned} \rho \frac{u}{h_1} \frac{\partial w}{\partial x} + \overline{\rho v} \frac{\partial w}{\partial y} - \rho \cot \theta K_2 w^2 + \rho \csc \theta K_1 u^2 + \rho K_{21} u w \\ = \rho_e \left( \frac{u_e}{h_1} \frac{\partial w_e}{\partial x} - \cot \theta K_2 w_e^2 + \csc \theta K_1 u_e^2 + K_{21} u_e w_e \right) + \frac{\partial}{\partial y} \left( \mu \frac{\partial w}{\partial y} - \overline{\rho w' v'} \right) \end{aligned} \quad (22)$$

Energy

$$\rho \frac{u}{h_1} \frac{\partial H}{\partial x} + \overline{\rho v} \frac{\partial H}{\partial y} = \frac{\partial}{\partial y} \left[ \frac{\mu}{Pr} \frac{\partial H}{\partial y} + \mu \left( 1 - \frac{1}{Pr} \right) \frac{\partial}{\partial y} \left( \frac{u_t^2}{2} \right) - \overline{\rho v' H'} \right] \quad (23)$$

The boundary conditions are the same as those given by (9) except that  $u_e$  and  $w_e$  are independent of  $z$ .

### Turbulence Model

The method uses the eddy-viscosity formulation of reference 2. According to this formulation the eddy viscosity defined by

$$-\overline{\rho u' v'} = \rho \epsilon_m \frac{\partial u}{\partial y}, \quad -\overline{\rho w' v'} = \rho \epsilon_m \frac{\partial w}{\partial y} \quad (24)$$

is represented by two separate formulas across the boundary layer. In the so-called inner region of the boundary layer ( $\epsilon_m$ ) is defined by the following formula

$$(\epsilon_m)_i = L^2 \left[ \left( \frac{\partial u}{\partial y} \right)^2 + \left( \frac{\partial w}{\partial y} \right)^2 + 2 \cos \theta \left( \frac{\partial u}{\partial y} \right) \left( \frac{\partial w}{\partial y} \right) \right]^{1/2} \quad (25)$$

where

$$L = 0.4y[1 - \exp(-y/A)] \quad (26a)$$

$$A = 26 \frac{v}{u_\tau} \left( \frac{\rho}{\rho_w} \right)^{1/2}, \quad u_\tau = \left( \frac{\tau_{tw}}{\rho_w} \right)^{1/2} \quad (26b)$$

$$\tau_{tw} = \mu_w \left[ \left( \frac{\partial u}{\partial y} \right)_w^2 + \left( \frac{\partial w}{\partial y} \right)_w^2 + 2 \cos \theta \left( \frac{\partial u}{\partial y} \right)_w \left( \frac{\partial w}{\partial y} \right)_w \right]^{1/2} \quad (26c)$$

In the outer region  $\epsilon_m$  is defined by the following formula

$$(\epsilon_m)_o = 0.0168 \left| \int_0^\infty (u_{te} - u_t) dy \right| \quad (27)$$

where

$$u_{te} = (u_e^2 + w_e^2 + 2u_e w_e \cos \theta)^{1/2} \quad (28a)$$

$$u_t = (u^2 + w^2 + 2uw \cos \theta)^{1/2} \quad (28b)$$

The inner and outer regions are established by the continuity of the eddy-viscosity formula.

The local heat flux term  $-\rho \overline{v'H'}$ , appearing in the energy equation is modeled by the turbulent Prandtl number concept; the term  $-\rho \overline{v'H'}$  is written as

$$-\rho \overline{v'H'} = \rho \frac{\epsilon_m}{Pr_t} \frac{\partial H}{\partial y} \quad (29)$$

and the value of  $Pr_t$  is assumed to be constant and equal to 0.90.

### Solution Procedure

We use the numerical method of reference 2 to solve the governing system of equations described above. Before they are solved, however, they are expressed in transformed variables defined by

$$x = x, \quad z = z, \quad d\eta = \left( \frac{u_e}{\rho_e \mu_e S_1} \right)^{1/2} \rho dy \quad (30)$$

A two-component vector potential defined by

$$uh_2 \sin \theta = \frac{\partial \psi}{\partial y}, \quad \rho wh_1 \sin \theta = \frac{\partial \Phi}{\partial y} \quad (31)$$

$$\overline{\rho v} h_1 h_2 \sin \theta = - \left( \frac{\partial \psi}{\partial x} + \frac{\partial \Phi}{\partial z} \right)$$

is introduced to satisfy the continuity equation. They are made dimensionless by using new variables  $f$  and  $g$  defined by

$$\begin{aligned}\psi &= (\rho_e \nu_e u_e s_1)^{1/2} h_2 \sin \theta f(x, z, \eta) \\ \Phi &= (\rho_e \nu_e u_e s_1)^{1/2} u_{ref}/u_e h_1 \sin \theta g(x, z, \eta)\end{aligned}\quad (32)$$

The present method is developed in such a way that nonuniform net spacings can be used in the streamwise and in the spanwise directions as well as across the boundary layer. In the latter case, the variable grid is a geometric progression having the property that the ratio of lengths of any two adjacent intervals is a constant; that is,  $\Delta \eta_j = K \Delta \eta_{j-1}$ . The distance to the  $j$ -th line is given by the following formula:

$$\eta_j = \Delta \eta_1 (K^j - 1)/(K - 1) \quad K > 1 \quad (33)$$

There are two parameters:  $\Delta \eta_1$ , the length of the first  $\Delta \eta$  step, and  $K$ , the ratio of two successive steps. The total number of points  $J$  can be calculated by the following formula:

$$J = \frac{\ln[1 + (K - 1)(\eta_\infty/\Delta \eta_1)]}{\ln K} \quad (34)$$

In the computer program, we select  $\Delta \eta_1$  and  $K$ . Typical values for  $\Delta \eta_1 = 0.01$  and  $K = 1.2$ . For further details see reference 5.

In the present program for a given spanwise station we march in the streamwise direction. Whether the initial calculations start at the root section or at the tip section is determined by the sign of the external spanwise velocity component  $w_e$ . To illustrate our marching procedure, let us assume that the wing has three regions defined by the sign of  $w_e$ . In region 1,  $w_e$  is positive; in region 2,  $w_e$  is negative; and in region 3,  $w_e$  is positive (see figure 2). Let us also assume that region 1 starts from the leading edge. In this case, our calculations start at the root section. At the leading edge we use the stagnation-line equations for one  $x$ -station and switch to either chordwise attachment-line equations (if  $w \equiv 0$ ) or to the infinite swept-wing

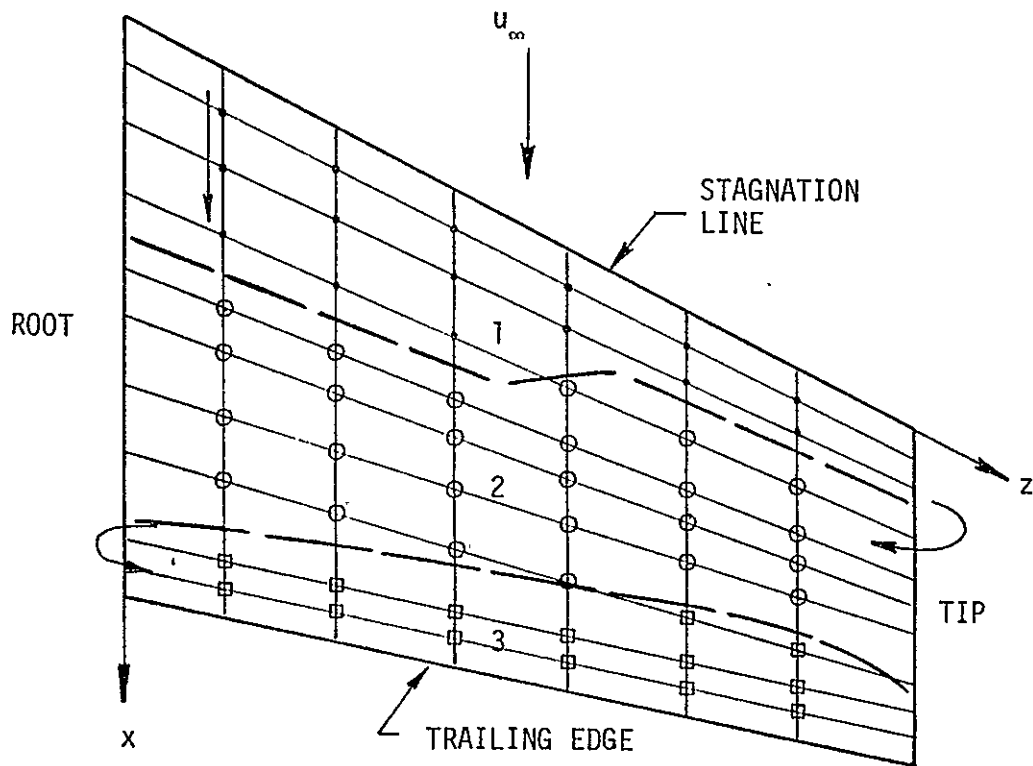


Figure 2. Definitions of various regions on the wing for marching procedure.

equations. With either one of these equations we march in the streamwise direction to the net point before  $w_e$  changes sign. Then we go back to the stagnation line and after solving the stagnation line equations, we start solving the general three-dimensional flow equations at the second  $x$ -station. This procedure is repeated as before for all stations up to and including the tip section in region 1. There the solutions are obtained for positive  $w_e$  by using the general three-dimensional flow equations; they are continued into region 2 by solving the chordwise attachment-line or infinite swept-wing equations up to the beginning of region 3. At that time we go back to the next spanwise station of region 2. For the first chordwise station we solve the chordwise attachment-line or infinite swept-wing equations and then continue on to the next chordwise station by solving the general three-dimensional flow equations for region 2. This procedure is again repeated for region 2 up to and including the root section in region 2. The calculations at the root section are extended to region 3 by solving either the infinite-swept-wing equations or the chordwise attachment-line equations, and the procedure used for region 2 is repeated for this region.



## DESCRIPTION OF THE COMPUTER PROGRAM

Detailed descriptions of the three separate programs; i.e., the geometry, external-velocity and boundary-layer programs, are provided below.

### INPUT FOR THE GEOMETRY PROGRAM

#### Case Data

Card 1 Punched as an 80-column alphanumeric field.

TITLE Description of the case.

1	2	3	4	5	6	7	8	9	10	11	12	13	14	15	16	17	18	19	20	21	22	23	24	25	26	27	28	29	30	31	32	33	34	35	36	37	38	39	40	41	42	43	44	45	46	47	48	49	50	51	52	53	54	55	56	57	58	59	60	61	62	63	64	65	66	67	68	69	70	71	72	73	74	75	76	77	78	79	80
TITLE																																																																															

Load Sheet for Card 1.

Card 2 Namelist/Input/IY, NC, NS, IFLG, NT, IPUNCH, SB, SP, RL

- IY Number of wing defining stations to be read in. Numbering starts with the most inboard station.
- NC The desired number of chordwise output stations.
- NS The desired number of spanwise output stations.
- IFLG = 0, program calculates and prints all geometrical data needed for boundary-layer calculations.  
= 1, program calculates and punches cards for geometrical data needed for the velocity program.
- NT Chordwise station number in the NC array at which the punched output is started.
- IPUNCH This flag applies only when IFLG=0  
= 0, output printed only.  
= 1, output both printed and punched on cards.
- SB Multiplicative factor which will convert the input  $\bar{y}$ -values into feet.
- SP Nominal span in feet. This constant can be used to scale the spanwise dependent variable  $z$ .

RL Reference length L in feet. All calculated quantities with dimension of length are output in nondimensionalized form with respect to this reference length.

Card 3 Cards for input  $\bar{y}$ -station punched in 6F10.0 format.

YI  $\bar{y}$ -values of wing defining stations. Total number of entries is IY.

1	2	3	4	5	6	7	8	9	10	11	12	13	14	15	16	17	18	19	20	21	22	23	24	25	26	27	28	29	30	31	32	33	34	35	36	37	38	39	40
YI										YI										YI										YI									
41	42	43	44	45	46	47	48	49	50	51	52	53	54	55	56	57	58	59	60																				
YI															YI																								

Load Sheet for Card 3.

Card 4 Cards for chordwise output stations punched in 6F10.0 format.

CX Desired chordwise output stations in terms of decimal fraction of chord (based on maximum length line). Total number of entries is NC. Note: If calculations extend around the leading edge, 0.0 must be one of the inputs.

1	2	3	4	5	6	7	8	9	10	11	12	13	14	15	16	17	18	19	20	21	22	23	24	25	26	27	28	29	30	31	32	33	34	35	36	37	38	39	40
CX										CX										CX										CX									
41	42	43	44	45	46	47	48	49	50	51	52	53	54	55	56	57	58	59	60																				
CX															CX																								

Load Sheet for Card 4.

Card 5 Cards for spanwise output stations punched in 6F10.0 format.

CY Desired spanwise output stations in terms of the coordinate  $\bar{y}$ . Note that the following must be satisfied:  $YI(1) \leq CY(1)$  and  $CY(NS) \leq YI(IY)$ . Total number of entries is NS. The spanwise coordinate  $z$  is made zero at  $CY(1)$  in the program.

1	2	3	4	5	6	7	8	9	10	11	12	13	14	15	16	17	18	19	20	21	22	23	24	25	26	27	28	29	30	31	32	33	34	35	36	37	38	39	40
CY					CY					CY					CY																								
41	42	43	44	45	46	47	48	49	50	51	52	53	54	55	56	57	58	59	60																				
CY										CY																													

Load Sheet for Card 5.

Station Data

Card 1 First card for each input station punched in 2I3, 5F10.0 format.

- NP Number of  $\bar{x} - \bar{z}$  input pairs. Note: Values for the leading edge defined by the maximum length line must be part of the input array if calculations proceed from or around the leading edge.
- NN Sequence number for the leading-edge point in the input array. Note: If calculations do not include the leading edge, then  $NN = 0$ .
- CL Multiplicative factor which will convert the input  $\bar{x}$  and  $\bar{z}$  values into feet.
- XLE  $\bar{x}$ -value for the leading edge.
- ZLE  $\bar{z}$ -value for the leading edge.
- XTE  $\bar{x}$ -value for the trailing edge.
- ZTE  $\bar{z}$ -value for the trailing edge.

1	2	3	4	5	6	7	8	9	10	11	12	13	14	15	16	17	18	19	20	21	22	23	24	25	26	27	28	29	30	31	32	33	34	35	36				
NP		NN		CL					XLE					ZLE																									
37	38	39	40	41	42	43	44	45	46	47	48	49	50	51	52	53	54	55	56																				
XTE										ZTE																													

Load Sheet for Card 1.

Card 2

Cards for  $\bar{x}$ -values at a given input station punched in 6F10.0 format.

XI  $\bar{x}$ -values for a defining section. Total number of entries is NP.

1	2	3	4	5	6	7	8	9	10	11	12	13	14	15	16	17	18	19	20	21	22	23	24	25	26	27	28	29	30	31	32	33	34	35	36	37	38	39	40
XI										XI										XI										XI									
41	42	43	44	45	46	47	48	49	50	51	52	53	54	55	56	57	58	59	60																				
XI																				XI																			

Load Sheet for Card 2.

Card 3

Cards for  $\bar{z}$ -values at a given input station, punched in 6F10.0 format.

ZI  $\bar{z}$ -values for a defining section. Total number of entries is NP.

Note: The range of the input values in terms of the coordinate  $x$  must be at least equal to the range of  $x$  specified by the output variable CX.

1	2	3	4	5	6	7	8	9	10	11	12	13	14	15	16	17	18	19	20	21	22	23	24	25	26	27	28	29	30	31	32	33	34	35	36	37	38	39	40
ZI										ZI										ZI										ZI									
41	42	43	44	45	46	47	48	49	50	51	52	53	54	55	56	57	58	59	60																				
ZI																				ZI																			

Load Sheet for Card 3.

INPUT FOR THE EXTERNAL VELOCITY PROGRAM

Case Data

Card 1

Punched as an 80-column alphanumeric field.

TITLE Description of the case.

1	2	3	4	5	6	7	8	9	10	11	12	13	14	15	16	17	18	19	20	21	22	23	24	25	26	27	28	29	30	31	32	33	34	35	36	37	38	39	40	41	42	43	44	45	46	47	48	49	50	51	52	53	54	55	56	57	58	59	60	61	62	63	64	65	66	67	68	69	70	71	72	73	74	75	76	77	78	79	80
TITLE																																																																															

Load Sheet for Card 1.

Card 2

Namelist/Input/IY, NC, NS, IFLG, FM, AL, SP, SB, CR, CT, NI

- IY Number of spanwise wing stations where pressure is given.
- NC The number of chordwise output stations.
- NS The number of spanwise output stations.
- IFLG = 0, output is printed only.  
= 1, output is both printed and punched on cards.
- FM Freestream Mach number.
- AL Angle of attack in degrees. (Freestream angle with respect to the  $\bar{x}$  axis in the  $\bar{x}\bar{z}$ -plane.)
- SP Nominal span in feet (see geometry program).
- SB Multiplicative factor which will convert the input  $\bar{y}$ -values into feet.
- CR Length of root chord in feet. Corresponds to chord at CY(1).
- CT Length of tip chord, in feet. Corresponds to chord at CY(NS).
- NI { NI = 5 expects geometry data to be read from cards.  
NI = 8 expects geometry data to be read from Tape 8.

Cards for Input  $\bar{y}$ -Stations

Card 3 Punched in 6F10.0 format.

YI  $\bar{y}$ -values of spanwise stations on which the pressure distribution is input. Total number of entries is IY.

1	2	3	4	5	6	7	8	9	10	11	12	13	14	15	16	17	18	19	20	21	22	23	24	25	26	27	28	29	30	31	32	33	34	35	36	37	38	39	40
YI										YI										YI										YI									
-----																																							
41																				42																			
43																				44																			
45																				46																			
47																				48																			
49																				50																			
51																				52																			
53																				54																			
55																				56																			
57																				58																			
59																				60																			
-----																				-----																			
YI																				YI																			
-----																																							

Load Sheet for Card 3.

Card 4

Punched in 6F10.0 format.

CX

Chordwise output stations in terms of fraction of chord. Must be the same stations as output in geometry program. Total number of entries is NC. Note: If calculations extend around the leading edge, 0.0 must be one of the inputs.

1	2	3	4	5	6	7	8	9	10	11	12	13	14	15	16	17	18	19	20	21	22	23	24	25	26	27	28	29	30	31	32	33	34	35	36	37	38	39	40
CX										CX										CX										CX									

41	42	43	44	45	46	47	48	49	50	51	52	53	54	55	56	57	58	59	60
CX										CX									

Load Sheet for Card 4.

Card 5

Punched in 6F10.0 format.

CY

Spanwise output stations in terms of the coordinate  $\bar{y}$ . Must be the same stations as output in geometry program. Total number of entries is NS. Note that the following must be satisfied:  $YI(1) \leq CY(1)$  and  $CY(NS) \leq YI(IY)$

1	2	3	4	5	6	7	8	9	10	11	12	13	14	15	16	17	18	19	20	21	22	23	24	25	26	27	28	29	30	31	32	33	34	35	36	37	38	39	40
CY										CY										CY										CY									

41	42	43	44	45	46	47	48	49	50	51	52	53	54	55	56	57	58	59	60
CY										CY									

Load Sheet for Card 5.

Geometry Data

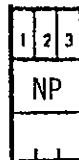
Cards Generated by the Geometry Program:

<u>Column</u>	<u>Symbol</u>	<u>Format</u>	<u>Description</u>
1-12	TH	E12.5	The angle between coordinate lines.
13-24	H2	E12.5	The metric coefficient $h_2$ .
25-36	C12	E12.5	The derivative $\partial(\bar{x}/L)/\partial z$ .
37-48	C21	E12.5	The derivative $\partial(\bar{z}/L)/\partial z$ .

Note: Data is read in for one spanwise station at a time. There will be NX x NS cards.

Pressure Data

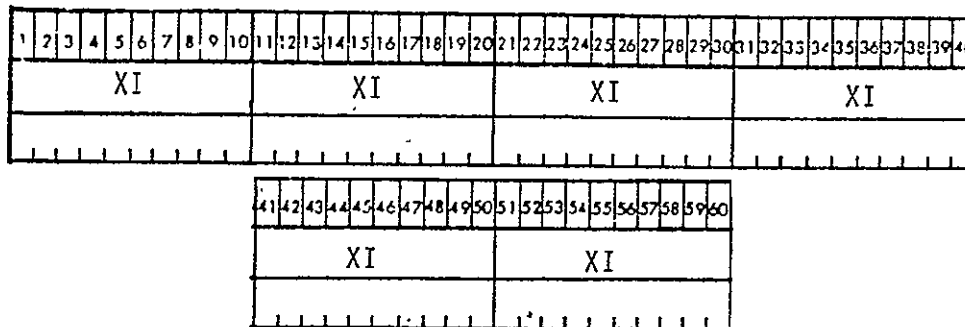
- Card 1 First card for each input station. Punched in I3 format.
- NP Number of input points for chordwise location and  $C_p$  at a given spanwise station.



Load Sheet for Card 1.

- Card 2 Cards for chordwise location of pressures. Punched in 6F10.0 format.

- XI Chordwise location of pressure data in terms of fraction of chord (maximum length line). If data is specified around the leading edge, the chordwise location 0.0 must be one of the inputs.



Load Sheet for Card 2.

Card 3 Cards for pressure data. Punched in 6F10.0 format.

P Input pressure data in terms of Cp.

Note: The range of the input pressure data in terms of the coordinate x (XI) must be greater than or equal to the range of the specified output points in x (CX).

1	2	3	4	5	6	7	8	9	10	11	12	13	14	15	16	17	18	19	20	21	22	23	24	25	26	27	28	29	30	31	32	33	34	35	36	37	38	39	40
P										P										P										P									

41	42	43	44	45	46	47	48	49	50	51	52	53	54	55	56	57	58	59	60
P										P									

Load Sheet for Card 3.

INPUT FOR THE BOUNDARY-LAYER PROGRAM

Description of Data

Data for the boundary-layer program is input in two manners. First, the body geometry and the velocity distribution are each loaded onto disk, thus eliminating cumbersome loading of a large number of cards for each run. These two data sets need to be defined in the JCL, and the numbers on the DD card must correspond to the tape numbers defined in the MAIN program for the particular data sets (i.e., IBM - FT01 and TAPEVL=1; CDC - TAPE1 and TAPEVL=1). Secondly, three cards are input with each run.

Input for Each Run

Card 1 Punched as an 80-column alphanumeric field.

TITLE Case description

1	2	3	4	5	6	7	8	9	10	11	12	13	14	15	16	17	18	19	20	21	22	23	24	25	26	27	28	29	30	31	32	33	34	35	36	37	38	39	40	41	42	43	44	45	46	47	48	49	50																														
TITLE																																																																															

Load Sheet for Card 1.



NAMelist/NAME/NXSTRT, NZSTRT, NXT, NZT, NTR, IFLOW, ICHORD, ICMP, ISPAN, IFPRNT, VGP, DETA, ITMAX, EPS, IPZ, IPX, EPSV, EPST

NXSTRT Number of chordwise station (NX) where calculations begin.  
NZSTRT Number of spanwise station (NZ) where calculations begin.  
NXT Number of last chordwise station (NX) to be calculated.  
NZT Number of last spanwise station (NZ) to be calculated.  
NTR Number of chordwise station (NX) where transition is specified.  
IFLOW = 1 Start with outboard calculations (root to tip).  
= 2 Start with inboard calculations (tip to root).  
Note: This is dependent on the sign of  $w_e$ . A positive sign is outboard flow, negative is inboard.  
ICHORD = 1 Chordwise attachment line equations used on root, tip and spanwise attachment line.  
= 2 Infinite swept wing equations used on root and tip, stagnation line equations used on spanwise attachment line.  
ICMP = 1 Specifies incompressible flow.  
= 2 Specifies compressible flow.  
ISPAN = 1 Stagnation line equations used.  
= 2 Flat plate.  
IFPRNT = 0 Input data sets are not printed.  
= 1 Input data sets are printed.  
VGP Variable-grid parameter - K  
DETA(1) Initial  $\Delta\eta$  spacing -  $\Delta\eta_1$   
ITMAX maximum iterations allowed per column before proceeding on  
EPS laminar flow convergence criterion (use  $10^{-4}$ )  
IPZ controls printing in the Z direction (prints at every IPZ station)  
IPX controls printing in the X direction (prints at every IPX station)  
EPSV turbulent flow convergence criterion on V (fractional change; typical value = .1)  
EPST turbulent flow convergence criterion on T (fractional change; typical value = .1)

Card 3 Punched in (3E12.5) format.

Incompressible flow (NAMelist/NAME/ICMP = 1)

TFRS Freestream temperature,  $^{\circ}\text{R}$ .  
UFRS Freestream velocity, ft/sec.  
PFRS Freestream pressure,  $\text{lb}_f/\text{ft}^2$ .

Compressible flow (NAMelist/NAME/ICMP = 2)

TFRS Freestream temperature,  $^{\circ}\text{R}$ .  
CMFRS Mach number.  
PFRS Freestream pressure,  $\text{lb}_f/\text{ft}^2$ .

1	2	3	4	5	6	7	8	9	10	11	12	13	14	15	16	17	18	19	20	21	22	23	24	25	26	27	28	29	30	31	32	33	34	35	36
TFRS										UFRS or CMFRS										PFRS															
+										E +										+															

Load Sheet for Card 3.

Input for Data Sets

TAPEDT Contains the wing geometry - permanent information for a given wing.

TAPEVL Contains the pressure (velocity) distribution. Several different distributions may be used for a given wing.

TAPEDT

Card 1 Punched in (2I3) format.

NXTL Total number of chordwise stations (NX) in this data set.

NZTL Total number of spanwise stations (NZ) in this data set.

1	2	3	4	5	6
NXTL			NZTL		

Load Sheet for Card 1.

Card 2 Punched in (8F10.0) format.

X Chordwise coordinate. Will have NXTL values.

1	2	3	4	5	6	7	8	9	10	11	12	13	14	15	16	17	18	19	20	21	22	23	24	25	26	27	28	29	30	31	32
X							X							X																	

63	64	65	66	67	68	69	70	71	72	73	74	75	76	77	78	79	80
X								X									

Load Sheet for Card 2.

Card 3 Punched in (8F10.0) format.

Z Spanwise coordinate. Will have NZTL values.

1	2	3	4	5	6	7	8	9	10	11	12	13	14	15	16	17	18	19	20	21	22	23	24	25	26	27	28	29	30	31	32
Z							Z							Z																	

63	64	65	66	67	68	69	70	71	72	73	74	75	76	77	78	79	80
Z								Z									

Load Sheet for Card 3.

Card 4 Punched in (8F10.0) format.

XC Fraction of chord corresponding to x-values. Will have NXTL values.

1	2	3	4	5	6	7	8	9	10	11	12	13	14	15	16	17	18	19	20	21	22	23	24	25	26	27	28	29	30	31	32	33	34	35	36	37	38	39	40
XC										XC										XC																			

Load Sheet for Card 4.

Card 5 Punched in (8E10.3) format (IBM - punched in 8E10.4 format). Will have (NXTL\*NZTL) of these cards.

- H1 Metric coefficient,  $h_1$ .
- H2 Metric coefficient,  $h_2$ .
- CK1 Geodesic curvature,  $K_1$ .
- CK2 Geodesic curvature,  $K_2$ .
- CK12 Curvature parameter,  $K_{12}$ .
- CK21 Curvature parameter,  $K_{21}$ .
- THETA Coordinate angle,  $\theta$ .
- PS1 Surface distance,  $S_1$ .

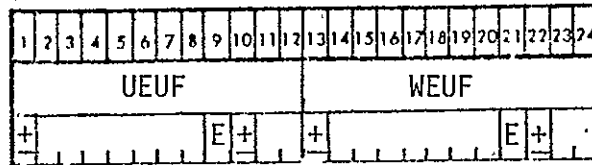
1	2	3	4	5	6	7	8	9	10	11	12	13	14	15	16	17	18	19	20	21	22	23	24	25	26	27	28	29	30	31	32	33	34	35	36	37	38	39	40
H1										H2										CK1										CK2									
+					E	+		+					E	+		+					E	+		+					E	+		+					E	+	
41	42	43	44	45	46	47	48	49	50	51	52	53	54	55	56	57	58	59	60	61	62	63	64	65	66	67	68	69	70	71	72	73	74	75	76	77	78	79	80
CK12										CK21										THETA										PS1									
+					E	+		+					E	+		+					E	+		+					E	+		+					E	+	

Load Sheet for Card 5.

TAPEVL

Card 1 Punched in (2E12.5) format. Will have (NXTL\*NZTL) of these cards.

UEUF  $u_e/u_\infty$   
 WEUF  $w_e/u_\infty$



Load Sheet for Card 1.

OUTPUT FROM THE GEOMETRY PROGRAM

Geometrical data for boundary-layer calculations (IFLG = 0)

Printed output (IFLG = 0, IPUNCH = 0 or 1)

Output is organized in such a way that all data for a given spanwise station appears on one page. The top line of each page contains the nondimensional spanwise boundary-layer coordinate  $z$  and the case description. The rest of the data is printed in columns. There are NS pages and NC lines on each page corresponding to the number of  $z$  and  $x$  stations, respectively.

<u>Column Heading</u>	<u>Variable</u>	<u>Description</u>
X	$x$	The chordwise nondimensional boundary-layer coordinate, expressed in radians. $x = 0$ corresponds to the leading edge, and $x = \pi/2$ corresponds to the trailing edge. Negative values are points near the leading edge on the opposite surface, that is, if upper surface is being considered the points are on the lower surface and vice versa if the lower surface is considered.
XB	$\bar{x}$	The Cartesian coordinate $\bar{x}$ in feet of an output point on the wing.
ZB	$\bar{z}$	The Cartesian coordinate $\bar{z}$ in feet of an output point on the wing.
H1	$h_1/L$	Metric coefficient associated with the coordinate $x$ in nondimensional form.

H2	$h_2/L$	Metric coefficient associated with the coordinate $z$ in nondimensional form.
K1	$K_1L$	The geodesic curvature of the $x$ -coordinate line in nondimensional form.
K2	$K_2L$	The geodesic curvature of the $z$ -coordinate line in nondimensional form.
K12	$K_{12}L$	The geometric parameter $K_{12}$ in nondimensional form.
K21	$K_{21}L$	The geometric parameter $K_{21}$ in nondimensional form.
THETA	$\theta$	The angle between the coordinate line in radians.
S	$S_1/L$	The nondimensional surface distance $S_1$ measured along the $x$ -coordinate line from the first $x$ -value specified.

### Punched Output (IPUNCH = 1)

In addition to the printed output, the following information is punched out for the use in the boundary-layer programs:

$x$ -values over the range from NT to NC in format 8F10.6.

$z$ -values over the range from 1 to NS in format 8F10.6.

$\xi/\zeta$ -values over the range from NT to NC in format 8F10.6.

Station data with geometrical quantities  $h_1/L$ ,  $h_2/L$ ,  $K_1L$ ,  $K_2L$ ,  $K_{12}L$ ,  $K_{21}L$ ,  $\theta$ , and  $S_1/L$  in the format 8E10.3. The sequence of card output is from NT to NC at each spanwise station. The spanwise stations are sequenced from 1 to NS. There will be  $(NC + 1 - NT) \times NS$  cards.

### Optional Output of Geometrical Data for Velocity Component Calculation

The following four quantities are punched out for each station:  $\theta$ ,  $h_2/L$ ,  $\partial(\bar{x}/L)/\partial z$ ,  $\partial(\bar{z}/L)/\partial z$  in the format 4E12.5. The sequence of card output is identical to the previous case. There will be  $(NC + 1 - NT) \times NS$  cards. This data is needed as input for the calculation of approximate inviscid velocity components from a known pressure distribution.

## OUTPUT FROM THE VELOCITY PROGRAM

### Printed Output (IFLG = 0 or 1)

Output is organized in such a way that all data for a given spanwise station appear on one page. The top line of each page contains the nondimensional spanwise coordinate  $z$  and the case description. The rest of the data is printed in columns. There are NS pages and NC lines on each page corresponding to the number of  $z$  and  $x$  stations respectively. Output for the compressible and incompressible ( $M_\infty = 0$ ) case differ somewhat.

#### Compressible Case:

<u>Column Heading</u>	<u>Variable</u>	<u>Description</u>
X	$x$	The chordwise coordinate $x$ in terms of radians (same meaning as in the geometry program)
PR	$P_e/P_\infty$	Local static to free stream pressure ratio
TR	$T_e/T_\infty$	Local static to free stream temperature ratio
U	$u_e/u_\infty$	Vector component of the inviscid velocity in the direction of the $x$ -coordinate line.
W	$w_e/u_\infty$	Vector component of the inviscid velocity

#### Incompressible Case:

<u>Column Heading</u>	<u>Variable</u>	<u>Description</u>
X	$x$	Same as above
USQ	$(u_s/u_\infty)^2$	Local to free stream velocity ratio squared
U	$u_e/u_\infty$	Same as above
W	$w_e/u_\infty$	Same as above

### Punched Output (IFLG = 1)

Only the vector components of the velocity vectors are punched out. All fluid property calculations are done in the boundary layer program from the velocity ratio and free stream conditions. The punched output is again organized in the sequence of chordwise locations for each spanwise station, and the spanwise stations are arranged from root to tip. Each card contains the  $u_e/u_\infty$  &  $w_e/u_\infty$  values for a  $x, z$  location in the format 2E12.5. There are a total of NC x NS cards.

## OUTPUT FROM THE BOUNDARY-LAYER PROGRAM

The output for the boundary-layer program is divided into two sections. The first, which is optional, prints the input geometry and velocity. This print can be suppressed by setting the IFPRNT flag on input Card 2 equal to 0. Output from boundary-layer calculations is printed in the second section.

### Section 1

For explanation of variables, refer to "Input for Data Sets" under INPUT FOR THE BOUNDARY LAYER PROGRAM.

### Section 2

#### Initial Print

The title, input flags, and variables are printed as an aid to the identification of each case. At the beginning of the output and with each change of direction, a message is printed stating which direction the calculations are moving: inboard being tip to root, and outboard being root to tip.

#### Station Data

Each station header gives the location of that station from leading edge down and root out along with the values of the chordwise coordinate ( $x$ ), the spanwise coordinate ( $z$ ), and the fraction of chord for each  $x$ -value ( $x/c$ ). Following the station header is a message stating which type of coefficients were used to solve that station. To determine how the three-point derivatives used to calculate the pressures were found, two messages are printed. One pertains to derivatives with respect to  $z$ , the other to derivatives with respect to  $x$ . The codes A, B, C are defined as follows:

A = present station plus the next two to be calculated.

B = present station (used as the midpoint) plus the preceding station and the next station to be calculated.

C = present station plus the two preceding stations

Each iteration prints the wall values and the delta-wall values of the  $V$ - and  $T$ -profiles. When convergence is reached, or iterations exceed the maximum

allowable, the profiles are printed. Their description is as follows (for the definition of the boundary-layer parameters, see p. 31 of reference 1):

J	number of eta point in boundary layer
ETA	$\Delta\eta$ -spacing, $h_j$
Y	y-coordinate
F	f
U	f'
V	f''
G	g
W	g'
T	g''
B	$C(1 + \epsilon_m^+)$
BG	E
BT	E'
SVC	spanwise velocity component, $\bar{w}/\bar{w}_e$
CVC	chordwise velocity component, $\bar{u}/\bar{u}_e$
US/USE	resultant velocity in the boundary layer, $u_t/u_s$
BETA	flow deflection angle $\beta$ in the boundary layer measured from freestream direction. Positive $\beta$ is outboard.

Following the profiles, pressures used in calculation of the coefficients are printed. For the general case, pressure-bars are also printed. Body geometry and velocity values for that station are then printed as an aid in determining that the correct values were retrieved from the data set. Next, boundary-layer parameters are given, which are defined as follows:

CFC	chordwise local skin-friction coefficient, $cf_c$
CFN	spanwise local skin-friction coefficient, $cf_n$
DLSTS	chordwise displacement thickness, $\delta_c^*$
DLSTN	spanwise displacement thickness, $\delta_n^*$
THETAS	chordwise momentum thickness, $\theta_c$
THETAN	spanwise momentum thickness, $\theta_n$
BETA	flow deflection angle $\beta_w$
RX	Reynolds number based on $s$ , $R_s$
USE	resultant inviscid velocity $u_s$ , in feet per second
DUSED	derivative of the resultant inviscid velocity in the external streamline direction, $du_s/ds$



At end of each spanwise station (NXT) three additional parameters are printed.

DLSS displacement thickness  $\delta_{1s}^*$  in the direction of the external streamline, in feet.

$$\delta_{1s}^* = \int_0^{\delta} \left(1 - \frac{\rho \bar{u}}{\rho u_s}\right) dy$$

THSS momentum thickness  $\theta_{11s}$  in the direction of the external streamline, in feet

$$\theta_{11s} = \int_0^{\delta} \frac{\rho \bar{u}_s}{\rho_e u_s} \left(1 - \frac{\bar{u}_s}{u_s}\right) dy$$

TH21 momentum thickness  $\theta_{21}$ , formed by the velocity components  $\bar{u}$  and  $\bar{w}$

$$\theta_{21} = \int_0^{\delta} \frac{\rho \bar{u}}{\rho_e u_s} \left(\frac{\bar{w}}{u_s} - \frac{\bar{w}}{u_s}\right) dy$$

$\bar{u}_s$  orthogonal velocity component in the direction of the external streamline

### Summary Table

At the end of each spanwise station, or at the point on the spanwise station when flow direction will change, a summary table is printed. The table consists of:

NX	number of chordwise station
X/C	fractional chord of that x-station
VWALL	$f_w^i$
TWALL	$g_w''$
CFC	$cf_c$
CFN	$cf_n$
BETA	$\beta$
DLSTS	$\delta_c^*$
DLSTN	$\delta_n^*$

THTAS	$\theta_c$
THTAN	$\theta_n$
RX	$R_s$

### Description of Messages

#### "ITERATIONS EXCEED ITMAX"

Solutions did not converge within the maximum number of iterations allowed.

#### "\*\*SIGN CHANGE ON WE — CALCULATIONS GO TO NEXT SPANWISE STATION"

For outboard flow a negative  $w_e$  was read; for inboard flow a positive  $w_e$  was read. Station is flagged and calculations move to next spanwise station. If the root or tip calculations have been completed, a search is made to find the area of flow of opposite direction, or to see if entire wing has been calculated.

#### "\*\*CHORDWISE INFINITE-SWEPT WING EQUATIONS\*\*"

#### "\*\*STAGNATION LINE EQUATIONS\*\*"

#### "\*\*GENERAL CASE\*\*"

States which type of equations are used to calculate the coefficients.

#### "\*\*\*\*\*----- INBOARD CALCULATIONS STARTED -----\*\*\*\*\*"

Flow calculations are in the direction of tip to root

#### "\*\*\*\*\*----- OUTBOARD CALCULATIONS STARTED -----\*\*\*\*\*"

Flow calculations are in the direction of root to tip

#### "\*\*ERROR IN PROGRAM--CHECK FOR INCORRECT BRANCHING TO SOLUTIONS OF COEFFICIENTS\*\*"

Will most likely never occur. If it does, check MAIN program where an accumulative counter is used to determine which coefficients will be calculated. The counter has been calculated incorrectly.

#### "\*\*SEPARATION LINE — PROFILES CALCULATED USING CHORDWISE EQUATIONS\*\*"

The first spanwise line of a flow with opposite direction is being calculated using the chordwise equations specified. Here, by separation line, we mean the line separating the regions.

\*\*\*\*V(WALL) BECAME NEGATIVE"

Flow separation occurred. NXT is set to last station, and calculations go to next spanwise station.

\*\*\*\*SEPARATION TOO CLOSE TO LEADING EDGE — CALCULATIONS TERMINATED\*\*\*\*"

Flow separation occurred within the first two stations of the leading edge and the calculations are terminated because three stations are needed to compute the three-point derivatives for the external velocity gradients.

"NP EXCEEDED NPT--PROGRAM TERMINATED"

The number of points exceeded the maximum dimension allowed. Check input for VGP and DELTA(1).

\*\*\*NOTE — EPS DISTRIBUTION OUTER ONLY\*\*"

There is no inner region. Something is definitely wrong.

\*\*\*NOTE — EPS DISTRIBUTION INNER ONLY\*\*"

There is no outer region.

\*\*\*X-PRESSURES=A\*\*" and \*\*\*Z-PRESSURES=A\*\*"

Three-point derivatives are calculated using values from present station and next two stations to be calculated

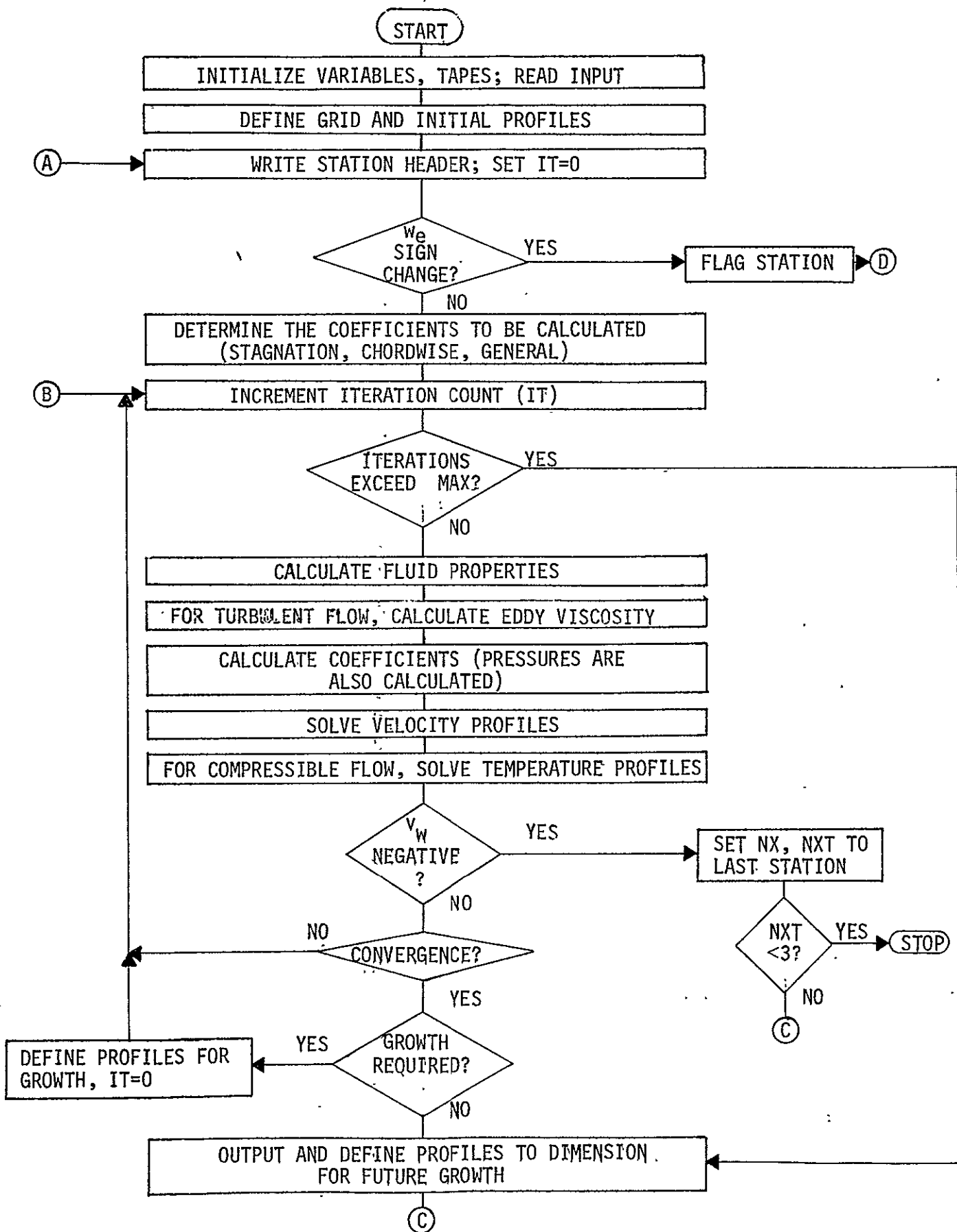
\*\*\*X-PRESSURES=B\*\*" and \*\*\*Z-PRESSURES=B\*\*"

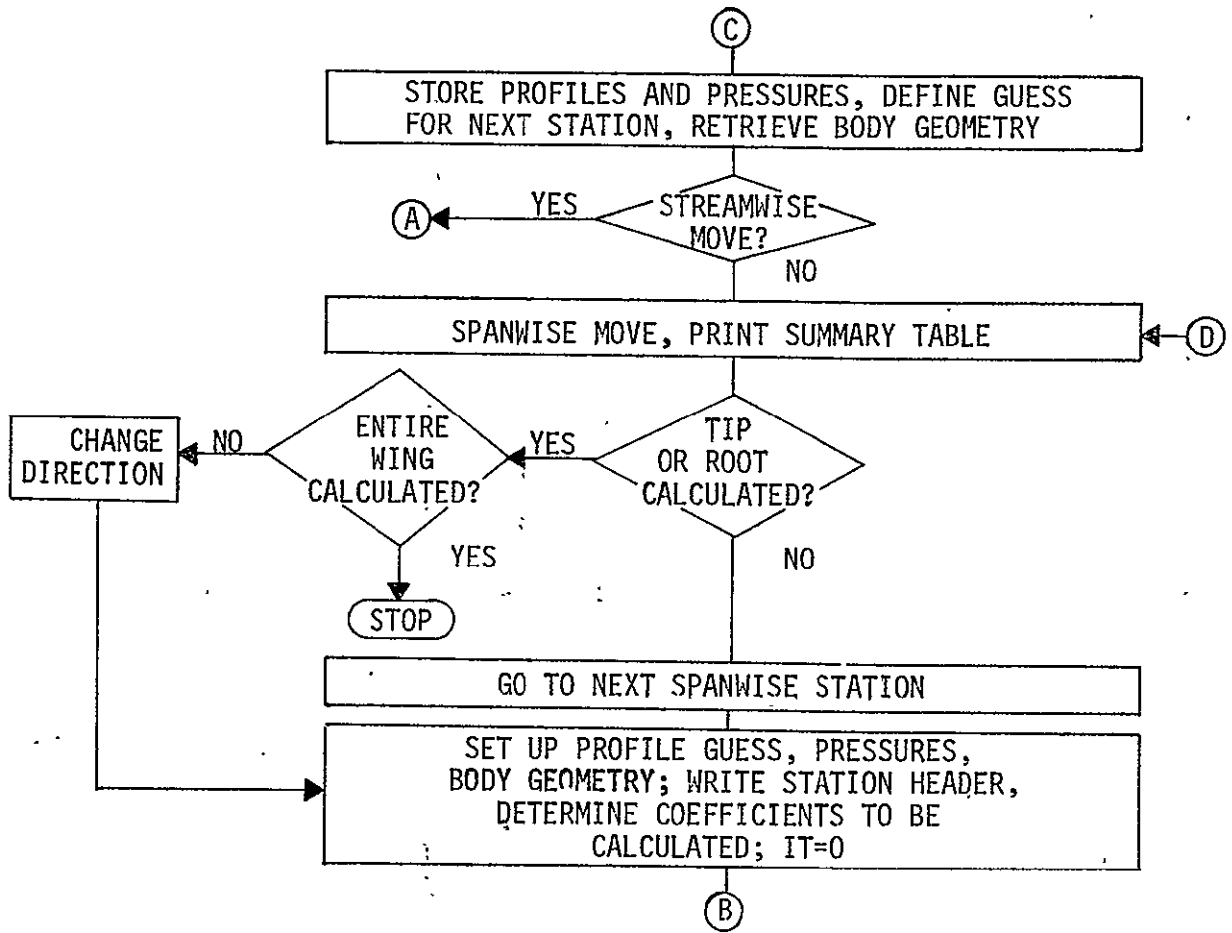
Three-point derivatives are calculated using values from present station (used as midpoint), previously calculated station, and next station to be calculated.

\*\*\*X-PRESSURES=C\*\*" and \*\*\*Z-PRESSURES=C\*\*"

Three-point derivatives are calculated using values from present station and the two previously calculated stations.

BASIC FLOW CHART OF MAIN FOR BOUNDARY-LAYER PROGRAM





## SAMPLE CALCULATIONS

To illustrate the use of the computer program, we present three sample calculations discussed in reference 1.

### Test Case 1

The first test case deals with the calculation of an infinite swept wing tested by Brebner and Wyatt<sup>5</sup>. Calculations for the upper surface were done in: (a) the orthogonal coordinate system fitting the yawed infinite wing geometry, and (b) the nonorthogonal system employed in reference 1.

The untapered wing had a sweep of 45 degrees, the streamwise airfoil was a 12-percent thick RAE 101 section on a 20-inch chord, and tests were run at a chord Reynolds number of  $2.1 \times 10^6$ . Calculations were done with the measured pressure distribution at wing angle of attack of 2.1 degrees and transition was specified at  $x'/c = 0.35$ . To run the present boundary-layer program for orthogonal coordinate system, we set  $h_1 = h_2 = 1$ ,  $K_1 = K_2 = K_{12} = K_{21} = 0$  and  $\theta = \pi/2$  for all chordwise and spanwise stations. The inviscid velocity components were obtained directly from the simple sweep theory:

$$\bar{u}_e = u_\infty [\cos^2 \lambda - C_p]^{1/2} \quad (35a)$$

and

$$\bar{w}_e = u_\infty \sin \lambda \quad (35b)$$

Here  $C_p$  is the measured pressure distribution,  $u_\infty = 200\text{fps}$ , and  $\lambda = \pi/4$ . Note that the geometry and velocity programs were not used and that, because all spanwise stations are identical, we have for convenience let the independent variable  $x$  be the surface distance normal to the leading edge instead of the polar angle  $\phi$ .

For calculation in the nonorthogonal coordinate system, one can take advantage of the similarity in airfoil profiles and pressure distribution in the spanwise direction to simplify geometry and velocity calculations. Because of similarity we can calculate the quantities  $h_1$ ,  $K_1$ , and  $\theta$  for one streamwise section only, and set  $K_2 = K_{12} = K_{21} = 0$ ,  $h_2 = 1.0$  for all stations. Calculation of the needed quantities follows the procedure discussed in detail for Test Case 2 except that the analytic expression for

streamwise airfoil definition was obtained by spline-fitting the tabulated data by a cubic spline. The inviscid velocity components were calculated directly from the velocity components determined for the infinite yawed wing calculations using the following relationships:

$$u_e = \bar{u}_e / \sin\theta \quad (36a)$$

and

$$w_e = u_\infty \sin\lambda - \bar{u}_e \cot\theta \quad (36b)$$

Here bars denote the inviscid velocity components in the orthogonal-coordinate system used previously.

To illustrate the input for this test case, we present only the load sheets for the boundary-layer program. The input for the geometry and velocity programs are quite straightforward, and the load sheets for them are not shown here. However, the data for them are shown below in the printout.

Load Sheets for the Boundary-Layer Program

Card 1

1	2	3	4	5	6	7	8	9	10	11	12	13	14	15	16	17	18	19	20	21	22	23	24	25	26	27	28	29	30	31	32	33	34	35	36	37	38	39	40	41	42	43	44	45	46	47	48	49	50	51
TITLE																																																		
BREBNER'S YAWED WING NONORTHOGONAL COORDINATE SYSTEM																																																		

Card 2

\$NAME NXSTRT = 1, NZSTRT = 1, NXT = 30, NZT = 3, NTR = 16, IFLOW = 1,  
 ICHORD = 1, ICMP = 1, ISPAN = 1; IFPRNT = 1, VGP = 1.26, DELTA(1) = .01,  
 ITMAX = 10, EPS = 1.0E-04, IPZ = 4, IPX = 4, EPSV = .1, EPST = .1\$

Card 3

1	2	3	4	5	6	7	8	9	10	11	12	13	14	15	16	17	18	19	20	21	22	23	24	25	26	27	28	29	30	31	32	33	34	35	36
TFRS										UFRS or CMFRS										PFRS															
+ 455 . E+00										+ 200 . E+00										+ 2047 . 68 E+00															

The printout of the velocity and geometry data are shown below for only one spanwise section since for test case 1 they are identical for all spanwise sections.

\*\* EXTERNAL VELOCITY DISTRIBUTION (FT/SEC) \*\*

Z	Y	U1	W1
0.0	0.0	0.0	0.141421E+02
1	0.447250E-01	0.467190E+02	0.128435E+03
2	0.632500E-01	0.687032E+02	0.116245E+03
3	0.774790E-01	0.865076E+02	0.104914E+03
4	0.100640E+00	0.115015E+03	0.846774E+02
5	0.141540E+00	0.137759E+03	0.451698E+02
6	0.200330E+00	0.222572E+03	0.348506E+02
7	0.245570E+00	0.243084E+03	-0.182142E+02
8	0.317560E+00	0.254628E+03	-0.211322E+02
9	0.402720E+00	0.260252E+03	-0.338567E+02
10	0.494730E+00	0.265200E+03	-0.449204E+02
11	0.594910E+00	0.268374E+03	-0.455844E+02
12	0.643500E+00	0.264750E+03	-0.451008E+02
13	0.722730E+00	0.262514E+03	-0.440190E+02
14	0.795400E+00	0.259714E+03	-0.422196E+02
15	0.863710E+00	0.255454E+03	-0.391560E+02
16	0.927500E+00	0.249956E+03	-0.351288E+02
17	0.983430E+00	0.243752E+03	-0.303012E+02
18	0.103720E+01	0.237099E+03	-0.251232E+02
19	0.110400E+01	0.230592E+03	-0.200936E+02
20	0.115950E+01	0.224360E+03	-0.160900E+02
21	0.121320E+01	0.218300E+03	-0.121768E+02
22	0.124010E+01	0.212694E+03	-0.813960E+01
23	0.125100E+01	0.205735E+03	-0.436104E+01
24	0.136740E+01	0.202104E+03	-0.671124E+00
25	0.142700E+01	0.196676E+03	0.314462E+00
26	0.147960E+01	0.189954E+03	0.787678E+00
27	0.152080E+01	0.182200E+03	0.110741E+02
28	0.155030E+01	0.182200E+03	0.15-176E+02
29	0.157080E+01	0.180902E+03	0.146329E+02
30	0.157080E+01	0.180902E+03	0.146329E+02

\*\* INPUT WING GEOMETRY \*\*

N7	NX	H1	H2	K1	K2	K12
1	1	0.17490E+00	0.10000E+01	0.26590E+02	0.0	0.0
1	2	0.18260E+00	0.10000E+01	0.28550E+02	0.0	0.0
1	3	0.20330E+00	0.10000E+01	0.22610E+02	0.0	0.0
1	4	0.21610E+00	0.10000E+01	0.18110E+02	0.0	0.0
1	5	0.23980E+00	0.10000E+01	0.12430E+02	0.0	0.0
1	6	0.25040E+00	0.10000E+01	0.61050E+01	0.0	0.0
1	7	0.37090E+00	0.10000E+01	0.24540E+01	0.0	0.0
1	8	0.42630E+00	0.10000E+01	0.12740E+01	0.0	0.0
1	9	0.54240E+00	0.10000E+01	0.53570E+00	0.0	0.0
1	10	0.66730E+00	0.10000E+01	0.22740E+00	0.0	0.0
1	11	0.86070E+00	0.10000E+01	0.10340E+00	0.0	0.0
1	12	0.38430E+00	0.10000E+01	0.60410E-01	0.0	0.0
1	13	0.10030E+01	0.10000E+01	0.22900E-01	0.0	0.0
1	14	0.11030E+01	0.10000E+01	0.18960E-01	0.0	0.0
1	15	0.11900E+01	0.10000E+01	0.22010E-02	0.0	0.0
1	16	0.12670E+01	0.10000E+01	-0.74530E-02	0.0	0.0
1	17	0.13350E+01	0.10000E+01	-0.11200E-01	0.0	0.0
1	18	0.13950E+01	0.10000E+01	-0.11970E-01	0.0	0.0
1	19	0.14430E+01	0.10000E+01	-0.10660E-01	0.0	0.0
1	20	0.14940E+01	0.10000E+01	-0.93430E-02	0.0	0.0
1	21	0.15350E+01	0.10000E+01	-0.75390E-02	0.0	0.0
1	22	0.15690E+01	0.10000E+01	-0.55530E-02	0.0	0.0
1	23	0.15990E+01	0.10000E+01	-0.29330E-02	0.0	0.0
1	24	0.16230E+01	0.10000E+01	-0.59320E-03	0.0	0.0
1	25	0.16420E+01	0.10000E+01	0.10320E-03	0.0	0.0
1	26	0.16570E+01	0.10000E+01	0.21420E-04	0.0	0.0
1	27	0.16630E+01	0.10000E+01	0.79410E-05	0.0	0.0
1	28	0.16740E+01	0.10000E+01	0.56230E-04	0.0	0.0
1	29	0.16760E+01	0.10000E+01	-0.14770E-03	0.0	0.0
1	30	0.16760E+01	0.10000E+01	-0.4170E-03	0.0	0.0



K21	THETA	SI	RHOE	CMUE
0.0	0.15710E+01	0.0	0.26226E-02	0.33708E-06
0.0	0.12890E+01	0.81470E-02	0.26226E-02	0.33708E-06
0.0	0.11960E+01	0.11790E-01	0.26226E-02	0.33708E-06
0.0	0.11350E+01	0.14770E-01	0.26226E-02	0.33708E-06
0.0	0.10580E+01	0.19910E-01	0.26226E-02	0.33708E-06
0.0	0.96120E+00	0.30900E-01	0.26226E-02	0.33708E-06
0.0	0.88630E+00	0.50310E-01	0.26226E-02	0.33708E-06
0.0	0.85430E+00	0.68570E-01	0.26226E-02	0.33708E-06
0.0	0.82510E+00	0.10380E+00	0.26226E-02	0.33708E-06
0.0	0.80710E+00	0.15530E+00	0.26226E-02	0.33708E-06
0.0	0.79670E+00	0.22300E+00	0.26226E-02	0.33708E-06
0.0	0.79250E+00	0.27350E+00	0.26226E-02	0.33708E-06
0.0	0.78850E+00	0.35720E+00	0.26226E-02	0.33708E-06
0.0	0.78640E+00	0.44060E+00	0.26226E-02	0.33708E-06
0.0	0.78540E+00	0.52400E+00	0.26226E-02	0.33708E-06
0.0	0.73570E+00	0.60730E+00	0.26226E-02	0.33708E-06
0.0	0.78650E+00	0.69070E+00	0.26226E-02	0.33708E-06
0.0	0.73750E+00	0.77410E+00	0.26226E-02	0.33708E-06
0.0	0.78840E+00	0.85770E+00	0.26226E-02	0.33708E-06
0.0	0.78930E+00	0.94130E+00	0.26226E-02	0.33708E-06
0.0	0.79000E+00	0.10250E+01	0.26226E-02	0.33708E-06
0.0	0.79060E+00	0.11090E+01	0.26226E-02	0.33708E-06
0.0	0.79090E+00	0.11920E+01	0.26226E-02	0.33708E-06
0.0	0.79110E+00	0.12760E+01	0.26226E-02	0.33708E-06
0.0	0.79110E+00	0.13600E+01	0.26226E-02	0.33708E-06
0.0	0.79110E+00	0.14440E+01	0.26226E-02	0.33708E-06
0.0	0.79110E+00	0.15280E+01	0.26226E-02	0.33708E-06
0.0	0.79110E+00	0.16110E+01	0.26226E-02	0.33708E-06
0.0	0.79110E+00	0.16620E+01	0.26226E-02	0.33708E-06
0.0	0.79110E+00	0.16950E+01	0.26226E-02	0.33708E-06

The printout of the boundary-layer program is shown below for a few representative chordwise stations together with a summary table containing the boundary-layer parameters.

```

THREE-D BOUNDARY-LAYER PROGRAM
FOR INCOMPRESSIBLE AND COMPRESSIBLE LAMINAR AND TURBULENT FLOWS
BREDNERS VAWEC WING, NLY-ORTHOGONAL COORD. SYSTEM

NXSTRT= 1      NZSTRT= 1      NXT = 30
NXT = 3      NTK = 16      IFLOW = 1
ICHORD= 7      ICOMP = 1      ISPAN = 1
IFPPNT= 1      FTAE = 8.00000      DELTA = 0.05000
VGP = 1.30000      FRFS = 0.45500E+03      PFRS = 0.204768E+04
UFRS = 0.200000E+03      MFRS = 0.0      MUFRS = 0.337078E-06
RHOFRS= 0.26226E-02      TT = 0.455000E+03

***----- CUTBOARD CALCULATIONS STARTED -----***

*** AX = 1      VZ = 1      X = 0.0      Z = 0.0      X/C = 0.0
** STAGNATION LINE EQUATIONS **
** Z-PRESSURES=A **
** X-PRESSURES=A **

V(WALL)      DFLV(I)      T(WALL)      DELT(I)
1 0.337000E+03  0.167527E+C1  0.322000E+03  0.222931E+00
2 0.140777E+01  -0.167262E+00  0.254921E+00  -0.144610E+00
3 0.124031E+01  -0.131129E-01  0.419321E+00  -0.130612E-01
4 0.122880E+01  0.267405E-00  0.357266E+00  -0.133523E-01
5 0.122880E+01  0.267405E-00  0.397127E+00  -0.266507E-01

J      STA      Y      F      U      V      G      W      T      B
1 0.0  0.0  0.0  0.0  0.0  0.122880E+01  0.0  0.0  0.397127E+00  0.100000E+01
4 0.157950  0.0  0.0  0.230525E-01  0.0  0.225362E+00  0.103125E+01  0.790082E-02  0.791881E-01  0.396473E+00  0.100000E+01
7 0.637801  0.0  0.0  0.77656E+00  0.0  0.89372E+00  0.641796E+00  0.403068E-01  0.250101E+00  0.378958E+00  0.100000E+01
10 1.600748  0.0  0.0  0.972169E+00  0.0  0.31949E+00  0.776715E+00  0.0  0.54921E+00  0.22241E+00  0.100000E+01
13 3.716345  0.0  0.0  0.305826E+01  0.0  0.100015E+01  -0.505416E-03  0.187662E+01  0.706955E+00  0.434229E-03  0.100000E+01
15 6.395623  0.0  0.0  0.573755E+01  0.0  0.100000E+01  -0.762987E-04  0.377112E+01  0.707107E+00  0.403236E-04  0.100000E+01

J      STA      SVC      CVC      US/USE      BETA
4 0.199500  0.0  0.111989E+00  0.0  0.275362E+00  0.0  0.111989E+00  0.0
7 0.637801  0.0  0.353695E+00  0.0  0.589372E+00  0.0  0.353695E+00  0.0
10 1.600748  0.0  0.776715E+00  0.0  0.776715E+00  0.0  0.776715E+00  0.0
13 3.716345  0.0  0.100015E+01  0.0  0.100015E+01  0.0  0.100015E+01  0.0
15 6.395623  0.0  0.100000E+01  0.0  0.100000E+01  0.0  0.100000E+01  0.0

P1      P2      P3      P4      P5      P6      P7      P8      P9
0.100000E+01  0.100000E+01  0.0  0.0  0.0  -0.217319E-06  0.334679E-01  0.0  0.0
0.0  0.100000E+01  0.0  0.0  0.0  0.0  0.0  0.0  0.0

BODY GEOMETRY FROM STORED DATA SFT
SI = 0.0      THETA = 0.15710E+01      H1 = 0.174800E+00      H2 = 0.100000E+01      KI = 0.385900E+02
K2 = 0.0      CMUE = 0.337078E-06      UE = 0.0      WE = 0.141421E+03
RHCE = 0.262261E-02
LFC = 0.0      DLSTG = 0.0      THIAS = 0.0      BETAI = 0.0
CFN = 0.0      RLSTG = 0.0      THIAN = 0.0
USE = 0.141421E+03      DUSED = 0.0

```

```

*** NX = 7  NZ = 1  X = C.2CC  Z = 0.0  X/C = 0.020
** CHORDWISE INFINITE-SWLP1 WING EQUATIONS **
** 7-PRESSURES=4 **
** X-PRESSURES=C **
  V(WALL) DELV(1) T(WALL) DELT(1)
  1 0.776718F+00 -0.145290E+00 -0.115555E+00 -0.154981E+00
  2 0.810428E+00 -0.447523E-02 -0.250536E+00 -0.151886E-02
  3 0.805937E+00 -0.944115E-05 -0.292955E+00 -0.328544E-05
  J ETA 0.0 Y 0.0 F 0.0 U 0.0 V 0.0 W 0.0 T 0.0 B
  1 0.0 0.0 0.0 0.0 0.0 0.0 0.0 0.0 0.0 0.0 0.0
  4 0.159500 0.418271E-03 0.155442E-01 0.153793E+00 0.757335E+00 -0.464385E-02 -0.457237E-01 -0.199356E+00 0.100000E+01
  7 0.637801 0.130526E-02 0.148258E+00 0.441640E+00 0.576777E+00 -0.396682E-01 -0.107681E+00 -0.880221E-01 0.100000E+01
  10 1.607148 0.727589E-02 0.787575E+00 0.822039E+00 0.245526E+00 -0.152719E+00 -0.104882E+00 0.657013E-01 0.100000E+01
  13 3.716345 0.741539E-02 0.279745E+01 0.598940E+00 0.226288E-02 -0.230017E+00 0.766636E-02 0.96045E-02 0.100000E+01
  15 6.395623 0.130889E-01 0.547628E+01 0.100000E+01 0.784959E-04 -0.206540E+00 0.423253E-02 -0.109518E-02 0.100000E+01
  J ETA 0.0 SVC 0.0 CVC 0.0 LS/USE 0.0 BETA
  1 0.0 0.0 0.0 0.0 0.0 0.0 0.0 0.0 0.0 0.0
  4 0.195500 -0.106375E+02 0.127876E+00 0.131511E+00 -0.137548E+02
  7 0.637801 -0.254413E+02 0.374481E+00 0.396753E+00 -0.11601E+02
  10 1.607148 -0.247152E+02 0.710541E+00 0.773979E+00 -0.540494E+01
  13 3.716345 0.727375E+01 0.100000E+01 0.100000E+01 0.384211E+00
  15 6.395623 0.544444E+01 0.100000E+01 0.100000E+01 0.168601E+00
  P1 P2 P3 P4 P5 P6 P7 P8 P9
  0.638585E+00 0.350244E+00 0.0 0.0 0.0 0.0 0.452566E-01 0.0 0.173542E+00
  0.135643E+00 0.353240E+00 -0.744650E+00
  BODY GEOMETRY FROM STORED DATA SET
  S1 = 0.503160E-01 THETA = 0.386306E+00 H1 = 0.370900E+00 H2 = 0.120000E+01 K1 = 0.245000E+00
  X2 = 0.0 P12 = 0.0 K21 = 0.0
  RMFE = 0.262261E-02 CPWF = 0.337078E-06
  CFC = 0.555977E-02 DLS15 = 0.179012E-03 THIAS = 0.737437E-04 BETAI = -0.148492E+12
  CFN = -0.127876E-02 DLS18 = 0.117781E-02 THIAN = -0.222075E+00 RX = 0.870279E+35
  CSE = 0.127876E-02 DLS19 = 0.117781E-02 THIAN = -0.222075E+00

```

```

*** NX = 8  NZ = 1  X = C.246  Z = 0.0  X/C = 0.030
** SIGN CHANGE ON DEL - CALCULATIONS GO TO NEXT SPANWISE STATION
*** SUMMARY TABLE ***
NX  Y/C  V(WALL) T(WALL) CFC  CFN  HFTA  DLSTS  DLSTN  THIAS  THIAN  RK
  1 0.0 0.12797E+01 0.19711E+00 0.0 0.0 0.0 0.0 0.0 0.0 0.0
  2 0.1000E-02 0.1147E+01 0.2047E+00 0.3172E-02 0.2344E-02 0.3699E+02 0.1432E-03 0.2004E-33 0.6742E-04 0.8566E-04 0.2961E+04
  3 0.7000E-02 0.1190E+01 0.2146E+00 0.4217E-02 0.1178E-02 0.2229E+04 0.1383E-03 0.1944E-33 0.6715E-04 0.7859E-04 0.6302E+04
  4 0.1900E-02 0.1190E+01 0.4480E-02 0.1178E-02 0.1178E-02 0.1257E+02 0.1377E-03 0.7051E-03 0.6161E-04 0.7945E-04 0.9941E+04
  5 0.5700E-02 0.1103E+01 0.4463E-01 0.5702E-02 0.3638E-03 0.3451E+01 0.1480E-03 0.2239E-33 0.6074E-04 0.7083E-04 0.1791E+05
  6 0.1000E-01 0.1767E+01 0.1569E+00 0.6291E-02 0.7914E-03 0.1717E+01 0.1451E-03 0.2940E-03 0.6398E-04 0.2224E-04 0.4033E+05
  7 0.7600E-01 0.4005E+01 0.2571E+00 0.5551E-02 0.1472E-02 0.1485E+02 0.1790E-03 0.7413E-02 0.7374E-04 0.2221E+00 0.6705E+05

```

```

*** NX = 25  NZ = 2  X = 1.365  Z = 0.160  X/C = 0.900
** GENERAL CASE **
** 7-PRESSURES=0 **
** X-PRESSURES=C **
  V(WALL) DELV(1) T(WALL) DELT(1)
  1 0.172566E+01 -0.449451E-02 0.290474E+00 -0.107333E-03
  J ETA 0.0 Y 0.0 F 0.0 U 0.0 V 0.0 W 0.0 T 0.0 B
  1 0.0 0.0 0.0 0.0 0.0 0.0 0.0 0.0 0.0 0.0
  4 0.195500 0.272644E-02 0.312672E-01 0.240152E+00 0.172067E+01 0.498520E-02 0.445458E-01 0.296566E+00 0.100000E+01
  7 0.637801 0.111792E-02 0.205927E+00 0.457602E+00 0.119402E+00 0.401409E-01 0.44158E-01 0.139711E-01 0.100000E+01
  10 1.607148 0.179443E-01 0.719439E+00 0.562282E+00 0.622613E-01 0.949662E-01 0.67053E-01 0.487059E-03 0.33792E+02
  13 3.716345 0.414742E-01 0.200239E+01 0.648975E+00 0.278799E-01 0.237526E+00 0.641621E-01 -0.256358E-02 0.882678E+02
  16 8.364110 0.293551E-01 0.571059E+01 0.774957E+00 0.266157E-01 0.502478E+00 0.470207E-01 -0.490159E-02 0.931729E+02
  19 18.575382 0.257306E+00 0.143225E+02 0.745311E+00 0.546609E-02 0.751564E+00 0.561741E-02 -0.233327E-02 0.931729E+02
  22 41.010694 0.257677E+00 0.166187E+02 0.100000E+01 0.659890E-04 0.707314E+00 -0.33162E-02 -0.200561E-04 0.931729E+02
  25 41.010694 0.457677E+00 0.361587E+02 0.100000E+01 0.659890E-04 0.707314E+00 -0.33162E-02 -0.200561E-04 0.931729E+02
  J ETA 0.0 SVC 0.0 CVC 0.0 LS/USE 0.0 BETA
  1 0.0 0.0 0.0 0.0 0.0 0.0 0.0 0.0 0.0 0.0
  4 0.195500 -0.127750E+02 0.311892E+00 0.312430E+00 0.618122E+01
  7 0.637801 -0.191114E+02 0.212666E+00 0.212666E+00 0.504190E+01
  10 1.607148 -0.204747E+02 0.612138E+00 0.614425E+00 0.457388E+01
  13 3.716345 -0.194148E+02 0.095528E+00 0.657477E+00 0.377852E+01
  16 8.364110 -0.140606E+02 0.80957E+00 0.235722E+01
  19 18.575382 -0.167701E+01 0.571195E+00 0.571702E+00 0.234174E+00
  22 41.010694 0.555456E+00 0.100000E+01 0.555977E+00 -0.135616E+00
  25 41.010694 0.257677E+00 0.100000E+01 0.555977E+00 -0.135616E+00
  P1 P2 P3 P4 P5 P6 P7 P8 P9
  0.297452E+00 -0.411153E+00 0.0 0.0 0.162577E-05 0.110027E-05 0.134584E+00 0.0 0.199442E-03
  P10 P11 P12
  0.878758E+00 -0.418115E+00 0.256560E+00
  P13 P14 P15 P16 P17 P18 P19
  0.298246E+00 -0.403048E+00 0.0 0.0 0.768729E-06 0.541193E-06 0.128830E+01 0.0 -0.452595E-03
  0.807726E+00 -0.403947E+00 0.285827E+00
  BODY GEOMETRY FROM STORED DATA SET
  S1 = 0.176000E+01 THETA = 0.191106E+00 H1 = 0.164200E+01 H2 = 0.103000E+01 K1 = 0.103200E-03
  X2 = 0.0 P12 = 0.0 K21 = 0.0
  RMFE = 0.262261E-02 CPWF = 0.337078E-06
  CFC = 0.769119E-02 DLS15 = 0.350667E-02 THIAS = 0.246753E-02 BETAI = 0.618122E+01
  CFN = 0.291644E-03 DLS18 = 0.314342E+00 THIAN = -0.342000E+01 RX = 0.213953E+07
  CSE = 0.201643E+03 DLS19 = 0.314342E+02

```

```

*** NX = 26  NZ = 2  X = 1.42C  Z = 0.100  X/C = 0.850
** SIGN CHANGE ON WE - CALCULATIONS GO TO NEXT SPANWISE STATION

```

## Test Case 2

The second test case is for an incompressible flow past an untapered and untwisted, 30-degree swept wing having NACA 0012 streamwise airfoil sections. Its semispan is 9.131 feet and its streamwise chord is 3.776 feet. The inviscid velocity distribution was obtained by using Hess's potential flow method<sup>7</sup> at an angle of attack of 8 degrees which yielded a lift coefficient of 0.51. A total of 16 chordwise strips each subdivided into 50 elements were used to obtain the solution. Boundary-layer calculations were made for the lower surface of the wing at a chord Reynolds number of  $R_L = 5.88 \times 10^6$ .

Because the velocity distribution was calculated from the inviscid flow theory, it was not necessary to use the velocity program. However, since the output from Hess's potential-flow program is given in a Cartesian-coordinate system, all velocity components had to be rotated into the nonorthogonal coordinate system. Let the potential flow velocity vector  $\hat{v}$  be given by  $v_x i + v_y j + v_z k$ , then the dot products of this vector and the unit vectors  $\hat{t}_1$  and  $\hat{t}_2$  in the coordinate directions on the surface will give the projections of the resultant velocity vector along the surface coordinate directions. The velocity components in the nonorthogonal coordinate system case can then be obtained from

$$u_e = \frac{\hat{v} \cdot \hat{t}_1 - \hat{v} \cdot \hat{t}_2 \cos\theta}{\sin^2\theta} \quad (37)$$

$$w_e = \frac{\hat{v} \cdot \hat{t}_2 - \hat{v} \cdot \hat{t}_1 \cos\theta}{\sin^2\theta} \quad (38)$$

Also, because the output points from the potential-flow program are not necessarily the surface net points at which the boundary layer is calculated, interpolation in both spanwise and chordwise directions becomes necessary. Ideally, the velocity-component-calculation subroutine should be attached to the potential-flow program. Here we have done all the steps piecewise.

Another aspect of this test case is the simplified geometry which allows one to bypass the geometry program if so desired. Similar to the previous test case, the untapered and untwisted wing implies that  $K_2 = K_{12} = K_{21} = 0$ ,  $h_2 = \text{const}$ , and that  $h_1$ ,  $K_1$  and  $\theta$  are to be calculated on one streamwise section only.

Calculation of these quantities can be done analytically since the NACA 0012 is described by a closed formula. The procedure is as follows:

We denote the wing chord by  $c$ , the span by  $b$ , the sweep angle by  $\lambda$  and the nondimensional airfoil definition by  $(\xi = x)$

$$\frac{\bar{z}}{c} = f\left(\frac{x}{c}\right) \quad (39a)$$

For the NACA 0012 airfoil, the thickness distribution  $f$  is given by

$$f\left(\frac{x}{c}\right) = 0.6[0.2969 \sqrt{x/c} - 0.126(x/c) - 0.3516(x/c)^2 + 0.2843(x/c)^3 - 0.1015(x/c)^4] \quad (39b)$$

According to equation (B6) of reference 1, the metric coefficient  $h_1$  is given by

$$h_1^2 = \left(\frac{\partial \bar{x}}{\partial \phi}\right)_y^2 + \left(\frac{\partial \bar{z}}{\partial \phi}\right)_y^2 \quad (40)$$

If we select the root section to be the defining airfoil section, then  $\bar{x} = x$  and  $\bar{x}/c = 1 - \cos\phi$  since we have an untwisted untapered wing. Using (30a), we can write (40) as

$$h_1^2 = c^2 \sin^2\phi [1 + (f')^2] \quad (41)$$

Here prime on  $f$  denotes differentiation with respect to  $x/c$ . To obtain  $h_2$  we note that the distance along the wing generator is  $\bar{y}/\sin\lambda$ , and choose the other independent variable to be  $y = \bar{y}/b$  which results in

$$h_2 = b/\sin\lambda$$

The angle between the coordinate axis is given by equation (B12) from reference 1 by

$$\cos\theta = \frac{1}{h_1 h_2} \left( \frac{\partial \bar{x}}{\partial \phi} \frac{\partial \bar{x}}{\partial y} + \frac{\partial \bar{z}}{\partial \phi} \frac{\partial \bar{z}}{\partial y} \right) \quad (43)$$

By noting that  $\partial \bar{z}/\partial y \equiv 0$  and that for any point  $P$  in figure 3,  $\bar{x} = by \tan\lambda + c(1 - \cos\phi)$  we obtain

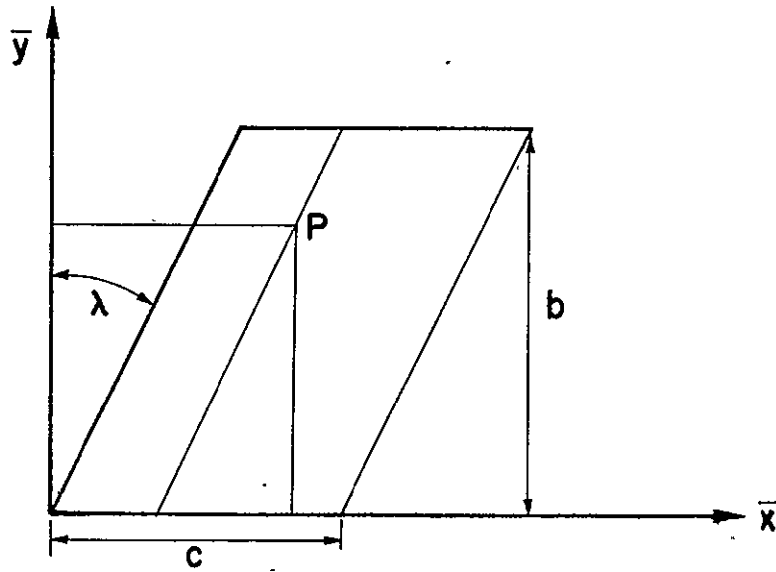


Figure 3. The notation for test case 2.

$$\cos\theta = \frac{\sin\lambda}{[1 + (f')^2]^{1/2}} \quad (44)$$

The expression for the geodesic curvature  $K_1$  can be obtained by differentiating the right-hand side of (44) and using the definition of  $K_1$ , that is,

$$K_1 = \frac{1}{h_1 h_2 \sin\theta} \left[ \frac{\partial}{\partial x} (h_2 \cos\theta) - \frac{\partial h_1}{\partial z} \right]$$

This gives

$$K_1 = \frac{1}{h_1 \sin\theta} \frac{d(\cos\theta)}{d\phi} = \frac{\sin\lambda f' f''}{c \sin\theta [1 + (f')^2]^{3/2}} \quad (45)$$

For reasons similar to those discussed in test case 1, we only present the load sheets for the boundary-layer program and the printout of the velocity, geometry data and a few representative chordwise stations for the boundary-layer calculations.

Load Sheets for the Boundary-Layer Program

Card 1

1	2	3	4	5	6	7	8	9	10	11	12	13	14	15	16	17	18	19	20	21	22	23	24	25	26	27	28	29	30	31	32	33	34	35	36	37	38	39	40	41	42	43	44
TITLE																																											
0 0 1 2 -- LOWER SURFACE, 30 DEGREE NEUMAN AL = 8.0																																											

Card 2

\$NAME NXSTRT = 1, NZSTRT = 1, NXT = 30, NZT = 22, NTR = 2, IFLOW = 1,  
 ICHORD = 2, ICMP = 1, ISPAN = 1, IFPRNT = 1, VGP = 1.26, DETA(1) = .01,  
 ITMAX = 10, EPS = 1.0E-04, IPZ = 4, IPX = 4, EPSV = .1, EPST = .1\$

Card 3

1	2	3	4	5	6	7	8	9	10	11	12	13	14	15	16	17	18	19	20	21	22	23	24	25	26	27	28	29	30	31	32	33	34	35	36			
TFRS						UFRS or CMFRS						PFRS																										
+				4	5	5	.	E	+	0	0	+					2	0	0	.	E	+	0	0	+					2	0	4	8	.	E	+	0	0

The external velocity data and the geometry data are shown for two spanwise stations:

\*\* EXTERNAL VELOCITY DISTRIBUTION (FT/SEC) \*\*

Z	X	UF	VE
0.0			
1	0.141539E+00	0.0	0.669840E+02
2	0.200335E+00	0.806720E+02	0.475240E+02
3	0.245565E+00	0.105664E+03	0.352300E+02
4	0.301136E+00	0.127110E+03	0.253260E+02
5	0.348166E+00	0.140244E+03	0.197070E+02
6	0.387761E+00	0.149324E+03	0.161100E+02
7	0.451027E+00	0.159619E+03	0.124202E+02
8	0.554811E+00	0.172158E+03	0.850306E+01
9	0.643501E+00	0.179616E+03	0.649020E+01
10	0.722734E+00	0.184542E+03	0.525760E+01
11	0.795399E+00	0.187888E+03	0.447780E+01
12	0.863212E+00	0.190320E+03	0.388260E+01
13	0.927295E+00	0.192192E+03	0.341480E+01
14	0.988432E+00	0.193618E+03	0.302920E+01
15	0.104720E+01	0.194680E+03	0.269300E+01
16	0.110403E+01	0.195448E+03	0.240980E+01
17	0.115928E+01	0.195972E+03	0.215680E+01
18	0.121322E+01	0.196272E+03	0.193790E+01
19	0.126610E+01	0.196400E+03	0.172818E+01
20	0.131812E+01	0.196382E+03	0.150894E+01
21	0.136944E+01	0.196190E+03	0.127510E+01
22	0.142023E+01	0.195746E+03	0.100348E+01
23	0.147063E+01	0.194858E+03	0.639560E+00
24	0.152077E+01	0.192732E+03	0.123824E+00
25	0.156080E+01	0.178220E+03	0.565240E+01
0.151515E+00			
1	0.141539E+00	0.0	0.759020E+02
2	0.200335E+00	0.768460E+02	0.539500E+02
3	0.245565E+00	0.104176E+03	0.399140E+02
4	0.301136E+00	0.127540E+03	0.279420E+02
5	0.348166E+00	0.141718E+03	0.208800E+02
6	0.387761E+00	0.151392E+03	0.162478E+02
7	0.451027E+00	0.162149E+03	0.114038E+02
8	0.554811E+00	0.174886E+03	0.628040E+01
9	0.643501E+00	0.182190E+03	0.377740E+01
10	0.722734E+00	0.186846E+03	0.240740E+01
11	0.795399E+00	0.189960E+03	0.165940E+01
12	0.863212E+00	0.192168E+03	0.115980E+01
13	0.927295E+00	0.193812E+03	0.824300E+00
14	0.988432E+00	0.195028E+03	0.590520E+00
15	0.104720E+01	0.195908E+03	0.432320E+00
16	0.110403E+01	0.196518E+03	0.313560E+00
17	0.115928E+01	0.196854E+03	0.229100E+00
18	0.121322E+01	0.197054E+03	0.175510E+00
19	0.126610E+01	0.197036E+03	0.129756E+00
20	0.131812E+01	0.196860E+03	0.775380E-01
21	0.136944E+01	0.196466E+03	0.267020E-01
22	0.142023E+01	0.195764E+03	0.302130E-01
23	0.147063E+01	0.194194E+03	0.261400E+00
24	0.152077E+01	0.190974E+03	0.123258E+01
25	0.156080E+01	0.176714E+03	0.840340E+01

\*\* INPUT WING GEOMETRY \*\*

N1	N2	H1	F2	K1	K2	K12
1	1	0.08600E+00	0.10750E+02	0.14060E+01	0.0	0.0
1	2	0.85630E+00	0.10750E+02	0.77080E+00	0.0	0.0
1	3	0.99820E+00	0.10750E+02	0.40800E+00	0.0	0.0
1	4	0.11780E+01	0.10750E+02	0.20220E+00	0.0	0.0
1	5	0.13330E+01	0.10750E+02	0.11860E+00	0.0	0.0
1	6	0.14700E+01	0.10750E+02	0.76650E-01	0.0	0.0
1	7	0.16700E+01	0.10750E+02	0.42120E-01	0.0	0.0
1	8	0.20000E+01	0.10750E+02	0.16000E-01	0.0	0.0
1	9	0.22700E+01	0.10750E+02	0.65190E-02	0.0	0.0
1	10	0.24990E+01	0.10750E+02	0.21880E-02	0.0	0.0
1	11	0.26970E+01	0.10750E+02	0.53700E-05	0.0	0.0
1	12	0.28710E+01	0.10750E+02	0.11520E-02	0.0	0.0
1	13	0.30240E+01	0.10750E+02	0.17340E-02	0.0	0.0
1	14	0.31580E+01	0.10750E+02	0.20010E-02	0.0	0.0
1	15	0.32770E+01	0.10750E+02	0.20930E-02	0.0	0.0
1	16	0.32820E+01	0.10750E+02	0.20960E-02	0.0	0.0
1	17	0.34750E+01	0.10750E+02	0.20640E-02	0.0	0.0
1	18	0.35520E+01	0.10750E+02	0.20350E-02	0.0	0.0
1	19	0.36200E+01	0.10750E+02	0.20340E-02	0.0	0.0
1	20	0.36770E+01	0.10750E+02	0.20830E-02	0.0	0.0
1	21	0.37230E+01	0.10750E+02	0.21950E-02	0.0	0.0
1	22	0.37600E+01	0.10750E+02	0.23850E-02	0.0	0.0
1	23	0.37370E+01	0.10750E+02	0.26630E-02	0.0	0.0
1	24	0.38050E+01	0.10750E+02	0.30580E-02	0.0	0.0
1	25	0.38130E+01	0.10750E+02	0.34590E-02	0.0	0.0
2	1	0.08600E+00	0.10750E+02	0.14060E+01	0.0	0.0
2	2	0.85630E+00	0.10750E+02	0.77080E+00	0.0	0.0
2	3	0.99820E+00	0.10750E+02	0.40800E+00	0.0	0.0
2	4	0.11780E+01	0.10750E+02	0.20220E+00	0.0	0.0
2	5	0.13330E+01	0.10750E+02	0.11860E+00	0.0	0.0
2	6	0.14700E+01	0.10750E+02	0.76650E-01	0.0	0.0
2	7	0.16700E+01	0.10750E+02	0.42120E-01	0.0	0.0
2	8	0.20000E+01	0.10750E+02	0.16000E-01	0.0	0.0
2	9	0.22700E+01	0.10750E+02	0.65190E-02	0.0	0.0
2	10	0.24990E+01	0.10750E+02	0.21880E-02	0.0	0.0
2	11	0.26970E+01	0.10750E+02	0.53700E-05	0.0	0.0
2	12	0.28710E+01	0.10750E+02	0.11520E-02	0.0	0.0
2	13	0.30240E+01	0.10750E+02	0.17340E-02	0.0	0.0
2	14	0.31580E+01	0.10750E+02	0.20010E-02	0.0	0.0
2	15	0.32770E+01	0.10750E+02	0.20930E-02	0.0	0.0
2	16	0.33820E+01	0.10750E+02	0.20960E-02	0.0	0.0
2	17	0.34730E+01	0.10750E+02	0.20640E-02	0.0	0.0
2	18	0.35520E+01	0.10750E+02	0.20350E-02	0.0	0.0
2	19	0.36200E+01	0.10750E+02	0.20340E-02	0.0	0.0
2	20	0.36770E+01	0.10750E+02	0.20830E-02	0.0	0.0
2	21	0.37230E+01	0.10750E+02	0.21950E-02	0.0	0.0
2	22	0.37600E+01	0.10750E+02	0.23850E-02	0.0	0.0
2	23	0.37370E+01	0.10750E+02	0.26630E-02	0.0	0.0
2	24	0.38050E+01	0.10750E+02	0.30580E-02	0.0	0.0
2	25	0.38130E+01	0.10750E+02	0.34590E-02	0.0	0.0



K21	THETA	S1	RHOE	CMUE
0.0	0.11720E+01	0.0	0.26230E-02	0.33708E-06
0.0	0.11160E+01	0.45340E-01	0.26230E-02	0.33708E-06
0.0	0.10930E+01	0.87280E-01	0.26230E-02	0.33708E-06
0.0	0.10750E+01	0.14780E+00	0.26230E-02	0.33708E-06
0.0	0.10660E+01	0.20680E+00	0.26230E-02	0.33708E-06
0.0	0.10610E+01	0.26510E+00	0.26230E-02	0.33708E-06
0.0	0.10550E+01	0.36130E+00	0.26230E-02	0.33708E-06
0.0	0.10500E+01	0.55170E+00	0.26230E-02	0.33708E-06
0.0	0.10480E+01	0.74100E+00	0.26230E-02	0.33708E-06
0.0	0.10470E+01	0.92990E+00	0.26230E-02	0.33708E-06
0.0	0.10470E+01	0.11190E+01	0.26230E-02	0.33708E-06
0.0	0.10470E+01	0.13080E+01	0.26230E-02	0.33708E-06
0.0	0.10480E+01	0.14960E+01	0.26230E-02	0.33708E-06
0.0	0.10480E+01	0.16850E+01	0.26230E-02	0.33708E-06
0.0	0.10480E+01	0.18740E+01	0.26230E-02	0.33708E-06
0.0	0.10490E+01	0.20630E+01	0.26230E-02	0.33708E-06
0.0	0.10490E+01	0.22530E+01	0.26230E-02	0.33708E-06
0.0	0.10500E+01	0.24430E+01	0.26230E-02	0.33708E-06
0.0	0.10500E+01	0.26320E+01	0.26230E-02	0.33708E-06
0.0	0.10500E+01	0.28220E+01	0.26230E-02	0.33708E-06
0.0	0.10510E+01	0.30120E+01	0.26230E-02	0.33708E-06
0.0	0.10510E+01	0.32020E+01	0.26230E-02	0.33708E-06
0.0	0.10520E+01	0.33920E+01	0.26230E-02	0.33708E-06
0.0	0.10530E+01	0.35820E+01	0.26230E-02	0.33708E-06
0.0	0.10530E+01	0.37730E+01	0.26230E-02	0.33708E-06
0.0	0.11160E+01	0.0	0.26230E-02	0.33708E-06
0.0	0.10930E+01	0.45340E-01	0.26230E-02	0.33708E-06
0.0	0.10750E+01	0.87280E-01	0.26230E-02	0.33708E-06
0.0	0.10660E+01	0.14780E+00	0.26230E-02	0.33708E-06
0.0	0.10610E+01	0.20680E+00	0.26230E-02	0.33708E-06
0.0	0.10550E+01	0.26510E+00	0.26230E-02	0.33708E-06
0.0	0.10500E+01	0.36130E+00	0.26230E-02	0.33708E-06
0.0	0.10480E+01	0.55170E+00	0.26230E-02	0.33708E-06
0.0	0.10470E+01	0.74100E+00	0.26230E-02	0.33708E-06
0.0	0.10470E+01	0.92990E+00	0.26230E-02	0.33708E-06
0.0	0.10470E+01	0.11190E+01	0.26230E-02	0.33708E-06
0.0	0.10470E+01	0.13080E+01	0.26230E-02	0.33708E-06
0.0	0.10480E+01	0.14960E+01	0.26230E-02	0.33708E-06
0.0	0.10480E+01	0.16850E+01	0.26230E-02	0.33708E-06
0.0	0.10480E+01	0.18740E+01	0.26230E-02	0.33708E-06
0.0	0.10490E+01	0.20630E+01	0.26230E-02	0.33708E-06
0.0	0.10490E+01	0.22530E+01	0.26230E-02	0.33708E-06
0.0	0.10500E+01	0.24430E+01	0.26230E-02	0.33708E-06
0.0	0.10500E+01	0.26320E+01	0.26230E-02	0.33708E-06
0.0	0.10500E+01	0.28220E+01	0.26230E-02	0.33708E-06
0.0	0.10510E+01	0.30120E+01	0.26230E-02	0.33708E-06
0.0	0.10510E+01	0.32020E+01	0.26230E-02	0.33708E-06
0.0	0.10520E+01	0.33920E+01	0.26230E-02	0.33708E-06
0.0	0.10520E+01	0.35820E+01	0.26230E-02	0.33708E-06
0.0	0.10530E+01	0.37730E+01	0.26230E-02	0.33708E-06

The printout of the boundary-layer program is shown below for a few representative chordwise stations together with a summary table containing the boundary-layer parameters.

ORIGINAL PAGE IS  
OF POOR QUALITY

THREE-D BOUNDARY-LAYER PROGRAM  
 FOR INCOMPRESSIBLE AND COMPRESSIBLE LAMINAR AND TURBULENT FLOWS  
 0017-LOWER SURFACE, 30 DEG, NEUM. AL = R.0

NXSTRT= 1                    NZSTRT= 1                    NXT = 25  
 NZT = 77                    NTR = 7                    IFLCN = 1  
 ICHORD= 2                    ICMP = 1                    ISPAN = 1  
 IFRNT= 1                    ETAC = 8.(C000)                    DETA = 0.01000  
 VGP = 1.26C00                    FFRS = 0.455CCCF+03                    PFRS = 0.204800E+04  
 UFPS = 0.200C00E+03                    VFPS = 0.0                    MFRS = 0.337078E-06  
 RHUFRS= 0.262302E-02                    IT = 0.455C00F+03

\*\*\*\*\*----- CUTBOARD CALCULATIONS STARTED -----\*\*\*\*\*

\*\*\*\* N1 = 1    N2 = 1    X = 0.142    Y = 0.0    X/C = 0.010

\*\* STAGNATION LINE EQUATIONS \*\*

\*\* 7-PRESSURES=A \*\*

\*\* X-PRESSURES=A \*\*

	V(HALL)	DFLV(1)	T(WALL)	DELTA(1)
1	0.332000E+00	0.108223E+01	0.332000E+00	0.104885E+00
2	0.141423E+01	-0.17354CE+00	0.436885E+00	-0.216905E+00
3	0.123589E+01	-0.127121E-01	0.226981E+00	-0.182313E-01
4	0.122237E+01	-0.958165E-04	0.207449E+00	-0.226131E-03
5	0.122238E+01	0.406281E-06	0.207622E+00	0.110748E-04

J	ETA	Y	F	U	V	G	X	T	B
1	0.0	0.0	0.0	0.0	0.122288E+01	0.0	0.0	0.207622E+00	0.100000E+01
4	0.038476	0.0	0.895231E-03	0.463710E-01	0.118492E+01	0.151591E-03	0.793168E-02	0.207265E+00	0.100000E+01
7	0.115442	0.0	0.790066E-03	0.134607E+00	0.110931E+01	0.138102E-02	0.239049E-01	0.206488E+00	0.100000E+01
10	0.269404	0.0	0.411373E-01	0.293493E+00	0.761533E+00	0.750066E-02	0.554236E-01	0.204337E+00	0.100000E+01
13	0.577386	0.0	0.172573E+00	0.547387E+00	0.690440E+00	0.341721E-01	0.117251E+00	0.195247E+00	0.100000E+01
16	1.19446	0.0	0.411438E+00	0.341817E+00	0.296340E+00	0.140917E+00	0.222174E+00	0.149790E+00	0.100000E+01
19	2.425854	0.0	0.177119E+01	0.91832E+00	0.219712E-01	0.497481E+00	0.351550E+00	0.302389E-01	0.100000E+01
22	4.891097	0.0	0.422353E+01	0.10003E+01	0.226536E-04	0.133731E+01	0.339987E+00	-0.257746E-02	0.100000E+01
24	7.787767	0.0	0.112017E+01	0.100000E+01	0.118875E-04	0.231426E+01	0.334920E+00	-0.132165E-02	0.100000E+01

J	ETA	SVC	CVC	US/USE	BETA
1	0.0	0.0	0.0	0.0	0.0
4	0.038476	0.238316E-01	0.483210E-01	0.239316E-01	0.0
7	0.115442	0.713340E-01	0.134607E+00	0.713340E-01	0.0
10	0.269404	0.165838E+00	0.293493E+00	0.165838E+00	0.0
13	0.577386	0.35683E+00	0.547387E+00	0.350088E+00	0.0
16	1.19446	0.72732E+00	0.341817E+00	0.672121E+00	0.0
19	2.425854	0.989938E+00	0.91832E+00	0.535938E+00	0.0
22	4.891097	0.101511E+01	0.10003E+01	0.101511E+01	0.0
24	7.787767	0.100000E+01	0.100000E+01	0.100000E+01	0.0

P1	P2	P3	P4	P5	P6	P7	P8	P9
0.100000E+01	0.100000E+01	0.0	0.0	-0.390160E-01	0.216369E-01	0.933188E-02	0.0	0.0
0.0	0.586933E+00	0.725261E-02						

BODY GEOMETRY FROM STORED DATA SET

S1 = 0.0	THETA = 0.11720CF+01	H1 = 0.686000E+00	H2 = 0.107500E+02	K1 = 0.190600E+01
K2 = 0.0	X12 = 0.0	X21 = 0.0	UF = 0.0	WE = 0.669840E+02
RH0 = 0.262302E-02	CMUF = 0.337078E-06			
CFL = 0.0	GLSIS = 0.0	THIAS = 0.0	BETA1 = 0.0	
CFN = 0.0	GLSIN = 0.0	THAN = 0.0	RY = 0.0	
USE = 0.669840E+02	BUSED = 0.154943E+02			

\*\*\* NX = 25 N2 = 2 X = 1.561 Z = 0.152 X/C = 0.990

\*\* GENERAL CASE \*\*

\*\* J-PRESSURES=B \*\*

\*\* X-PRESSURES=C \*\*

	V(WALL)	DELTV	T(WALL)	DELTT
1	0.255010E+01	-0.731784E+00	0.161103E+00	-0.363107E+00
2	0.181832E+01	-0.151914E+00	0.524710E+00	-0.140943E-01

J	ETA	Y	F	U	V	G	W	T	B
1	0.0	0.0	0.0	0.0	0.166440E+01	0.0	0.0	0.510126E+00	0.100000E+01
4	0.038476	0.762010E-03	0.125821E-02	0.658977E-01	0.178086E+01	0.365173E-03	0.186299E-01	0.459522E+00	0.101151E+01
7	0.118442	0.228632E-02	0.112474E-01	0.188629E+00	0.131732E+01	0.297451E-02	0.467734E-01	0.256688E+00	0.149506E+01
10	0.269404	0.533551E-02	0.516102E-01	0.317713E+00	0.508862E+00	0.120977E-01	0.674328E-01	0.603803E-01	0.446634E+01
13	0.577386	0.114350E-01	0.16015E+00	0.411129E+00	0.183544E+00	0.344442E-01	0.755022E-01	0.889598E-02	0.146993E+02
16	1.193465	0.236364E-01	0.44455E+00	0.484186E+00	0.87742E-01	0.816778E-01	0.770198E-01	-0.70870E-03	0.392553E+02
19	2.425954	0.430438E-01	0.128189E+01	0.254500E+00	0.341505E-01	0.175446E+00	0.743972E-01	-0.204275E-03	0.328898E+02
22	4.891097	0.866633E-01	0.255600E+01	0.628508E+00	0.21754E-01	0.54252E+00	0.705125E-01	-0.148544E-02	0.204889E+03
25	9.822512	0.194533E+00	0.585157E+01	0.724388E+00	0.186817E-01	0.685694E+00	0.635277E-01	-0.123315E-02	0.236678E+03
28	19.687195	0.389901E+00	0.138441E+02	0.631942E+00	0.125999E-01	0.126747E+01	0.246110E-01	-0.928029E-03	0.236678E+03
31	39.420258	0.737111E+00	0.27459E+02	0.598648E+00	0.327614E-01	0.230658E+01	0.516443E-01	0.47474E-02	0.236678E+03
32	49.679535	0.933895E+00	0.42583E+02	0.100000E+01	-0.564101E-03	0.273701E+01	0.420170E-01	-0.662455E-02	0.236678E+03

J	ETA	SV	CVC	LS/USE	QETA
1	0.0	0.0	0.0	0.0	0.144595E+02
4	0.038476	0.445054E+00	0.74430E-01	0.767226E-01	0.135699E+02
7	0.118442	0.111220E+01	0.214556E+00	0.214556E+00	0.121143E+03
10	0.269404	0.160409E+01	0.517395E+00	0.533128E+00	0.109299E+02
13	0.577386	0.175694E+01	0.442096E+00	0.449649E+00	0.922333E+01
16	1.193465	0.23306E+01	0.515291E+00	0.520180E+00	0.519464E+01
19	2.425954	0.178306E+01	0.227E49E+00	0.568292E+00	0.706283E+01
22	4.891097	0.167810E+01	0.652105E+00	0.55051E+00	0.593854E+01
25	9.822512	0.152147E+01	0.742770E+00	0.744708E+00	0.474022E+01
28	19.687195	0.129073E+01	0.891675E+00	0.87246E+00	0.317715E+01
31	39.420258	0.122913E+01	0.100356E+01	0.100437E+01	0.283730E+01
32	49.679535	0.555999E+00	0.100000E+01	0.100000E+01	0.221816E+01

P1	P2	P3	P4	P5	P6	P7	P8	P9
-0.483658E+00	-0.27929E+01	0.0	0.0	0.213182E+00	-0.977936E-01	0.394341E+00	0.0	-0.131001E-01
0.979544E+00	-0.279331E+01	0.115021E+01						

PIH	P2B	P3B	P4B	P5B	P6B	P7B	P8B	P9B
-0.461127E+00	-0.174427E+01	0.0	0.0	0.929685E-01	-0.434955E-01	0.369744E+00	0.0	-0.126372E-01
0.960458E+00	-0.174179E+01	0.749920E+00						

BODY GEOMETRY FROM STORED DATA SET  
 S1 = 0.373503E+01 THETA = 0.105300E+01 H1 = 0.381300E+01 H2 = 0.107500E+02 K1 = -0.345900E-02  
 K2 = 0.0 K12 = 0.0 UE = 0.176214E+03 ME = 0.840340E+01  
 RHOE = 0.262302E-02 CPLE = 0.337378E-06  
 CFC = 0.123845E-02 DLSTS = 0.101387E-01 THTAS = 0.702579E-02 BETAL = 0.144595E+02  
 CFN = 0.34138E-03 DLSTN = -0.27406E-01 THTAN = -0.40431E-01 RX = 0.512155E+07  
 USE = 0.183571E-03 DUSEC = -0.952150E+02

.DLSS = 0.100772E-01 TSS = 0.699259E-02 TH21 = -0.885350E-03

\*\*\*\* SUMMARY TABLE \*\*\*\*

NX	X/C	VWALL	TWALL	CFC	CFN	BETA	DLSTS	DLSTN	THTAS	THTAN	RX
1	0.1000E-01	0.1239E+01	0.1954E+00	0.0	0.0	0.0	0.0	0.0	0.0	0.0	0.0
2	0.2000E-01	0.1187E+01	0.1175E+00	0.2364E-02	0.4651E-03	0.1113E+02	0.2584E-03	0.4043E-03	0.1245E-03	0.1601E-03	0.2691E+05
3	0.3000E-01	0.1197E+01	0.4560E-01	0.2572E-02	0.2424E-03	0.5386E+01	0.3513E-03	0.6975E-03	0.1844E-03	0.2456E-03	0.7053E+05
4	0.4000E-01	0.1304E+01	0.3924E-01	0.2625E-02	0.1149E-03	0.2326E+01	0.4752E-03	0.9753E-03	0.2747E-03	0.3988E-03	0.1486E+06
5	0.6000E-01	0.1430E+01	0.2075E-01	0.2573E-02	0.5387E-04	0.1038E+01	0.5866E-03	0.1379E-02	0.3588E-03	0.5433E-03	0.2283E+06
6	0.7500E-01	0.1435E+01	0.5031E-02	0.3058E-02	0.2136E-04	0.6001E+00	0.6978E-03	0.1849E-02	0.4423E-03	0.6963E-03	0.3129E+06
7	0.1100E+00	0.1732E+01	0.4212E-02	0.3030E-02	0.310E-04	0.3183E+00	0.9378E-03	0.6934E-02	0.2768E-03	0.8989E-03	0.4555E+06
8	0.1500E+00	0.1732E+01	-0.3567E-01	0.3044E-02	0.310E-04	0.1003E+01	0.1239E-02	0.6986E-02	0.8277E-03	0.8989E-03	0.7499E+06
9	0.2000E+00	0.1874E+01	-0.3657E-01	0.2554E-02	0.5940E-04	0.1134E+01	0.1571E-02	0.9382E-02	0.1079E-02	0.1331E-02	0.1051E+07
10	0.2500E+00	0.2040E+01	-0.3945E-01	0.3031E-02	0.5489E-04	0.1038E+01	0.1890E-02	0.1446E-01	0.1330E-02	0.6092E-02	0.1352E+07
11	0.3000E+00	0.2177E+01	-0.3910E-01	0.3066E-02	0.5033E-04	0.9472E+00	0.2705E-02	0.2097E-01	0.1583E-02	0.1670E-01	0.1655E+07
12	0.3500E+00	0.2279E+01	-0.3866E-01	0.2584E-02	0.4602E-04	0.1188E+01	0.2561E-02	0.2985E-01	0.1843E-02	0.3190E-01	0.1952E+07
13	0.4000E+00	0.2380E+01	-0.3702E-01	0.2572E-02	0.4250E-04	0.8249E+00	0.2895E-02	0.4172E-01	0.2100E-02	0.6420E-01	0.2256E+07
14	0.4500E+00	0.2474E+01	-0.3716E-01	0.2911E-02	0.3926E-04	0.7727E+00	0.3226E-02	0.5736E-01	0.2535E-02	0.1219E+00	0.2557E+07
15	0.5000E+00	0.2551E+01	-0.4636E-01	0.2876E-02	0.3652E-04	0.7275E+00	0.3569E-02	0.7971E-01	0.2618E-02	0.2709E+00	0.2857E+07
16	0.5500E+00	0.2619E+01	-0.3557E-01	0.2828E-02	0.3477E-04	0.6902E+00	0.3912E-02	0.1104E+00	0.2881E-02	0.4236E+00	0.3159E+07
17	0.6000E+00	0.2681E+01	-0.3450E-01	0.2785E-02	0.3169E-04	0.6511E+00	0.4256E-02	0.1516E+00	0.3147E-02	0.7727E+00	0.3452E+07
18	0.6500E+00	0.2713E+01	-0.3761E-01	0.2745E-02	0.2969E-04	0.6195E+00	0.4604E-02	0.2001E+00	0.3412E-02	0.1288E+01	0.3745E+07
19	0.7000E+00	0.2822E+01	-0.2499E-01	0.2672E-02	0.2807E-04	0.5975E+00	0.4956E-02	0.2740E+00	0.3689E-02	0.2319E+01	0.4036E+07
20	0.7500E+00	0.282E+01	-0.3116E-01	0.2622E-02	0.2723E-04	0.5883E+00	0.5315E-02	0.4634E+00	0.3958E-02	0.4647E+01	0.4323E+07
21	0.8000E+00	0.2906E+01	-0.327E-01	0.2558E-02	0.2612E-04	0.5759E+00	0.5709E-02	0.1353E+01	0.4250E-02	0.5414E+01	0.4606E+07
22	0.8500E+00	0.2922E+01	-0.2865E-01	0.2522E-02	0.2205E-04	0.5008E+00	0.6135E-02	0.1134E+01	0.4572E-02	0.3676E+01	0.4878E+07
23	0.9100E+00	0.2968E+01	-0.2754E-01	0.2418E-02	0.2520E-05	0.1545E+00	0.6635E-02	0.9481E-01	0.4934E-02	0.2050E+01	0.5126E+07
24	0.9500E+00	0.2950E+01	0.1611E+00	0.2092E-02	0.1158E-05	0.3184E+01	0.7455E-02	0.9522E-01	0.5435E-02	0.2709E+01	0.5323E+07
25	0.9900E+00	0.1764E+01	0.2101E+00	0.1338E-02	0.3451E-05	0.1446E+02	0.1014E-01	-0.2746E-01	0.7026E-02	0.4043E-01	0.5122E+07

### Test Case 3

This test case represents the most general case that can be calculated by the program: the wing plan form is arbitrary, the wing has twist, and the pressure distribution is from experimental data. The wing selected for this case has a planform and dimensions similar to that given in figure 4 of reference 8 except that its trailing edge is straight, as shown in figure 17 of reference 1. Also, in our coordinate system the wing root is at  $\bar{y} = 30$  inches, corresponding to the  $z = 0$  degree plane in reference 8. The wing has a 220.42-inch root chord, 40-inch tip chord (which is at  $\bar{y} = 280$  inches). The 6-degree twist was generated by a linear variation of the trailing-edge height over the  $\bar{x}\bar{y}$ -plane, the leading edge of the wing remained on the  $\bar{x}\bar{y}$ -plane over its entire length. Thickness distribution was generated by supercritical airfoils of 12.38-percent thickness at the root, and 9.24-percent thickness at the tip, and with a parabolic variation in between. The airfoil coordinates were generated by a separate program and then fed into the geometry program.

The calculations were made for the upper surface at Mach numbers of  $M_\infty = 0.5$  and  $M_\infty = 0.99$ , with the experimental pressure distribution given in reference 8 as Table III-230 and Table III-28, respectively. The unit Reynolds number in both cases was  $1.5 \times 10^6$ /foot and transition was assumed to be at  $x/c = 0.10$ . The inviscid velocity components were obtained from the velocity program by the procedure described in Appendix A of reference 1. Since the experimental pressure distribution does not extend over the entire chord-length, boundary-layer calculations were started at  $x/c = 0.025$  and continued up to  $x/c = 0.975$ . The spanwise extent of calculations is from  $\bar{y} = 30$  inches to  $\bar{y} = 260$  inches and was again limited by the available pressure measurements. Note that the pressure distribution for the root section was obtained by extrapolating the experimental data. In terms of the boundary-layer coordinate  $z$ ,  $\bar{y} = 30$  inches corresponds to  $z = 0$  and  $\bar{y} = 260$  inches to  $z = 0.92$ , respectively.

The input and output data for  $M_\infty = 0.99$  and  $M_\infty = 0.50$  are similar. For this reason we only show the load sheets for  $M_\infty = 0.99$ .

For this test case we present a sample of the load sheets for both geometry and velocity programs as well as the boundary-layer program. The case data and the station data are shown for a few chordwise stations at the root section.

Load Sheets for the Geometry Program

Case Data

Card 1

1	2	3	4	5	6	7	8	9	10	11	12	13	14	15	16	17	18	19	20	21	22	23	24	25	26	27	28	29	30
TITLE																													
SUPERCRIT.															UPPER SURFACE														

Card 2

\$INPUT IY = 14, NC = 24, NS = 29, IFLG = 0, NT = 4, IPUNCH = 1, SB = .0833333,  
 SP = 20.83333, RL = 1.0\$

Card 3

1	2	3	4	5	6	7	8	9	10	11	12	13	14	15	16	17	18	19	20	21	22	23	24	25	26	27	28	29	30	31	32	33	34	35	36	37	38	39	40
YI					YI					YI					YI																								
30.0					40.0					50.0					60.0																								

41	42	43	44	45	46	47	48	49	50	51	52	53	54	55	56	57	58	59	60
YI										YI									
75.0										90.0									

Card 4

1	2	3	4	5	6	7	8	9	10	11	12	13	14	15	16	17	18	19	20	21	22	23	24	25	26	27	28	29	30	31	32	33	34	35	36	37	38	39	40
CX					CX					CX					CX																								
0.005					0.0075					0.015					0.025																								

41	42	43	44	45	46	47	48	49	50	51	52	53	54	55	56	57	58	59	60
CX										CX									
0.05										0.1									

Card 5

1	2	3	4	5	6	7	8	9	10	11	12	13	14	15	16	17	18	19	20	21	22	23	24	25	26	27	28	29	30	31	32	33	34	35	36	37	38	39	40
CY					CY					CY					CY																								
30.0					35.0					40.0					45.0																								

41	42	43	44	45	46	47	48	49	50	51	52	53	54	55	56	57	58	59	60
CY										CY									
50.0										55.0									

Station Data

Card 1

1	2	3	4	5	6	7	8	9	10	11	12	13	14	15	16	17	18	19	20	21	22	23	24	25	26	27	28	29	30	31	32	33	34	35	36
NP		NN		CL					XLE					ZLE																					
23		3		0.0833333					0.0					0.00003																					

37	38	39	40	41	42	43	44	45	46	47	48	49	50	51	52	53	54	55	56
XTE										ZTE									
220.4101										0.0									

Card 2

1	2	3	4	5	6	7	8	9	10	11	12	13	14	15	16	17	18	19	20	21	22	23	24	25	26	27	28	29	30	31	32	33	34	35	36	37	38	39	40
XI					XI					XI					XI																								
5.39405					1.35685					0.0					1.35689																								

41	42	43	44	45	46	47	48	49	50	51	52	53	54	55	56	57	58	59	60
XI										XI									
5.39413										12.01231									

Card 3

1	2	3	4	5	6	7	8	9	10	11	12	13	14	15	16	17	18	19	20	21	22	23	24	25	26	27	28	29	30	31	32	33	34	35	36	37	38	39	40
ZI					ZI					ZI					ZI																								
-7.36559					-4.13312					0.00003					3.75572																								

41	42	43	44	45	46	47	48	49	50	51	52	53	54	55	56	57	58	59	60
ZI										ZI									
6.45484										8.32452									

Load Sheets for the External Velocity Program

Case Data

Card 1

1	2	3	4	5	6	7	8	9	10	11	12	13	14	15	16	17	18	19	20	21	22	23	24	25	26	27	28	29	30
TITLE																													
S,U,P.,C,R,I,T.,M.,=.0.,99																													

Card 2

\$INPUT IY = 7, NC = 21, NS = 29, IFLG = 1, FM = .99, AL = .0, SP = 20.8333,  
 SB = .0833333, CR = 18.3684, CT = 3.91667, NI = 5\$

Card 3

1	2	3	4	5	6	7	8	9	10	11	12	13	14	15	16	17	18	19	20	21	22	23	24	25	26	27	28	29	30	31	32	33	34	35	36	37	38	39	40
YI					YI					YI					YI																								
30.0					37.24					85.96					134.4																								
41	42	43	44	45	46	47	48	49	50	51	52	53	54	55	56	57	58	59	60																				
YI										YI																													
182.84										225.12																													

Card 4

1	2	3	4	5	6	7	8	9	10	11	12	13	14	15	16	17	18	19	20	21	22	23	24	25	26	27	28	29	30	31	32	33	34	35	36	37	38	39	40
CX					CX					CX					CX																								
0.025					0.05					0.1					0.15																								
41	42	43	44	45	46	47	48	49	50	51	52	53	54	55	56	57	58	59	60																				
CX										CX																													
0.2										0.25																													

Card 5

1	2	3	4	5	6	7	8	9	10	11	12	13	14	15	16	17	18	19	20	21	22	23	24	25	26	27	28	29	30	31	32	33	34	35	36	37	38	39	40
CY										CY										CY										CY									
30.0										35.0										40.0										45.0									

41	42	43	44	45	46	47	48	49	50	51	52	53	54	55	56	57	58	59	60
CY										CY									
50.0										55.0									

Geometry Data

Card 1

1	2	3
NP		
21		

Card 2

1	2	3	4	5	6	7	8	9	10	11	12	13	14	15	16	17	18	19	20	21	22	23	24	25	26	27	28	29	30	31	32	33	34	35	36	37	38	39	40
XI										XI										XI										XI									
0.025										0.05										0.10										0.15									

41	42	43	44	45	46	47	48	49	50	51	52	53	54	55	56	57	58	59	60
XI										XI									
0.20										0.25									

Card 3

1	2	3	4	5	6	7	8	9	10	11	12	13	14	15	16	17	18	19	20	21	22	23	24	25	26	27	28	29	30	31	32	33	34	35	36	37	38	39	40
P										P										P										P									
-0.125										-0.16										-0.23										-0.29									

41	42	43	44	45	46	47	48	49	50	51	52	53	54	55	56	57	58	59	60
P										P									
-0.34										-0.38									



Load Sheets for the Boundary-Layer Program

Card 1

1	2	3	4	5	6	7	8	9	10	11	12	13	14	15	16	17	18	19	20	21	22	23	24	25	26	27	28	29	30	31	32	33	34	35	36	37	38	39	40
TITLE																																							
SUPER CRITICAL WING																				MACH NO. = 0.99																			

Card 2

\$NAME, NXSTRT = 1, NZSTRT = 29, NXT = 21, NZT = 1, NTR = 3, IFLOW = 2,  
 ICHORD = 1, ICMP = 2, ISPAN = 1, IFPRNT = 1, VGP = 1.26, DELTA(1) = .05,  
 ITMAX = 10, EPS = 1.0E-04, IPZ = 4, IPX = 4, EPSV = .1, EPST = .1\$

Card 3

1	2	3	4	5	6	7	8	9	10	11	12	13	14	15	16	17	18	19	20	21	22	23	24	25	26	27	28	29	30	31	32	33	34	35	36
TFRS										UFRS or CMFRS										PFRS															
+				3	9	0	.	E	+	00	+					0	.	99	E	+	00	+		3	1	1	.	1	8	8	E	+	00		

The external velocity data and the geometry data are shown for two spanwise stations:

\*\* EXTERNAL VELOCITY DISTRIBUTION (FT/SEC) \*\*

Z	X	UE	WE
0.0			
1	0.224076E+00	0.101814E+04	-0.343258E-12
2	0.317560E+00	0.103498E+04	-0.652243E-12
3	0.451027E+00	0.106983E+04	-0.142484E-11
4	0.554311E+00	0.109809E+04	-0.192607E-11
5	0.643501E+00	0.112269E+04	-0.231155E-11
6	0.722734E+00	0.114255E+04	-0.261288E-11
7	0.795399E+00	0.115004E+04	-0.273111E-11
8	0.863212E+00	0.115254E+04	-0.277449E-11
9	0.927295E+00	0.114354E+04	-0.272335E-11
10	0.988432E+00	0.113506E+04	-0.259237E-11
11	0.104720E+01	0.112517E+04	-0.259854E-11
12	0.110403E+01	0.111936E+04	-0.219056E-11
13	0.115928E+01	0.109975E+04	-0.191313E-11
14	0.121323E+01	0.107029E+04	-0.162157E-11
15	0.126610E+01	0.105333E+04	-0.137727E-11
16	0.131812E+01	0.103980E+04	-0.558219E-12
17	0.136944E+01	0.103161E+04	-0.520719E-12
18	0.142023E+01	0.103498E+04	-0.528049E-12
19	0.147063E+01	0.105187E+04	-0.621477E-12
20	0.152077E+01	0.106883E+04	-0.707371E-12
21	0.154579E+01	0.104463E+04	-0.519020E-12
0.200000E-01			
1	0.224075E+00	0.104261E+04	-0.253697E+00
2	0.317560E+00	0.106927E+04	-0.257529E+02
3	0.451027E+00	0.110926E+04	-0.450475E+02
4	0.554311E+00	0.114344E+04	-0.573850E+02
5	0.643501E+00	0.117030E+04	-0.659875E+02
6	0.722734E+00	0.118409E+04	-0.698695E+02
7	0.795399E+00	0.118578E+04	-0.697134E+02
8	0.863212E+00	0.118207E+04	-0.676700E+02
9	0.927295E+00	0.117228E+04	-0.637385E+02
10	0.988432E+00	0.116089E+04	-0.592967E+02
11	0.104720E+01	0.114435E+04	-0.533763E+02
12	0.110403E+01	0.112571E+04	-0.469450E+02
13	0.115928E+01	0.110587E+04	-0.403006E+02
14	0.121323E+01	0.108709E+04	-0.340854E+02
15	0.126610E+01	0.106907E+04	-0.282179E+02
16	0.131812E+01	0.105409E+04	-0.232193E+02
17	0.136944E+01	0.104863E+04	-0.204551E+02
18	0.142023E+01	0.105562E+04	-0.201344E+02
19	0.147063E+01	0.106921E+04	-0.205093E+02
20	0.152077E+01	0.107978E+04	-0.195285E+02
21	0.154579E+01	0.104926E+04	-0.129109E+02

ORIGINAL PAGE 1  
OF POOR QUALITY

\*\* INPUT WING GEOMETRY \*\*

NZ	NX	H1	H2	K1	K2	K1Z
1	1	0.44000E+01	0.84560E+02	0.51690E+00	0.33830E-02	0.18350E+00
1	2	0.58680E+01	0.82890E+02	0.19050E+00	0.49020E-02	0.17160E+00
1	3	0.80490E+01	0.79560E+02	0.48240E-01	0.65760E-02	0.57260E-01
1	4	0.96900E+01	0.76230E+02	0.15470E-01	0.77720E-02	0.47250E-01
1	5	0.11020E+02	0.72910E+02	0.62650E-02	0.86980E-02	0.47840E-01
1	6	0.12150E+02	0.69600E+02	0.35390E-02	0.95650E-02	0.52340E-01
1	7	0.13120E+02	0.66300E+02	0.17860E-02	0.10440E-01	0.54310E-01
1	8	0.13960E+02	0.63020E+02	0.13300E-02	0.11380E-01	0.58280E-01
1	9	0.14700E+02	0.59750E+02	0.76300E-03	0.12380E-01	0.61250E-01
1	10	0.15350E+02	0.56520E+02	0.63440E-03	0.13460E-01	0.65420E-01
1	11	0.15920E+02	0.53310E+02	0.36330E-03	0.14630E-01	0.69360E-01
1	12	0.16420E+02	0.50130E+02	0.31770E-03	0.15870E-01	0.74230E-01
1	13	0.16860E+02	0.46990E+02	0.14190E-03	0.17150E-01	0.79320E-01
1	14	0.17250E+02	0.43910E+02	0.11230E-04	0.18420E-01	0.85330E-01
1	15	0.17570E+02	0.40880E+02	0.32200E-03	0.19570E-01	0.91900E-01
1	16	0.17850E+02	0.37930E+02	0.72830E-03	0.20400E-01	0.99430E-01
1	17	0.18090E+02	0.35070E+02	0.12790E-02	0.20550E-01	0.10770E+00
1	18	0.18290E+02	0.32340E+02	0.17100E-02	0.19500E-01	0.11680E+00
1	19	0.18450E+02	0.29750E+02	0.17420E-02	0.16280E-01	0.12630E+00
1	20	0.18550E+02	0.27390E+02	0.11790E-02	0.11050E-01	0.13180E+00
1	21	0.18570E+02	0.26300E+02	0.30370E-03	0.60440E-02	0.13710E+00
2	1	0.40740E+01	0.80530E+02	0.54610E+00	0.40850E-02	0.19610E+00
2	2	0.54370E+01	0.73930E+02	0.19910E+00	0.58910E-02	0.17940E+00
2	3	0.74600E+01	0.75860E+02	0.45640E-01	0.76910E-02	0.60920E-01
2	4	0.89810E+01	0.72750E+02	0.15880E-01	0.90010E-02	0.51570E-01
2	5	0.10220E+02	0.69640E+02	0.64190E-02	0.10010E-01	0.52190E-01
2	6	0.11260E+02	0.66550E+02	0.36700E-02	0.10960E-01	0.56890E-01
2	7	0.12160E+02	0.63470E+02	0.18430E-02	0.11920E-01	0.58920E-01
2	8	0.12940E+02	0.60400E+02	0.13800E-02	0.12930E-01	0.63010E-01
2	9	0.13620E+02	0.57360E+02	0.78030E-03	0.14000E-01	0.68040E-01
2	10	0.14220E+02	0.54340E+02	0.65240E-03	0.15150E-01	0.73280E-01
2	11	0.14750E+02	0.51340E+02	0.36590E-03	0.16360E-01	0.74250E-01
2	12	0.15220E+02	0.48390E+02	0.32160E-03	0.17640E-01	0.79150E-01
2	13	0.15620E+02	0.45460E+02	0.13610E-03	0.18920E-01	0.84180E-01
2	14	0.15980E+02	0.42590E+02	0.26390E-03	0.20170E-01	0.90090E-01
2	15	0.16280E+02	0.39780E+02	0.34810E-03	0.21220E-01	0.96500E-01
2	16	0.16540E+02	0.37040E+02	0.78090E-03	0.21890E-01	0.10380E+00
2	17	0.16770E+02	0.34390E+02	0.13800E-02	0.21790E-01	0.11170E+00
2	18	0.16950E+02	0.31850E+02	0.18890E-02	0.20420E-01	0.12040E+00
2	19	0.17100E+02	0.29460E+02	0.20080E-02	0.16810E-01	0.12930E+00
2	20	0.17190E+02	0.27250E+02	0.14670E-02	0.11260E-01	0.13450E+00
2	21	0.17220E+02	0.26230E+02	0.52700E-03	0.60880E-02	0.13970E+00

K21	THETA	S1	RHOE	C MUE
0.163401+00	0.47610E+00	0.0	0.43614E-03	0.29071E-06
0.15103E+00	0.35273E+00	0.47993E+00	0.42793E-03	0.28885E-06
0.54483E-01	0.30169E+00	0.14083E+01	0.41131E-03	0.28500E-06
0.45020E-01	0.29430E+00	0.23293E+01	0.39685E-03	0.28155E-06
0.45530E-01	0.29950E+00	0.32473E+01	0.38463E-03	0.27856E-06
0.49650E-01	0.31003E+00	0.41663E+01	0.37475E-03	0.27609E-06
0.51310E-01	0.32350E+00	0.50843E+01	0.37101E-03	0.27514E-06
0.54760E-01	0.33950E+00	0.60023E+01	0.36977E-03	0.27483E-06
0.57170E-01	0.35780E+00	0.69203E+01	0.37176E-03	0.27533E-06
0.60570E-01	0.37863E+00	0.78383E+01	0.37648E-03	0.27653E-06
0.63550E-01	0.40220E+00	0.87573E+01	0.38340E-03	0.27826E-06
0.67250E-01	0.42890E+00	0.96753E+01	0.39076E-03	0.28007E-06
0.70830E-01	0.45940E+00	0.10595E+02	0.40048E-03	0.28243E-06
0.74830E-01	0.49440E+00	0.11515E+02	0.41059E-03	0.28483E-06
0.78780E-01	0.53490E+00	0.12435E+02	0.41894E-03	0.28678E-06
0.82760E-01	0.58220E+00	0.13355E+02	0.42557E-03	0.28831E-06
0.86190E-01	0.63790E+00	0.14275E+02	0.42957E-03	0.28922E-06
0.88710E-01	0.70380E+00	0.15205E+02	0.42793E-03	0.28885E-06
0.89040E-01	0.78170E+00	0.16125E+02	0.41965E-03	0.28694E-06
0.84610E-01	0.87310E+00	0.17055E+02	0.41131E-03	0.28500E-06
0.82150E-01	0.92420E+00	0.17525E+02	0.42320E-03	0.28776E-06
0.17430E+00	0.48070E+00	0.0	0.42431E-03	0.28802E-06
0.16790E+00	0.36120E+00	0.44460E+00	0.42291E-03	0.28770E-06
0.57350E-01	0.31310E+00	0.13056E+01	0.41246E-03	0.28527E-06
0.49170E-01	0.30710E+00	0.21586E+01	0.40141E-03	0.28265E-06
0.49580E-01	0.31310E+00	0.30096E+01	0.39208E-03	0.28039E-06
0.53870E-01	0.32410E+00	0.38606E+01	0.38692E-03	0.27913E-06
0.55540E-01	0.33820E+00	0.47116E+01	0.38580E-03	0.27885E-06
0.59050E-01	0.35460E+00	0.55626E+01	0.38654E-03	0.27903E-06
0.61460E-01	0.37330E+00	0.64136E+01	0.38936E-03	0.27973E-06
0.64850E-01	0.39450E+00	0.72645E+01	0.39274E-03	0.28055E-06
0.67820E-01	0.41840E+00	0.81166E+01	0.39799E-03	0.28182E-06
0.71380E-01	0.44540E+00	0.89675E+01	0.40405E-03	0.28328E-06
0.74790E-01	0.47810E+00	0.98196E+01	0.41063E-03	0.28484E-06
0.78560E-01	0.51110E+00	0.10670E+02	0.41689E-03	0.28630E-06
0.82180E-01	0.55140E+00	0.11530E+02	0.42295E-03	0.28771E-06
0.85750E-01	0.59810E+00	0.12380E+02	0.42793E-03	0.28885E-06
0.88640E-01	0.65270E+00	0.13230E+02	0.42916E-03	0.28913E-06
0.90620E-01	0.71670E+00	0.14090E+02	0.42522E-03	0.28823E-06
0.90390E-01	0.79190E+00	0.14950E+02	0.41811E-03	0.28659E-06
0.85820E-01	0.87920E+00	0.15310E+02	0.41200E-03	0.28516E-06
0.83330E-01	0.92770E+00	0.16240E+02	0.42471E-03	0.28811E-06

The printout of the boundary-layer program is shown below for a few representative chordwise stations together with a summary table containing the boundary-layer parameters.

THPEL-D BOUNDARY-LAYER PROGRAM  
 FOR INCOMPRESSIBLE AND COMPRESSIBLE LAMINAR AND TURBULENT FLOWS  
 SUPER CRITICAL WING MACH No. = 0.99

```

NXSTRT= 1          NZSTRT= 25          NXT = 21
NRT = 1           NTF = 3             IFLOW = 2
ICMORD= 1        ICOMP = 2          ISPAN = 1
IFPRINT= 1       ETAF = P.00000     DELTA = 0.05000
VGP = 1.26000    TFFS = 0.39000E+03 PFFS = 0.311188E+03
UFRS = 0.958191E+03 MFFS = C.99000E+00 MUFSS = 0.297031E+06
WDRFS = 0.4649E7E-03 TT = C.416447E+03
  
```

\*\*\*\*\* INWARD CALCULATIONS STARTED \*\*\*\*\*

\*\*\* NX = 1 N7 = 2% X = 0.224 Z = 0.920 X/C = 0.025

\*\* CHORDWISE INFINITE-SUBT WING EQUATIONS \*\*

\*\* Z-PRESSURE=C \*\*

\*\* X-PRESSURE=A \*\*

```

      V(WALL)      U(WALL)      T(WALL)      DELT(I)
1  0.342000E+00  0.220540E+00  0.32000E+00  -0.201740E+00
2  0.452535E+00  -0.191787E+00  0.13076E+00  -0.124980E+00
3  0.361252E+00  -0.267295E-01  0.527978E-02  -0.487959E-02
4  0.339523E+00  -0.111113E-02  -0.465482E-02  -0.265916E-03
5  0.334405E+00  -0.755528E-05  -0.456573E-02  -0.188233E-04

      J      ET      Y      F      U      V      G      h      T      B
1  0.0  0.0  0.0  0.0  0.0  0.0  0.0  0.0  0.0  0.0
2  0.192380  0.0  0.0  0.618764E-02  0.443241E-01  0.342800E+00  -0.918889E-04  -0.955238E-03  -0.496418E-02  0.963863E+00
7  0.477212  0.0  0.0  0.556548E-01  0.192650E+00  0.321134E+00  -0.826526E-03  -0.286974E-02  -0.493204E-02  0.964882E+00
10  1.347019  0.0  0.0  0.300270E+00  0.441392E+00  0.309623E+00  -0.446506E-02  -0.658404E-02  -0.459803E-02  0.969798E+00
13  2.886729  0.0  0.0  0.129804E+01  0.222298E+00  0.170385E+00  -0.152765E-01  -0.122119E-01  -0.253029E-02  0.985769E+00
16  4.767314  0.0  0.0  0.422124E+01  0.459617E+00  0.603987E-03  -0.628074E-01  -0.148447E-01  -0.895541E-05  0.999752E+00
17  7.568821  0.0  0.0  0.582246E+01  0.100000E+01  0.124976E-03  -0.064848E-01  -0.148906E-01  0.185586E-05  0.100034E+01

      J      ET      H0      IT      SVC      CVC      HS/USE      BETA
1  0.0  0.0  0.967728E+00  0.0  0.0  0.0  0.0  -0.572448E+00
4  0.192380  0.567581E+00  0.263015E-02  0.643240E-01  0.643241E-01  0.443241E-01  -0.572448E+00
7  0.477212  0.469995E+00  0.78070E-02  0.192650E+00  0.192651E+00  0.192651E+00  -0.572448E+00
10  1.347019  0.975457E+00  0.166477E-01  0.441392E+00  0.441392E+00  0.441392E+00  -0.572448E+00
13  2.886729  0.108337E+01  0.101584E-01  0.222298E+00  0.222298E+00  0.222298E+00  -0.572448E+00
16  4.767314  0.139137E+01  0.204650E-02  0.459617E+00  0.459617E+00  0.459617E+00  -0.572448E+00
17  7.568821  0.100000E+01  0.336119E-05  0.100000E+01  0.100000E+01  0.100000E+01  -0.572448E+00

      P1      P2      P3      P4      P5      P6      P7      P8      P9
0.500000E+00  0.0  0.0  0.0  0.0  0.0  0.0  0.0  0.0
0.0  0.0  0.0  0.0  0.0  0.0  0.0  0.0  0.0

      BODY LENGTH FROM STUPEL DATA SET
S1 = 0.0 THETA = 0.995490E+00 H1 = 0.889300E+00 H2 = 0.286200E+02 K1 = 0.950700E+00
K2 = 0.594200E-04 P17 = -0.252439E+00 K21 = 0.155800E+00 UE = 0.112057E+04 WE = -0.142295E+02
PHIC = 0.310075E-03 CWH = 0.275902E-06

      CFC = 0.0 DL S15 = 0.0 THIAS = 0.0 BETA1 = -0.572448E+00
      CCM = 0.0 DL S16 = 0.0 THIAN = 0.0 RX = 0.0
      USF = 0.111174E+04 HUSFD = C.117492E+04
  
```

\*\*\* NX = 70 NZ = 28 X = 1.521 Z = 0.860 X/C = 0.950

\*\* GENERAL CASE \*\*  
 \*\* Z-PRESSURES=B \*\*  
 \*\* X-PRESSURES=C \*\*

J	V(WALL)	DEL(V)	T(WALL)	DEL(T)					
1	0.149832E+01	0.578782E-01	0.551077E+00	0.431304E-01					
J	ETA	Y	F	U	V	G	W	T	S
1	0.0	0.0	0.0	0.0	0.0	0.0	0.0	0.0	0.0
2	0.192330	0.428648E-02	0.75521E-01	0.239216E+00	0.681835E+00	0.935898E-02	0.855968E-01	0.594208E+00	0.973347E+00
7	0.577212	0.127742E-01	0.14050E+00	0.358974E+00	0.143838E+00	0.510948E-01	0.121128E+00	0.33444E-01	0.125707E+02
10	1.347019	0.25357E-01	0.45191E+00	0.426538E+00	0.593386E-01	0.149897E+00	0.132519E+00	0.518025E-02	0.386301E+02
13	2.886925	0.622078E-01	0.116427E+01	0.493707E+00	0.237272E-01	0.355808E+00	0.133966E+00	-0.149216E-02	0.895795E+02
16	5.947319	0.127008E+00	0.280941E+01	0.568915E+00	0.176244E-01	0.753654E+00	0.124371E+00	-0.32367E-02	0.230302E+03
19	12.129251	0.253908E+00	0.667171E+01	0.648648E+00	0.208446E-01	0.143837E+00	0.956944E-01	-0.561565E-02	0.249840E+03
22	24.455440	0.491517E+00	0.165829E+02	0.804518E+00	0.128664E-01	0.220865E+00	0.342246E-01	-0.258429E-02	0.739279E+03
25	49.112488	0.962769E+00	0.406353E+02	0.100000E+01	-0.414720E-03	0.241527E+01	-0.132688E-02	-0.525490E-02	0.289466E+03
28	97.112488	0.962769E+00	0.406353E+02	0.100000E+01	-0.414720E-03	0.241527E+01	-0.132688E-02	-0.525490E-02	0.289466E+03

J	ETA	HG	HT	SVC	CVC	U/S/USE	BETA
1	0.0	0.0	0.0	0.0	0.0	0.0	0.0
4	0.152380	0.994171E+00	0.0	0.145348E-01	0.0	0.287740E+00	0.296129E+00
7	0.577212	0.994171E+00	0.0	0.11923E-03	-0.712981E+02	0.627338E+00	0.136709E+02
10	1.347019	0.994171E+00	0.0	0.144133E-03	-0.998728E+02	0.501355E+00	0.512824E+00
13	2.886925	0.994171E+00	0.0	0.452241E-04	-0.109934E+03	0.563676E+00	0.579330E+00
16	5.947319	0.994171E+00	0.0	0.122695E-04	-0.936942E+02	0.638327E+00	0.646296E+00
19	12.129251	0.994171E+00	0.0	0.109744E-04	-0.721199E+02	0.742959E+00	0.747028E+00
22	24.455460	0.100000E+01	0.0	0.250798E-05	-0.257933E+02	0.924493E+00	0.924911E+00
25	49.112488	0.100000E+01	0.0	0.120422E-05	-0.100000E+01	0.100000E+01	0.999999E+00
28	97.112488	0.100000E+01	0.0	0.120422E-05	-0.100000E+01	0.100000E+01	0.999999E+00

P1	P2	P3	P4	P5	P6	P7	P8	P9
0.517387E+00	-0.415311E+00	-0.261349E-04	0.115611E+00	-0.196789E+00	-0.291049E+00	0.144307E+00	0.454506E-04	-0.882484E-01
0.912231E+00	-0.415311E+00	0.189829E+00						

P10	P11	P12	P13	P14	P15	P16	P17	P18	P19
0.521647E+00	-0.566391E+00	-0.251724E-04	0.110615E+00	-0.191917E+00	-0.134897E+00	0.134004E+00	0.505969E-04	-0.720746E-01	
0.891939E+00	-0.566391E+00	0.183944E+00							

BODY GEOMETRY FROM STORED DATA SET  
 S1 = 0.371278E+01 THETA = 0.966300E+00 H1 = 0.407000E+01 H2 = 0.254300E+02 K1 = -0.193300E-01  
 K2 = 0.103100E-04 K17 = -0.528710E-01 K21 = 0.306000E-01 UE = 0.569430E+03 HE = -0.127140E+01  
 PHOF = 0.459716E-03 FNUC = 0.295994E-06  
 CFC = 0.157159E-02 DLSTS = 0.142435E-01 THTAS = 0.752591E-02 BETA1 = 0.143421E+02  
 CFN = 0.002134E-03 DLSTN = 0.235763E+01 THT4 = -0.208972E+03 RX = 0.559403E+07  
 USE = 0.468708E+03 DMSFD = -0.606319E+07

\*\*\* NX = 21 NZ = 28 X = 1.546 Z = 0.880 X/C = 0.975  
 \*\* SIGN CHANGE IN NF - CALCULATIONS GO TO NEXT SPANWISE STATION

\*\*\*\*\* SUMMARY TABLE \*\*\*\*\*

NX	X/C	V(WALL)	T(WALL)	CFI	CFN	BETA	DLSTS	DLSTN	THTAS	THTAN	RX
1	0.2500E-01	0.3357E+00	0.1310E-01	0.0	0.0	-0.1526E+01	0.0	0.0	0.0	0.0	0.0
2	0.5000E-01	0.4468E+00	0.1148E+00	0.2627E-02	-0.4013E-03	-0.8866E+01	0.5322E-03	0.6730E-03	0.1401E-03	0.2644E-03	0.1748E+06
3	0.7500E-01	0.1361E+01	0.3575E+00	0.4237E-02	-0.7054E-03	-0.1885E+01	0.1103E-02	0.6480E-03	0.4491E-03	0.1529E-04	0.5233E+06
4	0.1000E+00	0.1233E+01	0.4057E+00	0.4033E-02	-0.6212E-03	-0.7555E+01	0.1695E-02	0.1637E-02	0.9959E-03	0.6880E-03	0.8680E+06
5	0.2000E+00	0.1628E+01	0.4159E+00	0.3606E-02	-0.5448E-03	-0.8466E+01	0.2175E-02	0.2045E-02	0.9751E-03	0.8644E-03	0.1211E+07
6	0.3000E+00	0.1764E+01	0.4166E+00	0.3473E-02	-0.4824E-03	-0.7938E+01	0.2701E-02	0.2940E-02	0.1188E-02	0.1361E-02	0.1526E+07
7	0.4000E+00	0.1843E+01	0.4129E+00	0.3333E-02	-0.4378E-03	-0.7490E+01	0.3140E-02	0.3209E-02	0.1335E-02	0.1796E-02	0.1890E+07
8	0.5000E+00	0.1974E+01	0.4239E+00	0.3200E-02	-0.4172E-03	-0.7248E+01	0.3533E-02	0.4337E-02	0.1572E-02	0.2141E-02	0.2226E+07
9	0.6000E+00	0.2104E+01	0.4362E+00	0.3151E-02	-0.4013E-03	-0.7106E+01	0.3897E-02	0.5168E-02	0.1725E-02	0.2652E-02	0.2562E+07
10	0.7000E+00	0.1994E+01	0.4413E+00	0.3131E-02	-0.3836E-03	-0.6916E+01	0.4228E-02	0.6844E-02	0.1880E-02	0.3050E-02	0.2895E+07
11	0.8000E+00	0.2272E+01	0.4437E+00	0.3118E-02	-0.3673E-03	-0.6720E+01	0.4555E-02	0.8413E-02	0.2042E-02	0.3365E-02	0.3226E+07
12	0.9000E+00	0.2399E+01	0.4465E+00	0.3077E-02	-0.3533E-03	-0.6549E+01	0.4847E-02	0.7244E-02	0.2194E-02	0.3881E-02	0.3556E+07
13	0.9000E+00	0.2411E+01	0.4423E+00	0.3194E-02	-0.3214E-03	-0.6066E+01	0.5076E-02	0.8365E-02	0.2264E-02	0.4603E-02	0.3884E+07
14	0.8000E+00	0.2349E+01	0.4314E+00	0.2833E-02	-0.2313E-03	-0.5653E+01	0.5471E-02	0.1041E-01	0.2415E-02	0.5691E-02	0.4298E+07
15	0.7000E+00	0.2048E+01	0.4183E-01	0.2455E-02	-0.3034E-04	-0.7989E+00	0.6166E-02	0.1477E-01	0.2746E-02	0.7045E-02	0.4514E+07
16	0.7000E+00	0.1652E+01	0.2758E+00	0.1972E-02	0.1999E-03	0.5788E+01	0.3899E-02	0.2189E-01	0.3694E-02	0.3808E-02	0.4748E+07
17	0.8000E+00	0.1405E+01	0.3722E+00	0.1915E-02	0.2689E-03	0.7993E+01	0.8928E-02	0.3634E-01	0.4634E-02	0.1421E-01	0.4947E+07
18	0.8000E+00	0.1497E+01	0.4149E+00	0.1858E-02	0.7930E-03	0.8871E+01	0.1006E-01	0.6329E-01	0.4890E-02	0.3078E-01	0.5245E+07
19	0.9000E+00	0.1597E+01	0.5111E+00	0.1578E-02	0.3786E-03	0.1334E+02	0.1294E-01	0.1451E+00	0.9333E-02	0.2695E+00	0.5600E+07
20	0.9000E+00	0.1556E+01	0.5942E+00	0.1575E-02	0.4027E-03	0.1434E+02	0.1426E-01	0.2938E+01	0.7530E-02	0.1095E+00	0.5594E+07

## REFERENCES

1. Cebeci, T., Kaups, Kalle, and Ramsey, J.A.: A General Method for Calculating Three-Dimensional Compressible Laminar and Turbulent Boundary Layers on Arbitrary Wings. NASA CR-2777, 1977.
2. Cebeci, T.: Calculation of Three-Dimensional Boundary Layers. I. Swept Infinite Cylinders and Small Cross Flow. AIAA Journal, Vol. 12, June 1974, pp. 779-786.
3. Keller, H.B. and Cebeci, T.: Accurate Numerical Methods for Boundary Layers. II. Two-Dimensional Turbulent Flows. AIAA Journal, Vol. 10, Sept. 1972, pp. 1197-1200.
4. Cebeci, T.: Calculation of Three-Dimensional Boundary Layers. II. Three-Dimensional Flows in Cartesian Coordinates. AIAA Journal, Vol. 13, No. 8, Aug. 1975, pp. 1056-1064.
5. Cebeci, T. and Smith, A.M.O.: Analysis of Turbulent Boundary Layers. Academic Press, New York, 1974.
6. Brebner, G.G. and Wyatt, L.A.: Boundary-Layer Measurements at Low Speeds on Two Wings of 45° and 55° Sweep. Aeronautical Research Council Current Papers, C.P. No. 554, 1961.
7. Hess, J.L.: The Problem of Three-Dimensional Lifting Potential Flow and Its Solution by Means of Surface Singularity Distribution. Computer Methods in Applied Mechanics and Engineering, Vol. 4, No. 3, Nov. 1974.
8. Harris, C.D.: Wind-Tunnel Measurements of Aerodynamic Load Distribution on a NASA Supercritical-Wing Research Airplane Configuration. NASA TMX-2469, 1972 (title unclassified, paper classified).

**NASA TECHNICAL  
MEMORANDUM**

NASA TM X-73,215

NASA TM X-73,215

**INVESTIGATION OF INLET CONCEPTS FOR MANEUVER IMPROVEMENT  
AT TRANSONIC SPEEDS**

(NASA-TM-X-73215) INVESTIGATION OF INLET CONCEPTS FOR MANEUVER IMPROVEMENT AT TRANSONIC SPEEDS (NASA) 61 p HC A04/MF A01  
CSCL 01A  
N77-24060  
Unclas  
G3/02 30346

By Eldon Latham, John Gawienowski and Frank Meriwether

Ames Research Center  
Moffett Field, California 94035

April 1977





1. Report No. TM X-73,215		2. Government Accession No.		3. Recipient's Catalog No.	
4. Title and Subtitle INVESTIGATION OF INLET CONCEPTS FOR MANEUVER IMPROVEMENT AT TRANSONIC SPEEDS				5. Report Date April 1977	
				6. Performing Organization Code	
7. Author(s) Eldon Latham, John Gawienowski and Frank Meriwether				8. Performing Organization Report No. A-6952	
9. Performing Organization Name and Address NASA-Ames Research Center Moffett Field, Ca. 94035				10. Work Unit No. 505-04-11	
				11. Contract or Grant No.	
12. Sponsoring Agency Name and Address National Aeronautics and Space Administration Washington D.C. 20546				13. Type of Report and Period Covered Technical Memorandum	
				14. Sponsoring Agency Code	
15. Supplementary Notes					
16. Abstract  A 15-percent-scale lightweight fighter-type inlet-forebody was tested in the Ames 14-Foot Transonic Wind Tunnel at Mach numbers of 0.7, 0.9, and 1.04. The inlet was a two-dimensional horizontal-ramp system designed for a Mach number of 2.2. Four inlet devices designed to prevent or delay cowl-lip boundary-layer separation or to improve the inlet internal flow characteristics at high angles of attack were investigated. The devices used to control cowl-lip separation consisted of cowl leading-edge flaps, slotted flaps, and tangential blowing. To improve the internal flow characteristics, discrete jet-nozzle flows were directed downstream and parallel to the duct surface in the subsonic diffuser to energize the wall boundary layer. The discrete jets used in the subsonic diffuser were also tested in combination with each of the cowl leading-edge devices. The Reynolds number was about $11.9 \times 10^6$ per meter ( $3.9 \times 10^6$ per foot) for all Mach numbers. Angle of attack ranged from $0^\circ$ to $56^\circ$ and angle of sideslip from $0^\circ$ to $15^\circ$ . Test measurements included engine-face total pressure recovery, steady state distortion, dynamic distortion, duct boundary-layer profiles, and duct-surface static pressures. This report includes only representative data of some of the important parameters. No dynamic data are included.					
17. Key Words (Suggested by Author(s)) Inlet Transonic Maneuver High Angle of Attack			18. Distribution Statement  Unlimited  STAR Category 02		
19. Security Classif. (of this report) Unclassified		20. Security Classif. (of this page) Unclassified		21. No. of Pages 59	22. Price* \$4.25

INVESTIGATION OF INLET CONCEPTS FOR  
MANEUVER IMPROVEMENT AT TRANSONIC SPEEDS

By Eldon Latham, John Gawienowski and Frank Meriwether\*

Ames Research Center

SUMMARY

A 15-percent-scale lightweight fighter-type inlet-forebody was tested in the Ames 14-foot Transonic Wind Tunnel at Mach numbers of 0.7, 0.9, and 1.04. The inlet was a two-dimensional horizontal-ramp system designed for a Mach number of 2.2. Four inlet devices designed to prevent or delay cowl-lip boundary-layer separation or to improve the inlet internal flow characteristics at high angles of attack were investigated. The devices used to control cowl-lip separation consisted of cowl leading-edge flaps, slotted flaps, and tangential blowing. To improve the internal flow characteristics, discrete jet-nozzle flows were directed downstream and parallel to the duct surface in the subsonic diffuser to energize the wall boundary layer. The discrete jets used in the subsonic diffuser were also tested in combination with each of the cowl leading-edge devices. The Reynolds number was about  $11.9 \times 10^6$  per meter ( $3.9 \times 10^6$  per foot) for all Mach numbers. Angle of attack ranged from  $0^\circ$  to  $56^\circ$  and angle of sideslip from  $0^\circ$  to  $15^\circ$ . Test measurements included engine-face total pressure recovery, steady state distortion, dynamic distortion, duct boundary-layer profiles, and duct-surface static pressures. This report includes only representative data of some of the important parameters. No dynamic data are included.

INTRODUCTION

Aerodynamic design and control improvements have resulted in expanded stable-maneuver-envelopes for tactical aircraft. This type of aircraft requires advanced inlet concepts to provide good pressure recovery and low flow distortion to maintain continuous high thrust levels and prevent engine stall during severe maneuvers.

The purpose of this investigation was to evaluate the performance characteristics of selected inlet devices designed to prevent or delay cowl-lip boundary-layer separation or to control the inlet-duct flow properties so as to obtain maximum inlet pressure recovery and minimum flow distortion during severe transonic maneuvering. Four such devices were tested. Three

\* Project Engineer, ARO, Inc., Moffett Field, Calif. 94035

of these devices were derived from wing leading-edge high-lift devices and consisted of cowl leading-edge flaps, slotted flaps, and tangential blowing. The fourth device consisted of discrete jet-nozzle flow directed downstream and parallel to the duct surface in the subsonic diffuser so as to energize the wall boundary-layer. This fourth device was also tested in combination with each of the cowl leading-edge devices.

The test program, which was a cooperative effort between NASA Ames and General Dynamics, Fort Worth Division, was conducted in the Ames 14-Foot Transonic Wind Tunnel at Mach numbers of 0.7, 0.9, and 1.04. Angle of attack ranged from 0° to 56° and angle of sideslip from 0° to 15°. The Reynolds number was essentially constant and equal to  $11.9 \times 10^6$  per meter ( $3.9 \times 10^6$  per foot) for all Mach numbers. Test measurements included engine-face total-pressure recovery, steady state distortion, dynamic distortion, duct boundary-layer profiles and duct-surface static pressures.

#### NOMENCLATURE

<u>Symbol</u>	<u>Definition</u>
ALPHA, $\alpha$	angle of attack of model reference axis, deg
(AN/NSGRPT)MAX	maximum normalized Fourier coefficient parameter for ring 1 through ring 5, respectively
AO/AI	capture area ratio
BETA, $\beta$	angle of sideslip of model reference axis, deg
CFabb	compressor face total pressure ratios, <u>compressor pressure</u> a = ring number, bb = rake number PT
CONF	configuration code number
CMUL	actual combined lip and diffuser blowing momentum coefficient
CMUO	theoretical combined lip and diffuser blowing momentum coefficient
CMUxL	actual isolated blowing momentum coefficient, x - 1 = cowl lip, 2 = diffuser
CMUx0	theoretical isolated blowing momentum coefficient, x - 1 = cowl lip, 2 = diffuser

<u>Symbol</u>	<u>Definition</u>
DS	splitter diameter, calculated size of high compressor region, 1
D2	maximum compressor distortion, $\frac{\text{max. CFabb} - \text{min CFabb}}{PT}$
DX1	normalized KA2
DX2	normalized KC2
FLAP/SLAT	angle of cowl lip flap or slat relative to model reference axis, positive downward, deg
GX1	prediction of instantaneous DX1
ID	engine/inlet stability index
IDCy	compressor circumferential distortion index, y = compressor total-pressure ring number
IDCHUB	hub circumferential distortion index, $\frac{IDC1 + IDC2}{2}$
IDCMAX	larger of IDCHUB and TIP
IDCTIP	tip circumferential distortion index, $\frac{IDC4 + IDC5}{2}$
IDRMAX	larger of IDR4 and IDR5
IDRy	compressor radial distortion index, y = compressor total pressure-ring number
KA2	combined circumferential and radial distortion index
KC2	high compressor distortion parameter
KRA2	fan radial distortion parameter
KTHETA	fan circumferential distortion parameter
KTHETAS	fan circumferential distortion for rings with diameter < DS
MACH, M	free-stream Mach number
MTH	inlet throat Mach number

<u>Symbol</u>	<u>Definition</u>
P	free-stream static pressure, psf
PA1	lip blowing plenum pressure, psia
PA2	diffuser blowing plenum pressure, psia
PDcdd	duct wall static pressure ratios, $\frac{\text{duct pressure}}{P_T}$ c - 1 = upper wall, 2 = lower wall dd = tap number
PDX	lip blowing static pressure, $\frac{(PD201)(P_T)}{144}$ , psia
PDY	diffuser blowing static pressure, $\frac{(PD203)(P_T)}{144}$ , psia
PERCENT WC2	percent corrected airflow, $\frac{100(WC2)}{217}$
PH	phase
PREF	Kulite and scanivalve reference pressure, psf
PT	free-stream total pressure, psf
PT1	nose boom total pressure ratio, $\frac{\text{boom pressure}}{P_T}$
PT2	average compressor face total pressure, psf
(PT2R/PT2)BASE	base radial profile for ring 1 through ring 5, respectively
(PT2R/PT2)MEAS	measured radial profile for ring 1 through ring 5, respectively
P3	average throat plug exit pressure, psf
P30e	throat plug exit pressure ratios, e = tap number, $\frac{\text{exit pressure}}{P_T}$
PTRMS	average compressor RMS total pressure ratio, $\frac{\text{average compressor RMS pressure}}{P_T}$
Q	free-stream dynamic pressure, psf
QI/PT2	ratio of average inlet dynamic pressure to average compressor face total pressure

<u>Symbol</u>	<u>Definition</u>
Rf <sub>gg</sub>	duct boundary-rake total pressure ratios, f = rake number, gg = probe number, $\frac{\text{rake pressure}}{PT}$
RN/FT	Reynolds number, millions/ft
RUN	run number
SEQ	data sequence number
SPF <sub>h</sub>	forebody static pressure ratios, h = tap number, $\frac{\text{forebody pressure}}{PT}$
THETA	circumferential extent of distortion for ring 1 thru 5, respectively
TN	tunnel, 14 = Ames 14-Foot Transonic Wind Tunnel
TR	free-stream static temperature, °R
TST	test number
TTR	free-stream total temperature, °R
VIA <sub>xL</sub>	actual blowing velocity, ft/sec, x - 1 = lip, 2 = diffuser
VIA <sub>x0</sub>	theoretical blowing velocity, x - 1 = lip, 2 = diffuser
WAX	blowing air weight flow, lb/sec, x - 1 = lip, 2 = diffuser
WC2	duct full scale corrected weight flow, lb/sec
W2	model duct flow, lb/sec

## MODEL DESCRIPTION

Shown in figure 1 is the 15-percent-scale pressure model installed in the Ames 14-Foot Transonic Wind Tunnel. The model (fig. 2) consisted of a removable forebody assembly, an underslung inlet and subsonic duct with a simulated compressor face, and a remotely controlled conical-plug flow meter. The forebody (fig. 3) was removed for isolated inlet testing. The inlet (fig. 4) was a two-dimensional, horizontal-ramp system with a 6-degree initial ramp angle. A section of the inlet cowl was removable, allowing incorporation of the three different leading-edge devices. The entire forebody and inlet assembly was mounted on a remotely actuated pitch/yaw mechanism (fig. 5) which, in turn, was mounted on the wind tunnel model-support-system. This combination provided a capability of  $56^\circ$  angle of attack and  $15^\circ$  angle of sideslip.

The inlet cowl leading-edge devices consisted of a flap (fig. 6) deflected  $0^\circ$ ,  $30^\circ$  or  $50^\circ$ , a slotted flap (fig. 7) deflected  $30^\circ$ ,  $45^\circ$  or  $60^\circ$ , and a tangential blowing slot (fig. 8). Diffuser wall blowing jets, which were used independently and in combination with the leading-edge devices, are described in figure 4. It should be noted that the drawings are to scale, with only limited dimensions being given.

## INSTRUMENTATION

Steady state pressure instrumentation in the inlet subsonic-diffuser duct consisted of five total pressure boundary-layer rakes mounted downstream of the cowl-lip (fig. 9) and wall-static orifices on or near the duct centerline on both the ramp and cowl surfaces as well as near each rake location (fig. 10). Instrumentation at the simulated compressor face (fig. 11) consisted of 40 steady state and 40 high-response total pressure probes located on centroids of equal area. Kulite XDBL-093-25 pressure transducers were used to make high response measurements at the compressor face. A Kulite XCQ-093-25 pressure transducer mounted in the nose of the removable forebody was used to monitor the wind tunnel turbulence. Dynamic data were recorded on the NASA Ames high-response data acquisition system (ref. 1). All steady state pressures were measured with a multi-pressure scanning valve assembly mounted on the model support.

## TESTING AND PROCEDURE

The variation of engine-face total pressure recovery and distortion with inlet mass-flow ratio was established for each model configuration and test condition. All runs were made at constant Mach number and model attitude while the inlet mass flow was varied using the remotely-controlled,

conical-plug flowmeter. The number of data points for each model configuration and test condition varied from one to seven with at least one engine match point (based on the Pratt and Whitney Aircraft F100-PW-100(3) turbofan engine).

For each data point, tunnel and model conditions were set and 45 seconds of dynamic data were recorded on the NASA Ames high-response data acquisition system. Steady state data were then recorded.

Estimated uncertainties of the primary parameters, based on the accuracy of the measuring instrumentation and repeatability of data check points, are as follow:

$$\begin{array}{ll} \alpha = \pm 0.1 \text{ DEG.} & \text{PT2/PT} = \pm 0.005 \\ \beta = \pm 0.1 \text{ DEG.} & \text{AO/AI} = \pm 0.02 \\ \text{M} = \pm 0.005 & \end{array}$$

## RESULTS AND DISCUSSION

The run schedule for the present investigation is shown in table 1 and a sample of the tabulated data is shown in the appendix. A complete listing of the tabulated data is not presented in this report because of the large volume required. The data are available from NASA Ames Research Center, Moffett Field, California. Selected plots of the data are presented in figures 12 through 16.

For the isolated inlet, engine-face pressure recovery and steady state distortion as functions of inlet capture-area ratio and the angle of attack are presented for the basic cowl lip and each of the four inlet devices at a Mach number of 0.9 only. All data are for  $\beta = 0^\circ$ . Performance of the inlet with the basic cowl lip is shown in figure 12 from  $\alpha = 0^\circ$  to  $56^\circ$ . Performance is maintained up to  $\alpha = 20^\circ$  with a slight decrease in total pressure recovery at  $\alpha = 30^\circ$  and progressively increasing losses at  $\alpha = 40^\circ$  and  $56^\circ$ . Engine-face distortion increases with decreasing pressure recovery.

A comparison of inlet performance between the basic cowl lip and various cowl-lip flap deflections for inlet angles of attack of  $30^\circ$ ,  $40^\circ$ , and  $56^\circ$  is shown in figure 13. At  $\alpha = 30^\circ$  (fig. 13a), the  $30^\circ$  flap deflection provides a small increase in total pressure recovery and little change in distortion. The  $50^\circ$  flap deflection provides no increase in pressure recovery, and distortion at the lower capture-area ratios is increased. At  $\alpha = 40^\circ$  (fig. 13b) with a  $30^\circ$  flap deflection, large increases in total pressure recovery are seen along with a decrease in distortion. The  $50^\circ$  flap deflection at  $\alpha = 40^\circ$  also improves the inlet performance; however, the increase is only about one-half of that achieved with the  $30^\circ$  flap deflection. The distortion with the  $50^\circ$  flap deflection is improved



at the high capture-area ratios but increased at the lower values. At  $\alpha = 56^\circ$  (fig. 13c) no data are available with the  $30^\circ$  flap deflection, but a marked improvement in performance can be seen with the  $50^\circ$  flap deflection. Approximately a 7% increase in total pressure recovery is achieved at the engine match point. An improvement in engine-face distortion is also realized.

A comparison of the inlet performance for the basic cowl lip and slotted cowl flap is shown in figure 14 at  $\alpha = 30^\circ$ ,  $40^\circ$ , and  $56^\circ$ . At  $\alpha = 30^\circ$  (fig. 14a) there is a very small increase in total pressure recovery with the slotted flap deflected  $30^\circ$  and no improvement in engine face distortion. A slotted flap deflection of  $45^\circ$  provided no increase in pressure recovery but did result in a slight improvement in distortion. At  $\alpha = 40^\circ$  (fig. 14b) each position of the slotted flap ( $30^\circ$ ,  $45^\circ$  and  $60^\circ$  deflection) improved the inlet total pressure recovery. The  $30^\circ$  deflection resulted in the greatest gain in performance and the  $60^\circ$  deflection the least. Generally, the engine face distortion was reduced with all slotted flap deflections; however, an increase in distortion can be seen at the lower capture-area ratios for the  $60^\circ$  slotted flap deflection. At  $\alpha = 56^\circ$  (fig. 14c) all slotted flap positions improved the inlet performance significantly with the  $60^\circ$  deflection showing the greatest improvement and the  $30^\circ$  deflection the least. In addition to significant increases in total pressure recovery, the use of the slotted flap also resulted in a 0.05 increase in mass flow ratio. The engine face distortion was reduced in all cases.

The inlet performance achieved with tangential blowing at the cowl lip or discrete jet-nozzle blowing in the diffuser is compared to the basic cowl lip data in figure 15 over the angle of attack range. Data are shown at the engine match point with maximum blowing only for each of the devices. The tangential blowing at the cowl lip improves the total pressure recovery from 1.0 to 2.5 percent and decreases the engine-face distortion through most of the angle of attack range. The diffuser blowing provides slightly better total pressure recovery than tangential lip blowing at the high angles of attack; however, the engine face distortion is also increased at the higher angles.

The effect of an aircraft forebody on the performance of the basic inlet is shown in figure 16 from  $\alpha = 0^\circ$  to  $\alpha = 40^\circ$ . No data for  $\alpha = 56^\circ$  were available. At angles of attack of  $0^\circ$  (fig. 16a),  $20^\circ$  (fig. 16b), and  $30^\circ$  (fig. 16c), essentially no change in total pressure recovery or distortion was measured. At  $\alpha = 40^\circ$  (fig. 16d), however, significant improvements in total pressure recovery (up to 3.5 percent) and reduction in distortion were achieved.

## CONCLUDING REMARKS

The performance characteristics of four inlet devices (cowl-lip leading-edge flaps, slotted flaps, tangential blowing and discrete jet-nozzles in the subsonic diffuser) designed to prevent or delay cowl-lip boundary-layer separation or to improve the inlet internal-flow characteristics at high angles of attack were investigated at Mach numbers of 0.7, 0.9 and 1.04.

All of the inlet devices tested are capable of improving inlet performance at high angles of attack. However, parametric studies of each concept are required if optimum effectiveness is to be achieved.

Ames Research Center  
National Aeronautics and Space Administration  
Moffett Field, Calif. 94035

March 10, 1977

## REFERENCES

1. Garner, J. E.: Advanced Inlet/Airframe Integration Test of a 0.15-Scale Inlet Model in the NASA Ames 14-Foot Transonic Tunnel, Volume II: Report No. FZT-636-001, General Dynamics, Fort Worth Division, Fort Worth, Texas, December 1975.

TABLE 1. - RUN SCHEDULE

<u>ALPHA</u>	<u>SCHEDULES</u>	<u>NOTATION</u>
A1	15, 20	
A2	20, 30, 40, 50, 56	
A3	20, 30, 40, 50, 52, 56	
A4	0, 5, 10, 15, 20, 25, 30, 35, 40, 45, 50, 56	

BETA      SCHEDULES

B1	0, 5, 10, 15
B2	5, 10, 15
B3	0, 10
B4	5, 10
B5	10, 15
B6	0, 15
B7	0, 5

WC2      SCHEDULES

W1	227, 218, 203, 187, 169, 151, 140
W2	227, 211, 187, 162, 140
W3	227, 211, 140
W4	227, 140
W5	244, 235, 227, 212, 140
W6	244, 227, 140
W7	235, 227

PA1      SCHEDULES

L1	23, 32, 50, 67, 84, 102
L2	32, 67, 102
L3	air off, 32, 50, 67, 84, 102, 119, 136
L4	32, 50, 67, 84, 119, 136
L5	32, 67, 102, 136
L6	air off, 32, 50, 67, 84, 119, 136
L7	air off, 32, 50, 67, 102, 136
L8	air off, 32, 67, 102, 136

PA2      SCHEDULES

C1	37, 48, 60, 105, 150, 195, 240
C2	air off, 60, 150, 195, 240
C3	37, 60, 105, 150, 195, 240
C5	60, 105, 150, 195, 240
C6	air off, 60, 105, 150, 195, 240
C7	air off, 60, 150, 240
C10	60, 150, 240

TABLE 1. - Continued.

- B Forebody
- F<sub>x</sub> Cowl flap, x = flap angle, deg
- I Plain cowl lip
- L Blowing lip
- S<sub>x</sub> Cowl slotted flap (slat), x = flap angle, deg
- W Boundary layer rakes and diffuser blowing hardware installed in duct

Config. Code	Component Notation								
	B	F30	F50	I	L	S30	S45	S60	W
1				X					X
2		X							X
3			X						X
4						X			X
5							X		X
6								X	X
7					X				X
8	X				X				X
9	X						X		X
10	X		X						X
11	X			X					X
12	X			X					

TABLE 1. - Continued.

RUN	M	ALPHA	BETA	CONF	WC2	PA1	PA2	REMARKS
1	0.7	0	0	1	W1	air off	air off	WC2 out of limits at SEQ 30
2			0		W2			WC2 out of limits at SEQ 38
3			B2		227			
4		10	0		W3			WC2 out of limits at SEQ 45
5		15			W4			WC2 out of limits at SEQ 47
6		20			W4			WC2 out of limits at SEQ 49
7					227		C1	
8			B2				air off	
9		25	0					
10		35	B1					
11		40	0		W4			WC2 out of limits at SEQ 66
12		45	0		227			
13		56	B3					
14		30	0				C2	
15		56					C2	
16		56			140		air off	
17	0.9	0			W1			
18		20						
19		56						

TABLE 1. - Continued.

RUN	M	ALPHA	BETA	CONF	WC2	PA1	PA2	REMARKS
23	0.9	15	0	1	W6	air off	air off	
24		20			W5		air off	
25		20			227		C3	
28	0.9	30	0	1	W6		air off	
29		30	0		227		C2	
30		35	B1		227		air off	
31		40	0		W6			
32		45			227			
33		50			227			
34		56			W6			
35					227		C2	
36			10				air off	
37			15				C2	
38		35	15				C2	
39		45	0				C6	
40		45					air off	
41		20		2	W5		air off	
42					227		C5	
43			B2				air off	
44		25	0				air off	

TABLE 1. - Continued.

RUN	M	ALPHA	BETA	CONF	WC2	PA1	PA2	REMARKS
45	0.9	35	B1	2	227	air off	air off	
46		45	0					
47		50						
48		30			W6			
49		30			227		C5	
50		40			W6		air off	
51		40			227		C5	
52		45			W6		air off	
53		45			227		C5	
54		56			227		C5	
55				3	W6		air off	
56					227		C5	
57		50					air off	
58		45						
59		40			W6			
60		40			227		C5	
61		35	B1		227		air off	
62		30	0		W6		air off	
63		30			227		C5	
64		25			227		air off	
65		20			W5		air off	
66		20			227		C5	

TABLE 1. - Continued.

RUN	M	ALPHA	BETA	CONF	WC2	PA1	PA2	REMARKS
67	0.9	20	B2	3	227	air off	air off	
68		35	15				C5	
69		56	15					
70	0.7	56	0					
71	0.9	20		4	W5		air off	
72					227		C5	
73			B2				air off	
74		25	0					
75		30			W6			
76		30			227		C5	
77		35	B1		227		air off	
78		40	0		W6		air off	
79		40			227		C5	
80		45					air off	
81		50						
82		56			W6			
83					227		C5	
84			15				C6	
85		35	15				C6	
86		56	0	5	W6		air off	
87		56			227		C5	
88		50			227		air off	



TABLE 1. - Continued.

RIN	M	ALPHA	BETA	CONF	WC2	PA1	PA2	REMARKS
89	0.9	45	0	5	227	air off	air off	
90		40			W6		air off	
91		40			227		C6	
92		35	B1		227		air off	
93		30	0		W6		air off	
94		30			227		C6	
95		56		6	W6		air off	
96		56			227		C5	
97		50					air off	
98		45						
99		40			W6			
100		40			227		C5	
101		35					air off	
102	0.7	56					C7	
103		50					air off	
104		45					air off	
105		40					C7	
106	0.9	0		7	W5		air off	
107		0	15		227			
108		10	0					
109		15						
110		20			W5			

TABLE 1. - Continued.

RUN	M	ALPHA	BETA	CONF	WC2	PA1	PA2	REMARKS
111	0.9	20	0	7	227	L1	air off	
112			B2			air off		
113			15			L2		
114		25	0			L3		Regulator leakage PA2 = 22, SEQ 657-663
115		30			W6	air off		
116		30			227	L4		Regulator leakage PA2=18, SEQ 668&669
117		35				L3		
118			B2			air off		
119			15			L5		
120			15			67	C7	
121		30	0			50	C6	
122		40			W6	air off	air off	
123		40			227	L4		Regulator leakage, PA2=15, SEQ 717-721
124		45				L6		
125		50				L6		
126		56				L7		
127						67	C6	
128						136	C6	
129					SELECT	67	air off	WC2=215,200,182
130					182	136		
131		45			227	SELECT		PA1=air off,67,136
132		45			215	67		

TABLE 1. - Continued.

RUN	M	ALPHA	BETA	CONF	WC2	PA1	PA2	REMARKS
133	0.9	40	0	7	159	L8	air off.	
134					203			
135					214			
136					228			
137					SELECT	102	240	WC2=228, 214, 203
138		50			227	L8	air off	
139					212			
140					203			
141	0.7	40			219			
142					213			
143					204			
144					SELECT	102	240	WC2=204, 213
145	0.9	56		8	227	L8	air off	
146		56			204			
147		50			227			
148		50			203			
149		40			203			
150					212			
151					227			
152	1.04							
153	1.04	35						
154	0.9	40			SELECT	67	240	WC2=228, 213, 203

TABLE 1. - Continued.

RUN	M	ALPHA	BETA	CONF	WC2	PA1	PA2	REMARKS
155	0.9	35	0	8	227	L8	air off	
156		30		8	227	air off		
157		56		9	W6			
158		56			227		C10	
159		50					C7	
160		45					air off	
161		40			W6		air off	
162		40			227		C10	
163		35					air off	
164		30					C7	
165		25					air off	
166		20			W6		air off	
167					227		C10	
168			B2				air off	
169			15				240	
170		35	B2				air off	
171		35	15				C10	
172	1.01	56	0				C7	
173	0.7	56						
174		50						
175		40						
176	0.9	56		10	W6		air off	

TABLE 1. - Continued.

RUN	M	ALPHA	BETA	CONF	WC2	PA1	PA2	REMARKS
177	0.9	56	0	10	227	air off	C10	
178		50					C7	
179		45					air off	
180		40			W6		air off	
181		40			227		C10	
182		35					air off	
183		30					C7	
184		25					air off	
185		20			W6		air off	
186		20			227		C10	
187	0.7	50		3			C7	
188		45					air off	
189		40			W6		air off	
190		40			W6		C10	
191		35			227		air off	
192		30					C7	
193		25					air off	
194		20			W6		air off	
195		20			227		C10	
196		35	15				C7	
197		35	B4				air off	
198		56	B4				air off	

TABLE 1. - Continued.

RUN	M	ALPHA	BETA	CONF	WC2	PA1	PA2	REMARKS
199	0.7	56	15	3	227	air off	C10	
200		45	15				C7	
201		45	B2				air off	
202		56	0				240	
203		56		2			C7	
204		50					C7	
205		45					air off	
206		40					C7	
207		35					air off	
208		30					C7	
209		25					air off	
210		20					C7	
211		45	15				C7	
212		45	B2				air off	
213		56	B1				air off	
214		56	15				C10	
215		35	15				C7	
216		35	B5				air off	
217	0.9	56	0				air off	
218	0.9		15				SELECT	PA2=air off,10
219	0.7		0	5			C7	
220	0.7	50	0	5			C7	

TABLE 1. - Continued.

RUN	M	ALPHA	BETA	CONF	WC2	PA1	PA2	REMARKS
221	0.7	45	0	5	227	air off	air off	
222		40					C7	
223		35					air off	
224		30					C7	
225		25					air off	
226		20					C7	
227			15				C7	
228			B4				air off	
229		56	B4				air off	
232	0.7	45	B4	5	227	air off	air off	
233		50	0	4			C7	
234		45					air off	
235		40					C7	
236		35					air off	
237		30					C7	
238		56					C7	
239		25					air off	
240		20					C7	
241		45	15				C7	
242		45	B4				air off	

TABLE 1. - Continued.

RUN	M	ALPHA	BETA	CONF	WC2	PA1	PA2	REMARKS
243	0.9	0	0	1	W5	air off	air off	
244			5		W7			
245			10					
246			15					
247		5	0					
248		10	0					
249			5					
250			10					
251			15					
252		A1	0		235			For 2nd point of run BETA = 5
253		20	5		W7			
254		20	10		W7			
255		0	0	11	W5			
256		0	B2		227			
257		10	0		W6			
258		15			W6			
259		20			W5			
260			B2		227			
261			0				C10	
262		25					air off	
263		30			W6		air off	
264		30			227		C10	



TABLE 1. - Continued.

RUN	M	ALPHA	BETA	CONF	WC2	PA1	PA2	REMARKS
265	0.9	35	B1	11	227	air off	air off	
266		40	0		W6		air off	
267		40			227		C10	
268		45					air off	
269		50	B6					
270		56						
271		56					240	
272		50						
273	0.7	A2	0					
274		A3	15					
275		A4	0				air off	
276		56	B4					
277		45	B2					
278		35						
279		20						
280	0.9	0	0	12	W5			
281			B2		227			
282			B2		235			
283		5	0		W7			
284		10	0		W5			
285			B2		227			
286			B1		235			

TABLE 1. - Continued.

RUN	M	ALPHA	BETA	CONF	WC2	PA1	PA2	REMARKS
287	0.9	15	0	12	W7	air off	air off	
288		20	0		W5			
289			B2		227			
290			B2		235			
291		25	0		W7			
292		30	0		W5			
293			B2		227			
294			B2		235			
295		35	0		W7			
296		35	5		W7			
297		40	0		W6			
298		45	B1		227			
299		50	0		W6			
300		56	0		W6			
301		56	B2		227			
302		0	0		W3			
303		0	B2		227			
304		5	0		227			
305		10	0		W3			
306		10	B2		227			
307		15	0		227			
308		20	0		W3			

TABLE 1. - Concluded.

RUN	M	ALPHA	BETA	CONF	WC2	PA1	PA2	REMARKS
309	0.9	5	B2	12	227	air off	air off	
310		25	0		227			
311		30	0		W3			
312		30	B2		227			
313	0.7	0	0					
314		0	B2					
315		5	B7					
316		10	0					
317		10	B2					
318		15	0					
319		20	0					
320		5	B4					
321		20	B2					
322		25	0					
323		30	0					
324		30	B2					
325		35	B7					
326		40	0					
327		40	B2					
328		45	B6					
329		50	0					
330		56	0					
331		56	5					

TABLE 2. - INDEX OF FIGURES

Figure	Title	Page
1	Model installed in Ames 14-foot transonic wind tunnel	28
2	General arrangement of 15 percent scale inlet model	29
3	Model forebody	30
4	Model inlet	31
5	Representative test setups	32
6	Inlet cowl leading-edge flap	33
7	Inlet cowl leading-edge slotted-flap	34
8	Inlet cowl leading-edge tangential blowing slot	35
9	Static-pressure orifice locations in subsonic diffuser	36
10	Boundary-layer rake details	38
11	Compressor-face rake details	39
12	Performance of isolated inlet with basic cowl lip; $M = 0.9$ , $\beta = 0^\circ$	40
13	Performance of isolated inlet with cowl flap; $M = 0.9$ , $\beta = 0$	41
14	Performance of isolated inlet with slotted cowl flap; $M = 0.9$ , $\beta = 0$	44
15	Performance of isolated inlet with tangential blowing cowl slot and diffuser blowing; $M = 0.9$ , $\beta = 0$	47
16	Performance of inlet with basic cowl lip and forebody; $M = 0.9$ , $\beta = 0$	48



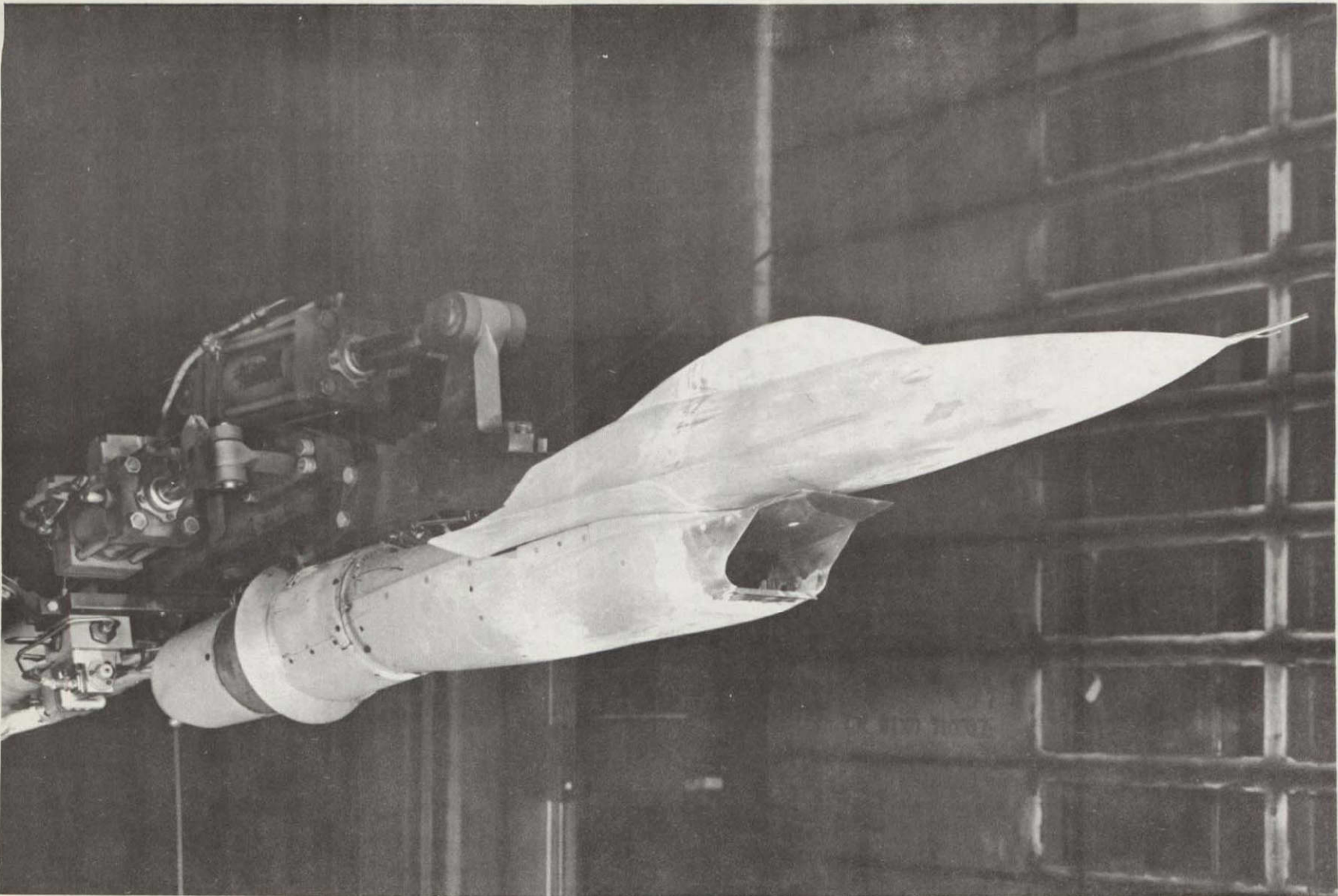


Figure 1. - Model installed in Ames 14-Foot Transonic Wind Tunnel.

ORIGINAL PAGE IS  
OF POOR QUALITY

28

ORIGINAL PAGE IS  
OF POOR QUALITY

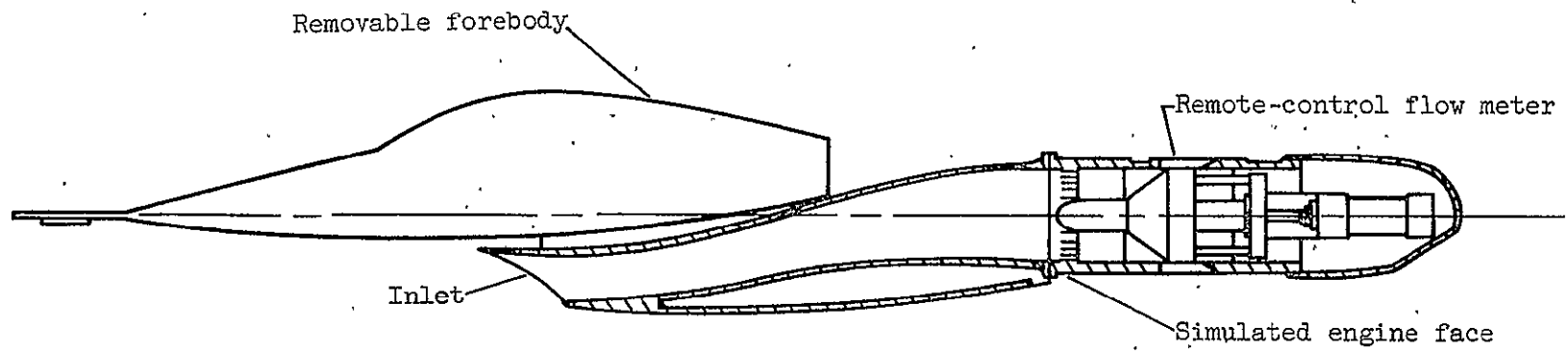


Figure-2. - General arrangement of 15 percent scale inlet model.

Note: All dimensions are  
in centimeters

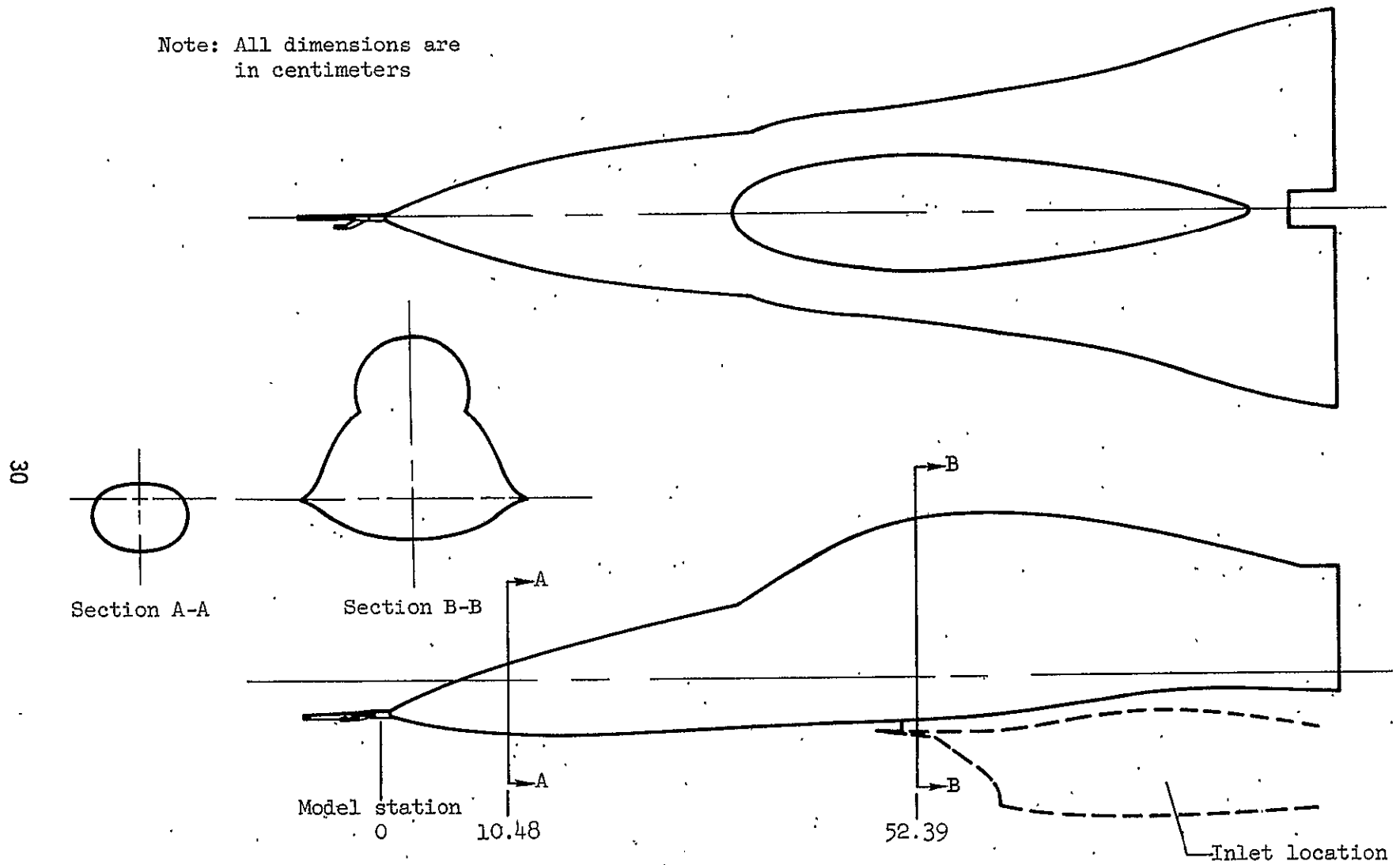
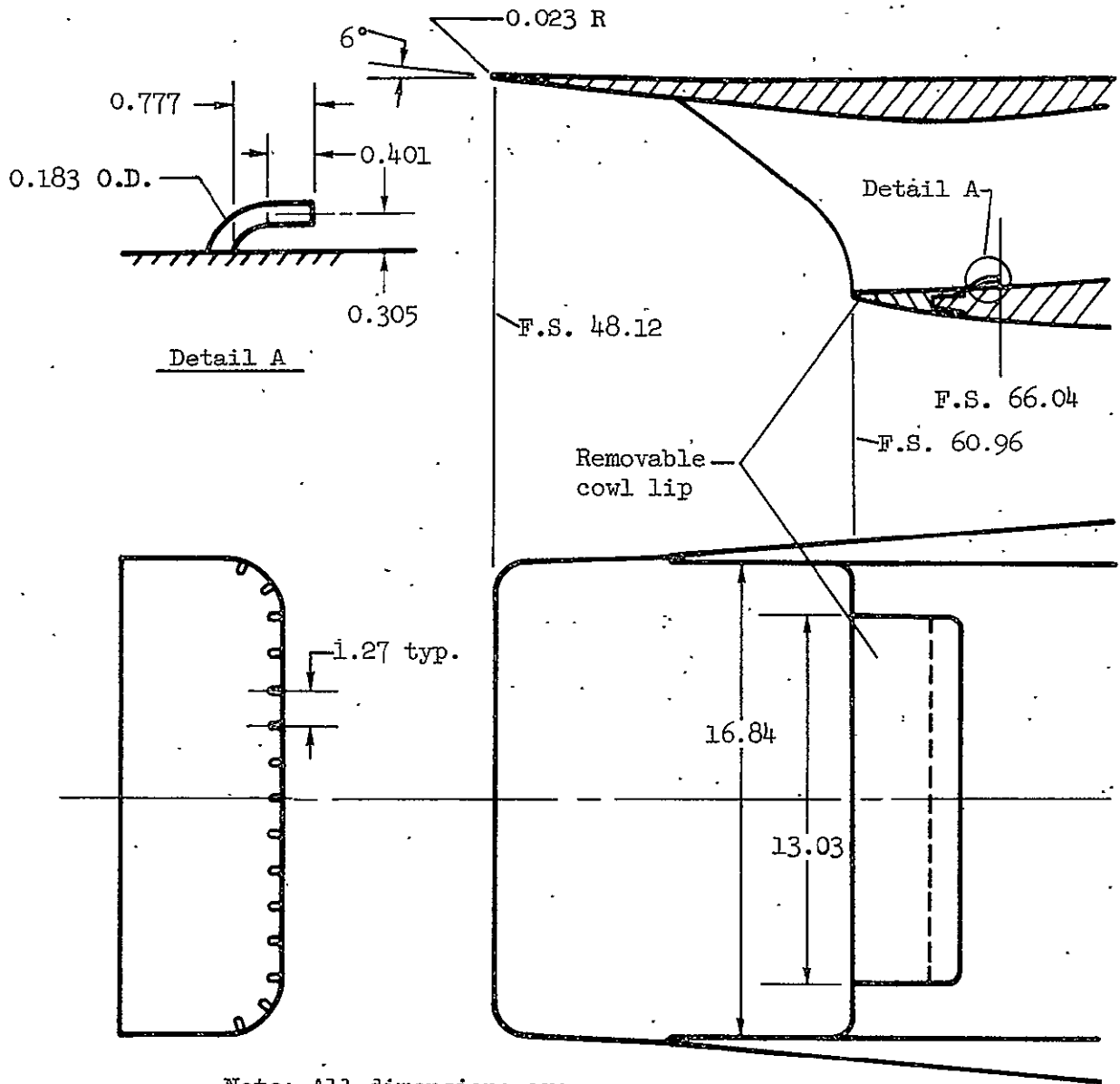


Figure 3. - Model forebody.



Note: All dimensions are in centimeters

Figure 4.- Model inlet.



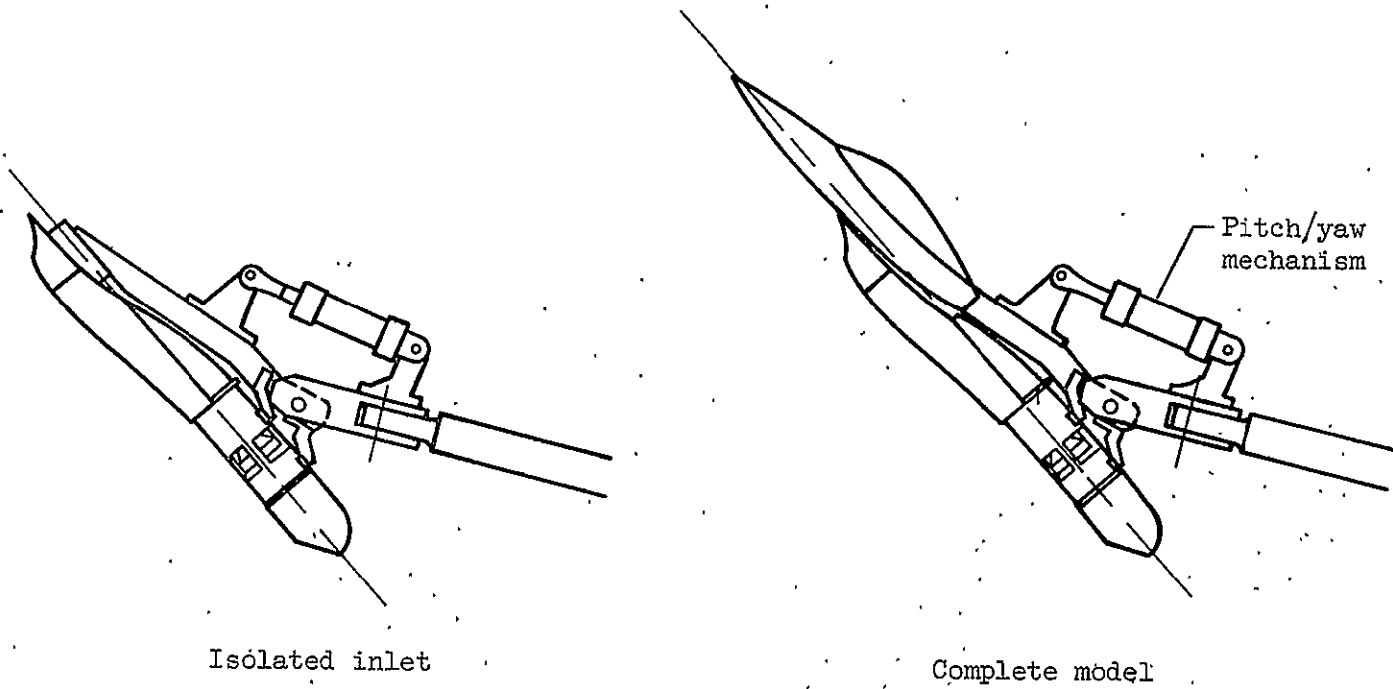
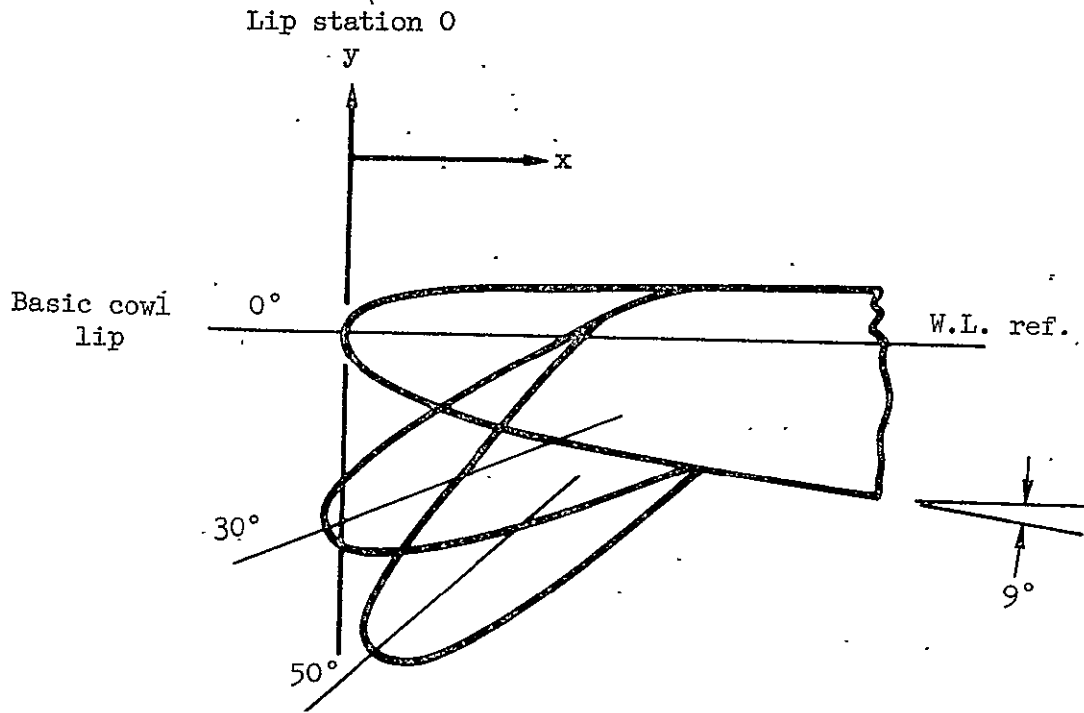


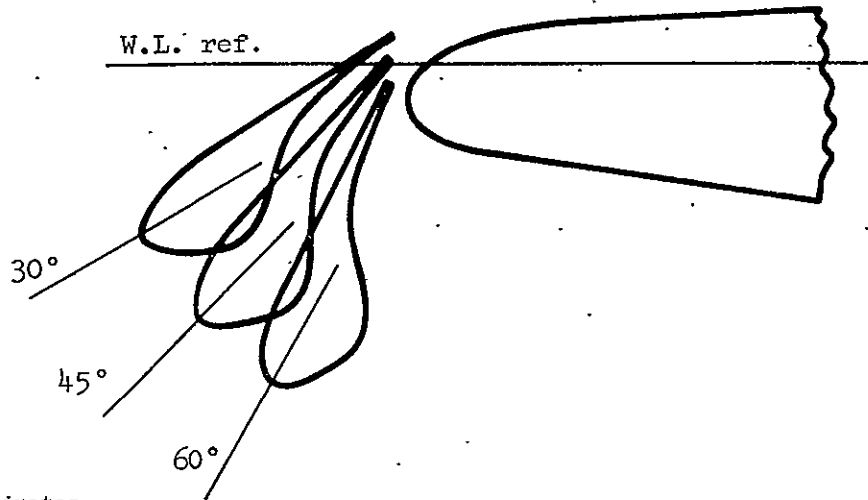
Figure 5.- Representative test setups.



Basic lip and flap ordinates

Basic lip, 0°			30° flap			50° flap		
Lip station, x, cm	Lower surface, y, cm	Upper surface, y, cm	Lip station, x, cm	Lower surface, y, cm	Upper surface, y, cm	Lip station, x, cm	Lower surface, y, cm	Upper surface, y, cm
0	0	0	-0.038	-0.483	-0.483	0.071	-0.800	-0.800
0.043	-0.084	0.053	-0.018	-0.541	-0.437	0.091	-0.846	-0.709
0.102	-0.130	0.079	0.051	-0.569	-0.353	0.127	-0.864	-0.638
0.180	-0.170	0.102	0.102	-0.577	-0.312	0.180	-0.861	-0.554
0.282	-0.206	0.117	0.178	-0.577	-0.254	0.231	-0.853	—
0.381	-0.234	0.124	0.282	-0.556	-0.185	0.282	-0.800	—
0.508	-0.257	0.127	0.348	—	-0.145	0.323	—	-0.368
0.660	-0.282	↑ straight line	0.381	-0.533	↑ straight line	0.381	-0.785	↑ straight line
—	↑ straight line	—	0.508	-0.495	—	0.508	-0.699	—
—	—	—	0.678	-0.434	—	—	—	—
—	—	—	—	↑ straight line	—	0.602	—	—
0.953	-0.328	—	—	—	—	0.632	-0.602	-0.028
1.092	—	0.142	0.721	—	0.071	—	—	—
—	—	—	—	—	—	0.734	-0.516	—
—	—	—	0.953	-0.328	0.140	—	—	—
—	—	—	1.092	—	0.142	—	↑ straight line	—
—	—	—	—	—	—	—	—	—
—	—	—	—	—	—	—	—	—
—	—	—	—	—	—	0.953	-0.328	0.140
—	—	—	—	—	—	1.092	—	0.142

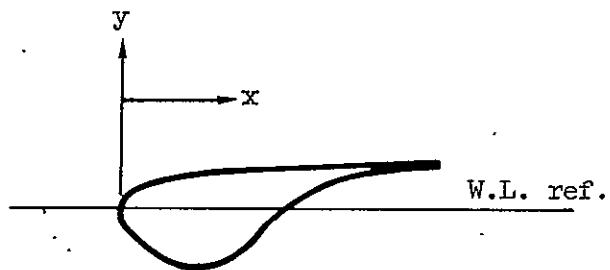
Figure 6.- Inlet cowl leading-edge flap.



Slotted flap ordinates

Lip station, x, cm	Lower surface, y, cm	Upper surface, y, cm
0.023	-0.069	0.043
0.061	-0.099	0.061
0.137	-0.147	0.097
0.259	-0.188	0.119
0.366	-0.155	
0.442	-0.097	↑
0.518	-0.020	straight line
0.594	-0.038	line
0.671	-0.074	↓
0.747	-0.097	
0.899	-0.130	
1.044	-0.142	0.157

Lip station 0



Slotted flap base ordinates

Lip station, x, cm	Lower surface, y, cm	Upper surface, y, cm
0.038	-0.193	-0.033
0.076	-0.231	0
0.152	-0.272	-0.004
0.305	↑	-0.099
0.330	straight line, -9°	-0.130
0.584	↓	-0.140

Lip station 0

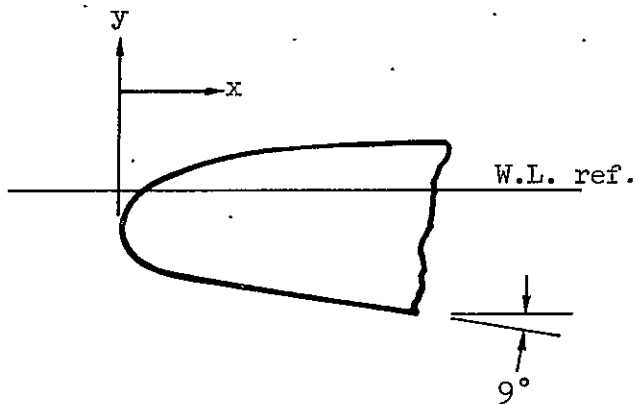
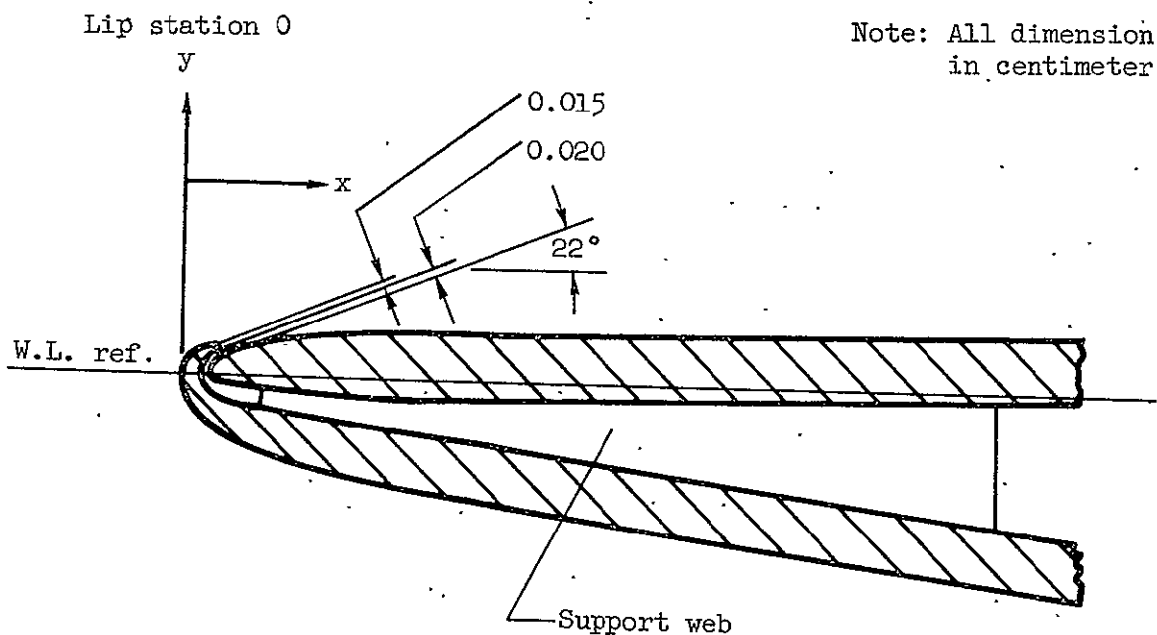


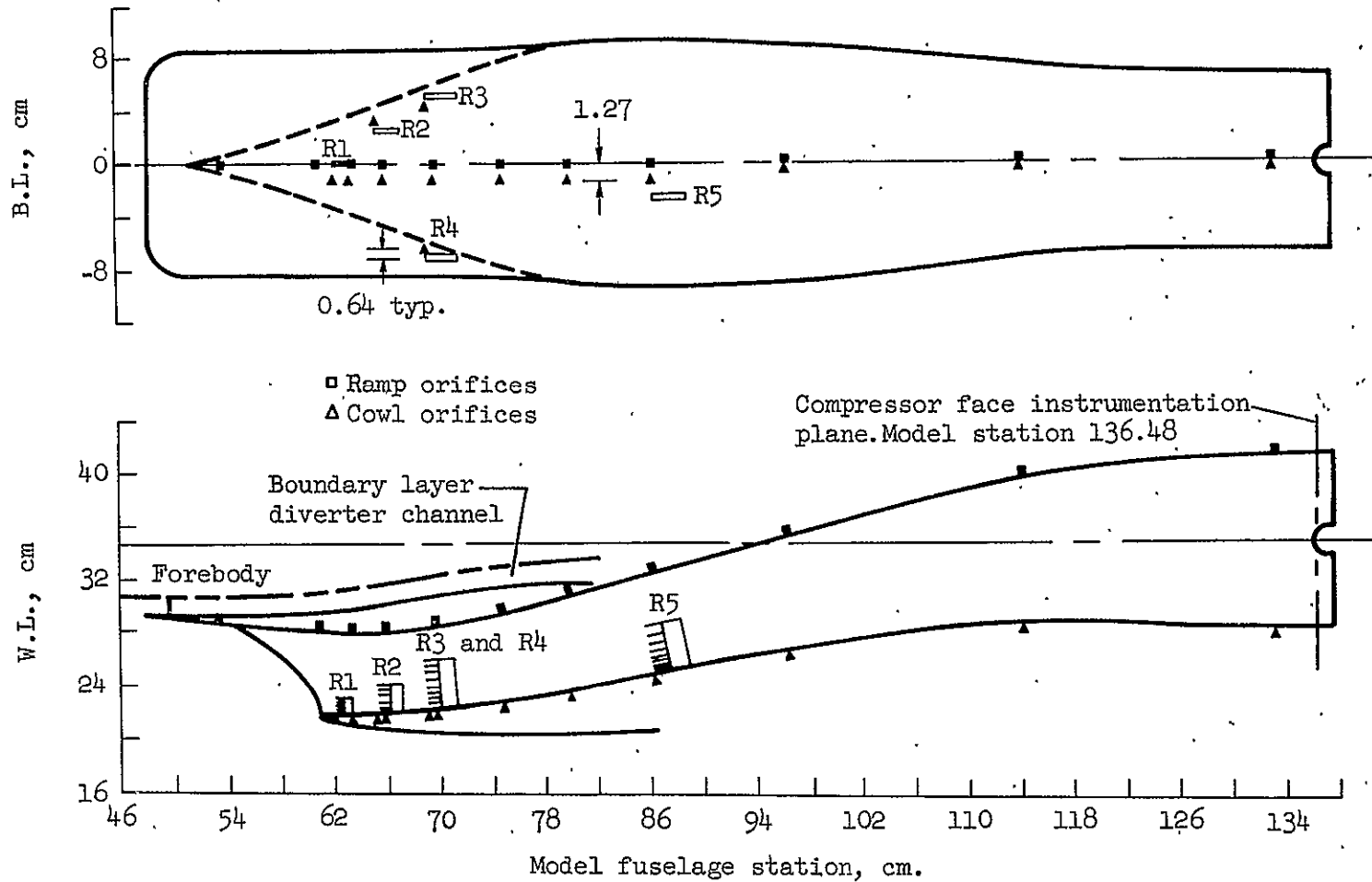
Figure 7.- Inlet cowl leading-edge slotted-flap.



Blowing lip ordinates

Lip station, x, cm	Lower surface, y, cm	Upper surface, y, cm
0.025	-0.079	0.051
0.051	-0.114	0.074
0.102	-0.150	0.086
0.114	—	0.053
0.152	-0.178	—
0.254	-0.208	0.097
0.381	-0.262	0.114
0.508	-0.295	—
0.521	—	0.125
0.635	-0.320	—
0.762	-0.343	—
3.810	straight line, -8°	straight line, 1°

Figure 8.- Inlet cowl leading-edge tangential blowing slot.



(a) Duct instrumentation.

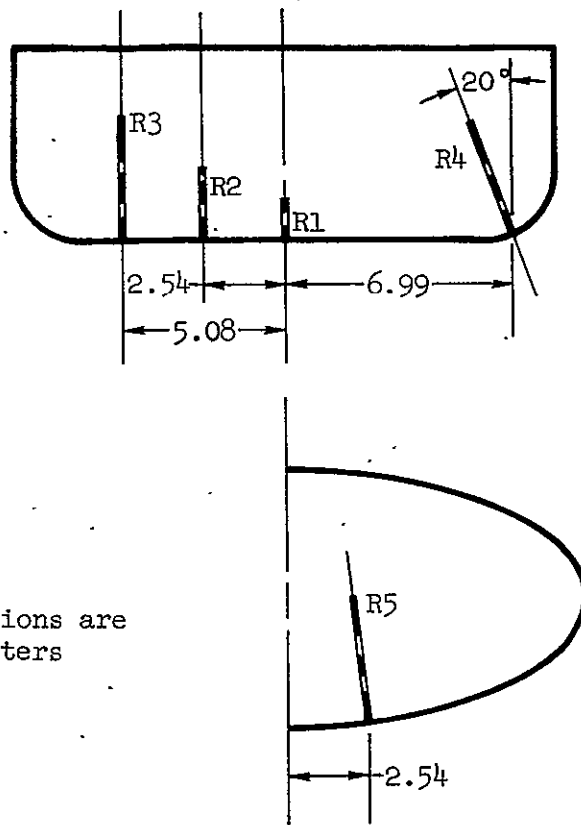
Figure 9.- Static-pressure orifice locations in subsonic diffuser.

Static orifice locations

Ramp orifice no.	Fuselage station, cm	Cowl orifice no.	Fuselage station, cm
D101	53.34	D201	62.23
D102	60.96	D202	63.37
D103	63.50	D203	65.41
D104	66.04	D204	66.04
D105	69.85	D205	69.22
D106	74.93	D206	69.22
D107	80.01	D207	69.85
D108	86.36	D208	74.93
D109	96.52	D209	80.01
D110	114.30	D210	86.36
D111	133.35	D211	96.52
—	—	D212	114.30
—	—	D213	133.35

(b) Static orifice locations.

Figure 9.- Concluded.

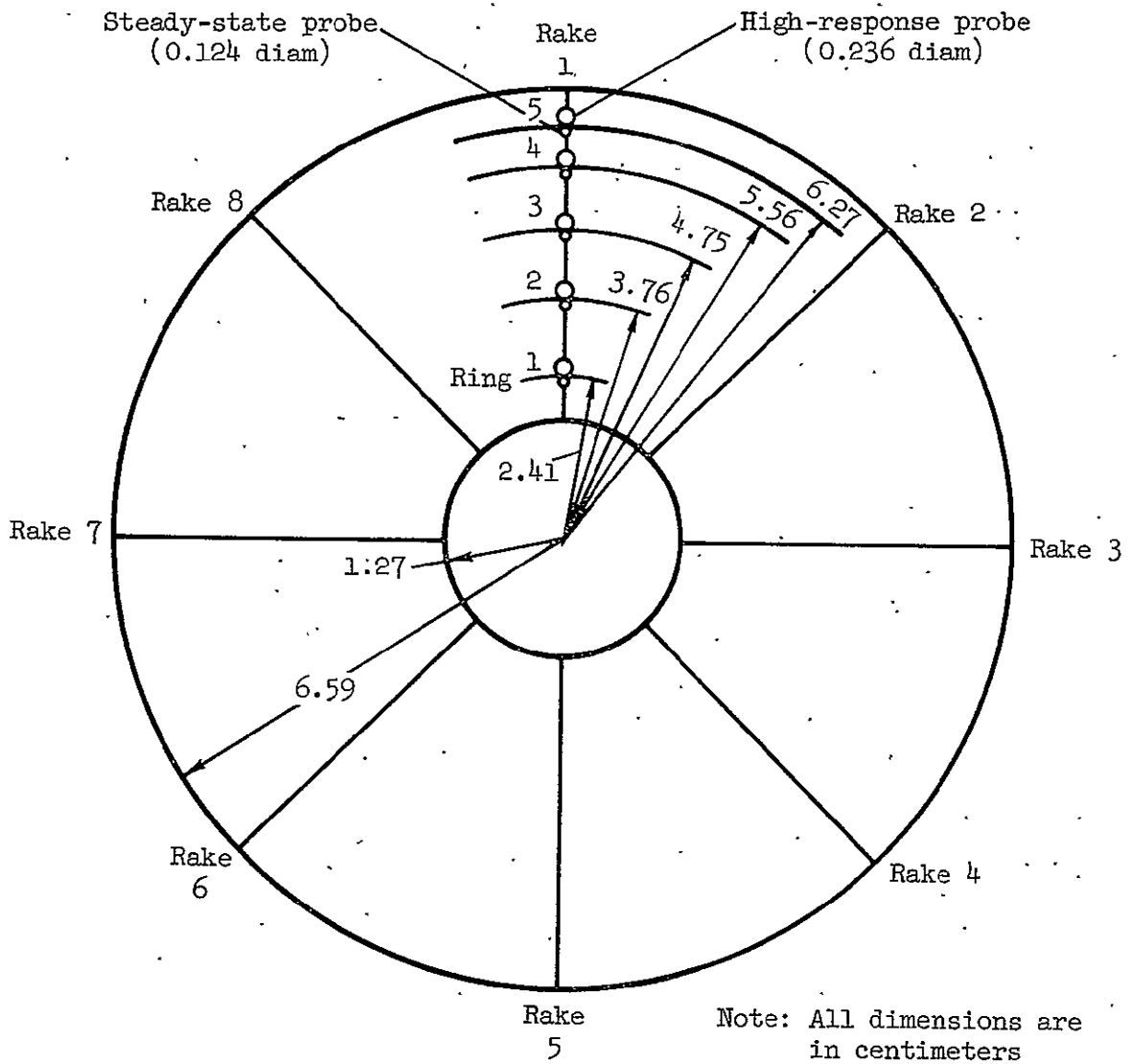


Note: All dimensions are in centimeters

Rake tube locations

Rake R1 Station 62.23	Rake R2 Station 65.41	Rake R3 Station 69.22	Rake R4 Station 69.22	Rake R5 Station 86.36	Height, cm
R101	R201	R301	R401	R501	0.046
R102	R202	R302	R402	R502	0.173
R103	R203	R303	R403	R503	0.351
R104	R204	R304	R404	R504	0.579
R105	R205	R305	R405	R505	0.884
R106	R206	R306	R406	R506	1.265
—	R207	R307	R407	R507	1.722
—	R208	R308	R408	R508	2.256
—	—	R309	R409	R509	2.967
—	—	R310	R410	R510	3.805

Figure 10.- Boundary-layer rake details.



Instrumentation plane; Model station 136.48

Figure 11. - Compressor face rake details



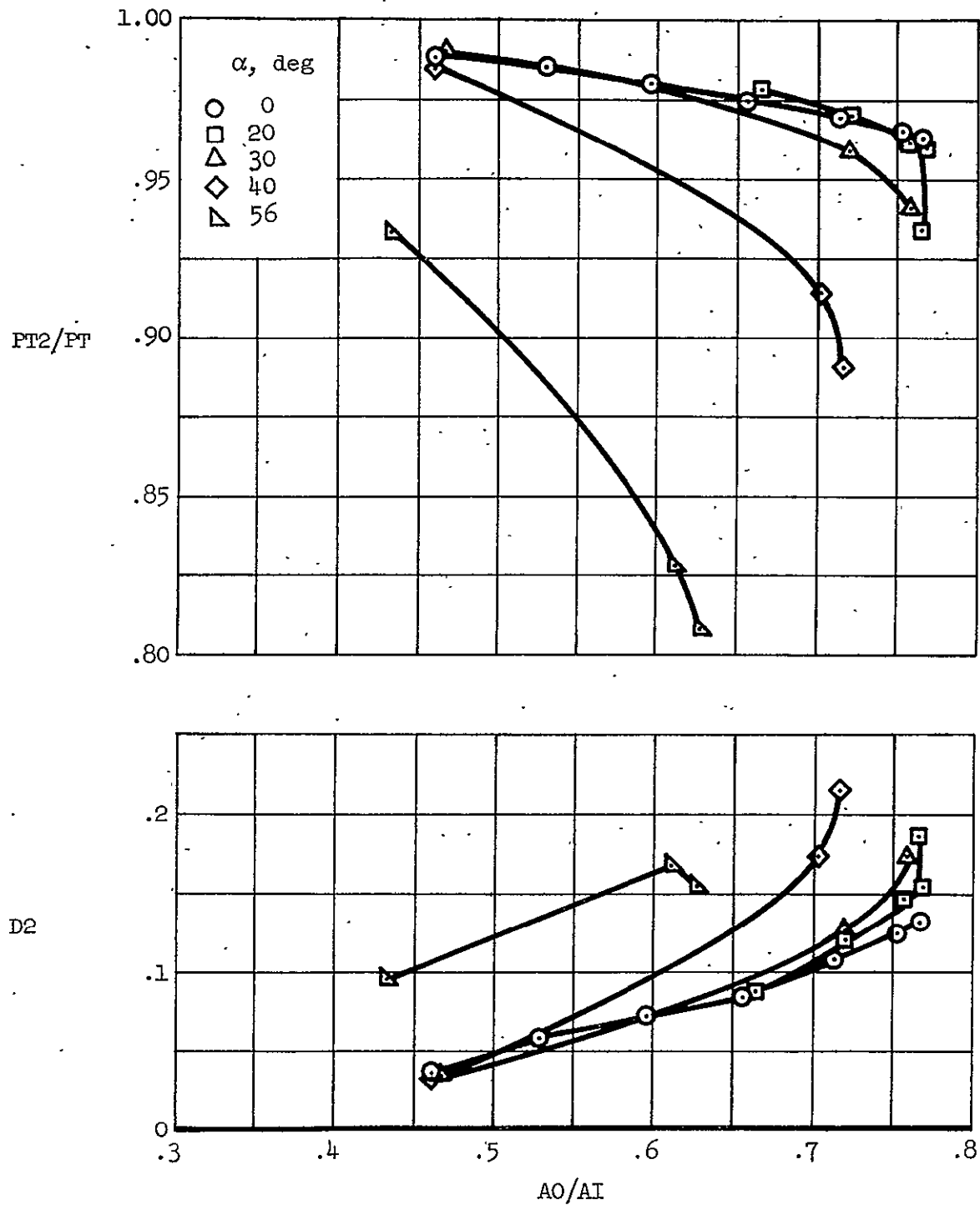
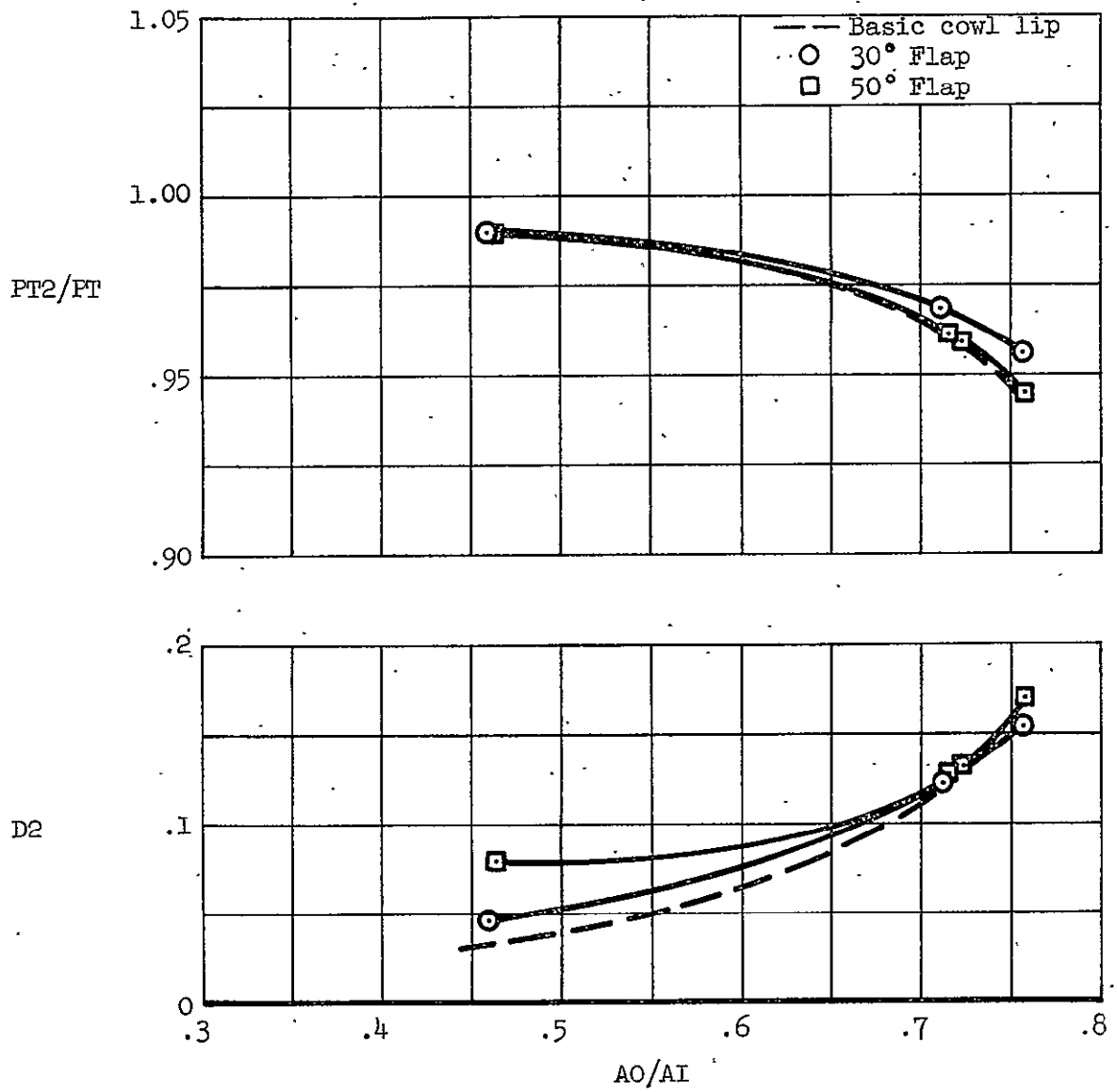
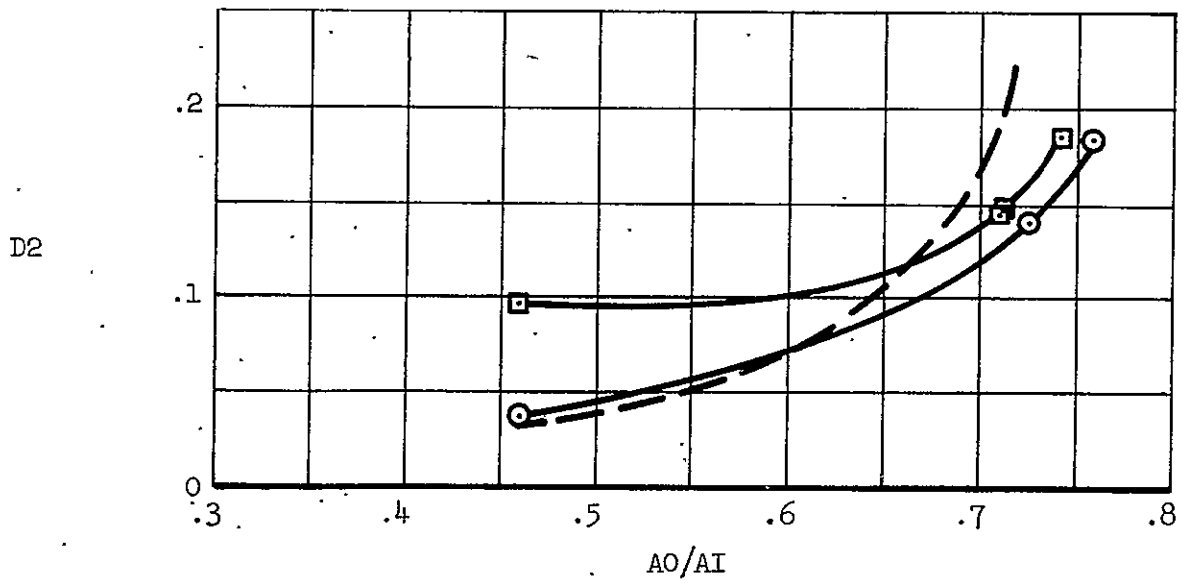
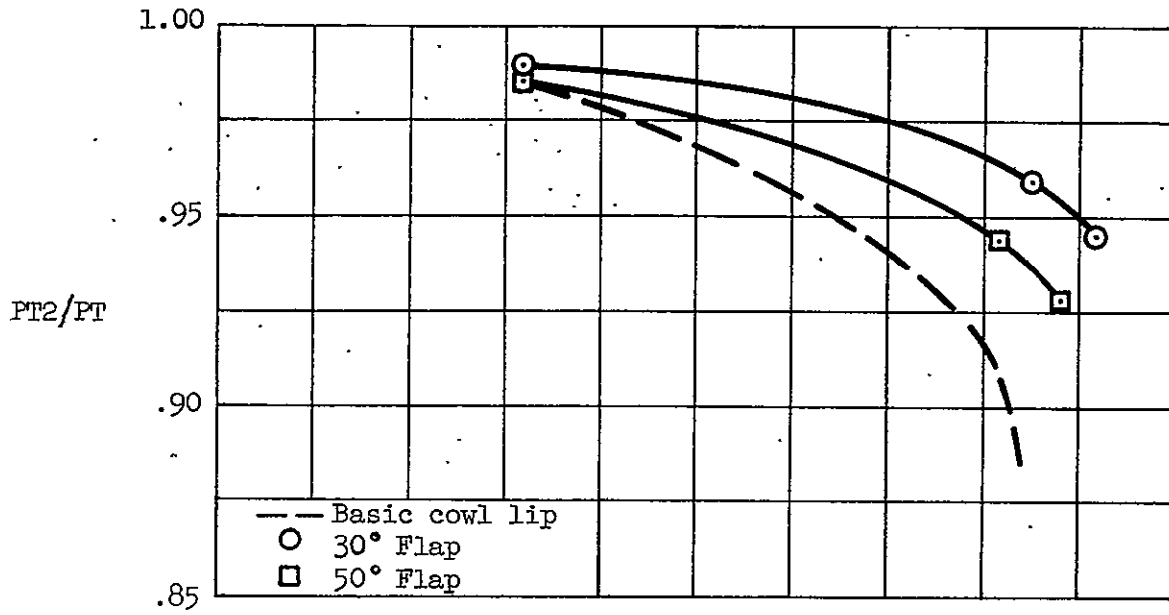


Figure 12.- Performance of isolated inlet with basic cowl lip;  $M = 0.9$ ,  $\beta = 0^\circ$ .



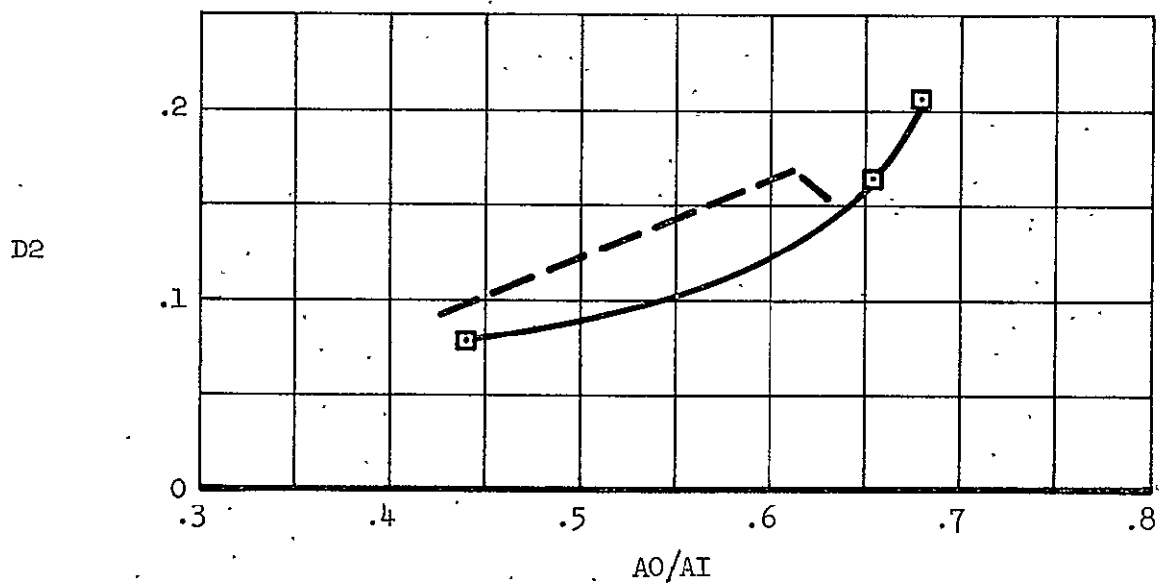
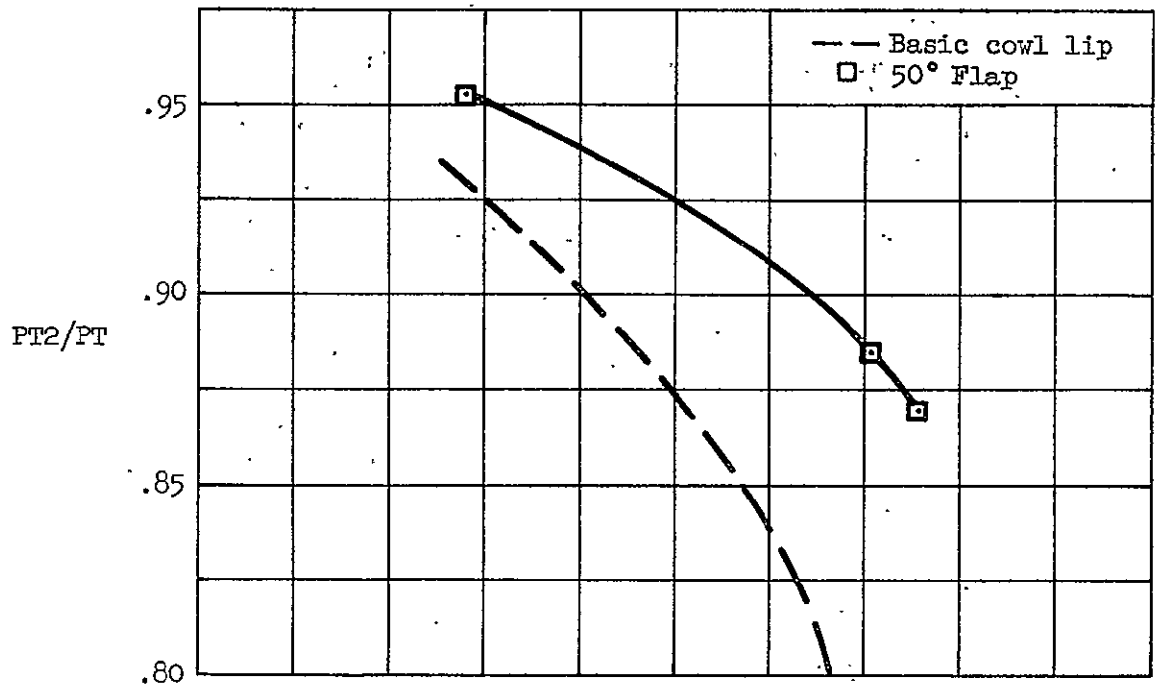
(a)  $\alpha = 30^\circ$

Figure 13.- Performance of isolated inlet with cowl flap;  $M = 0.9$ ,  
 $\beta = 0^\circ$ .



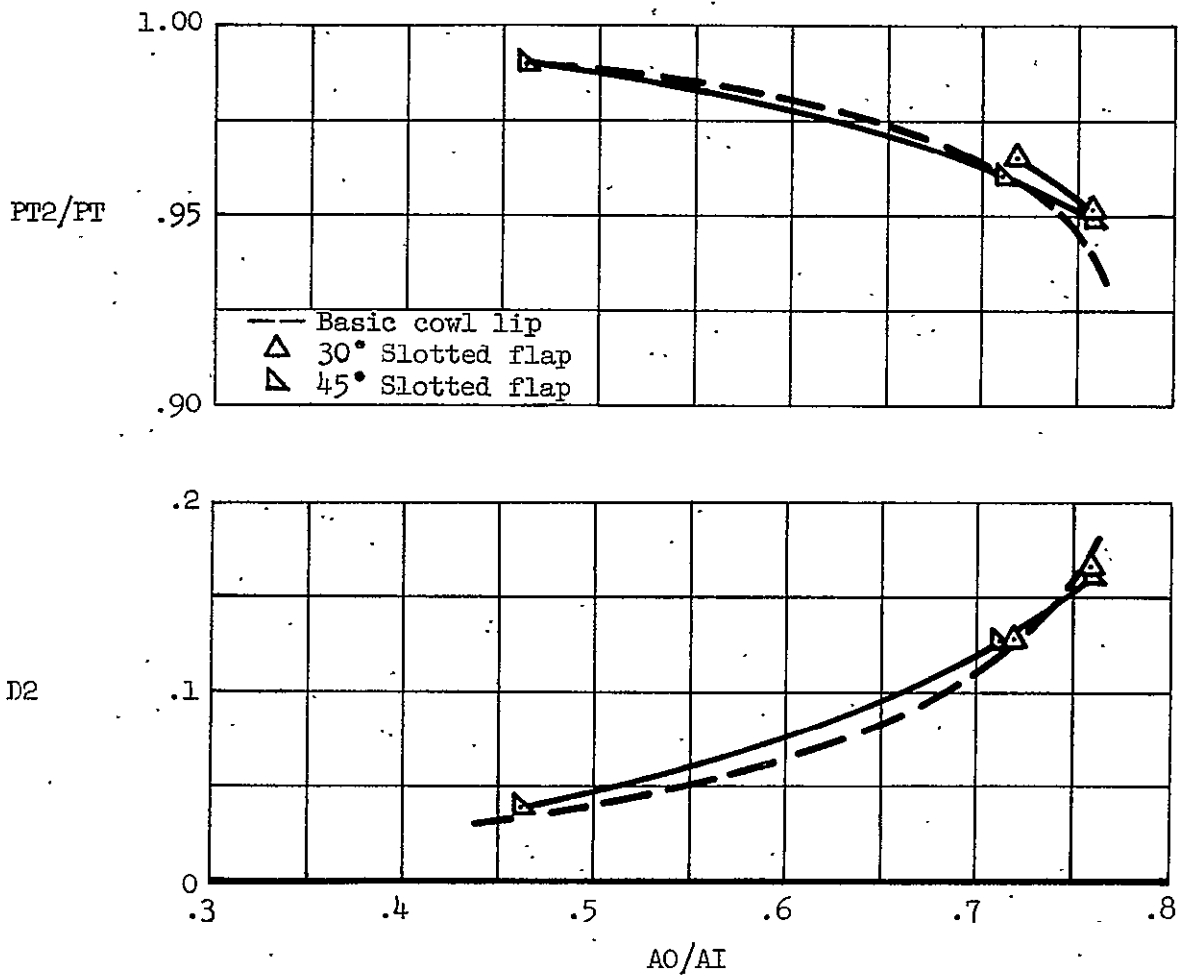
(b)  $\alpha = 40^\circ$

Figure 13.- Continued.



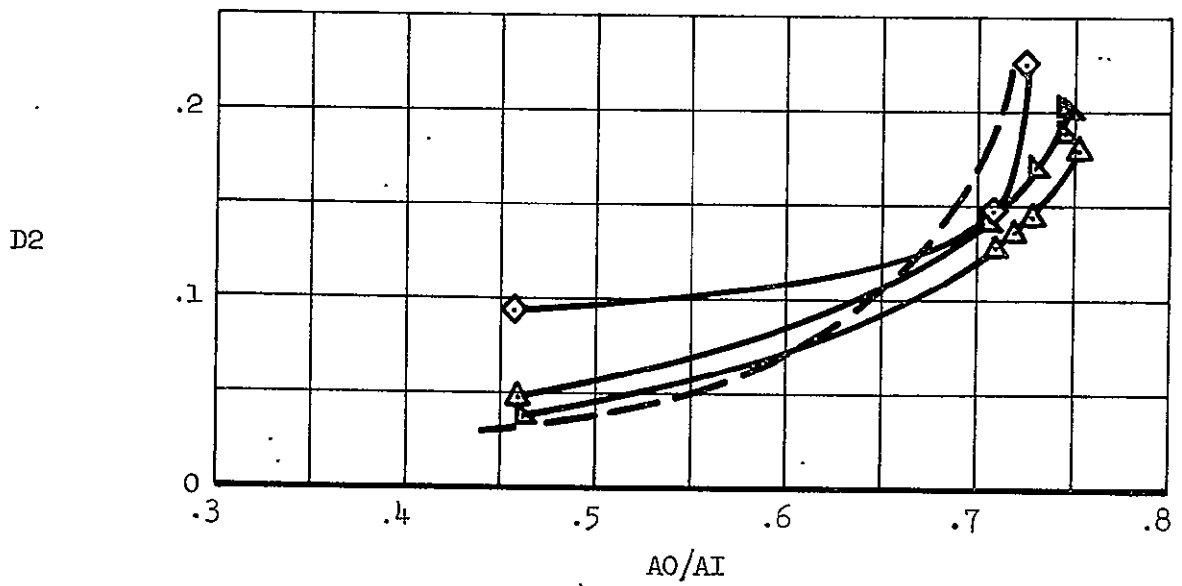
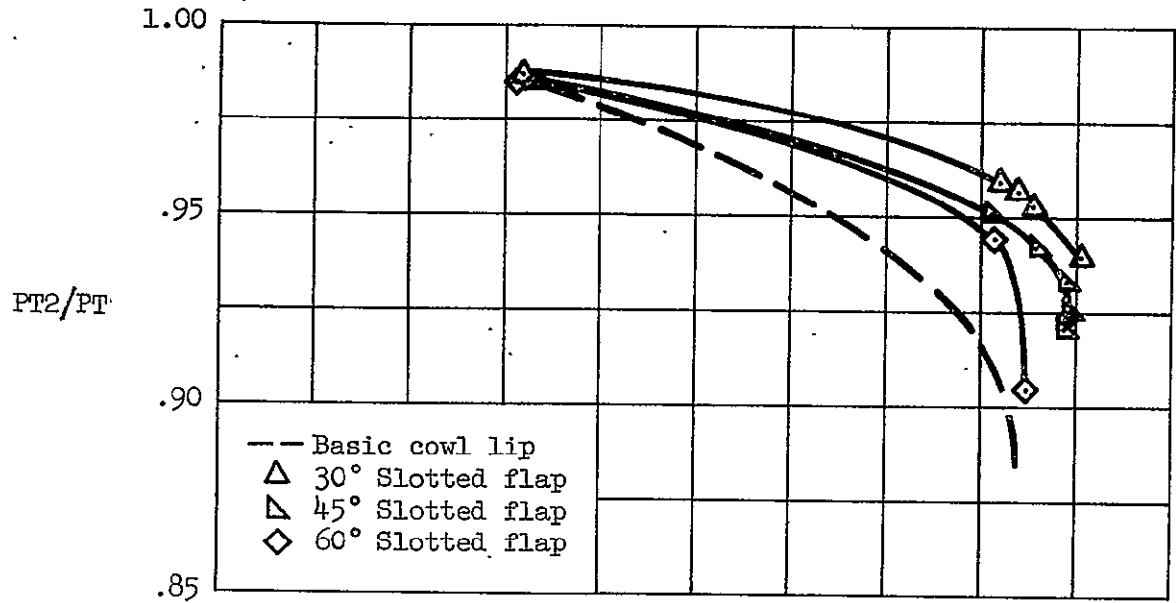
(c)  $\alpha = 56^\circ$

Figure 13.- Concluded.



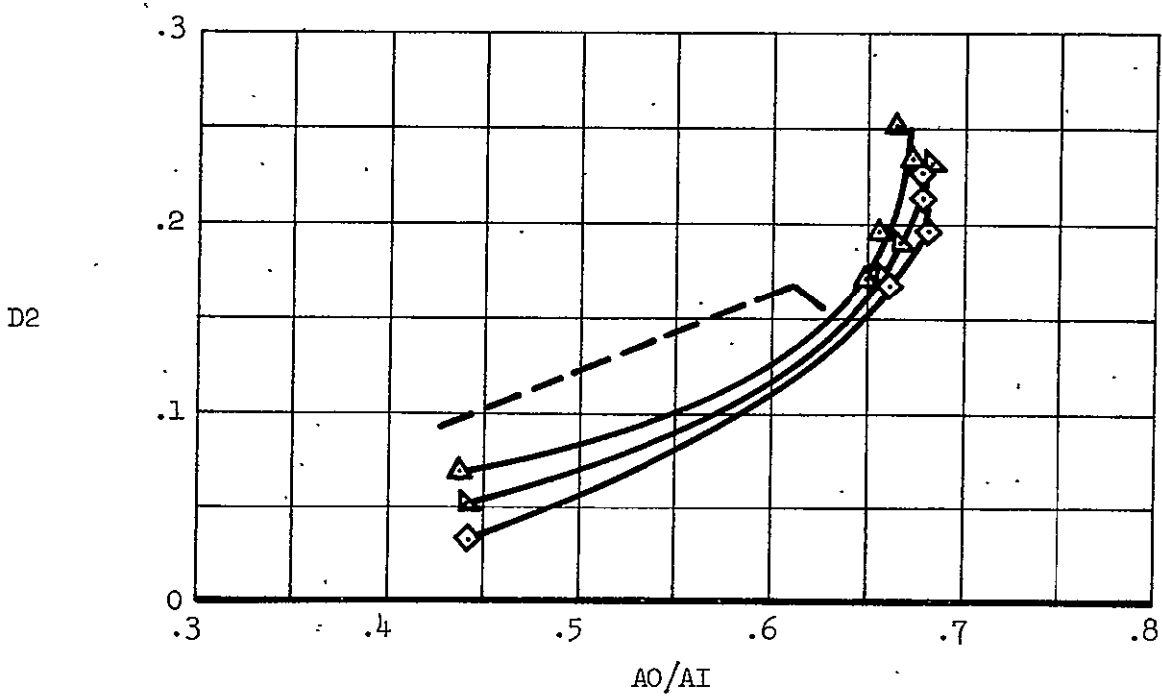
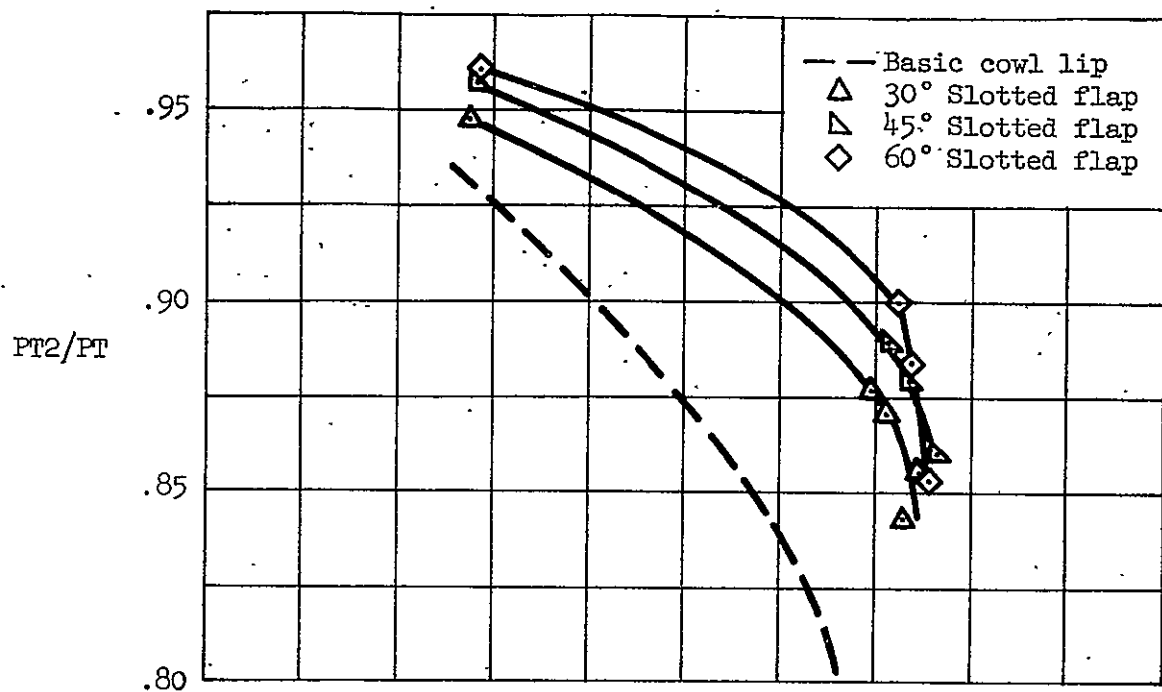
(a)  $\alpha = 30^\circ$

Figure 14.- Performance of isolated inlet with slotted cowl flap;  $M = 0.9$ ,  $\beta = 0^\circ$ .



(b)  $\alpha = 40^\circ$

Figure 14.- Continued.



(c)  $\alpha = 56^\circ$

Figure 14.- Concluded.

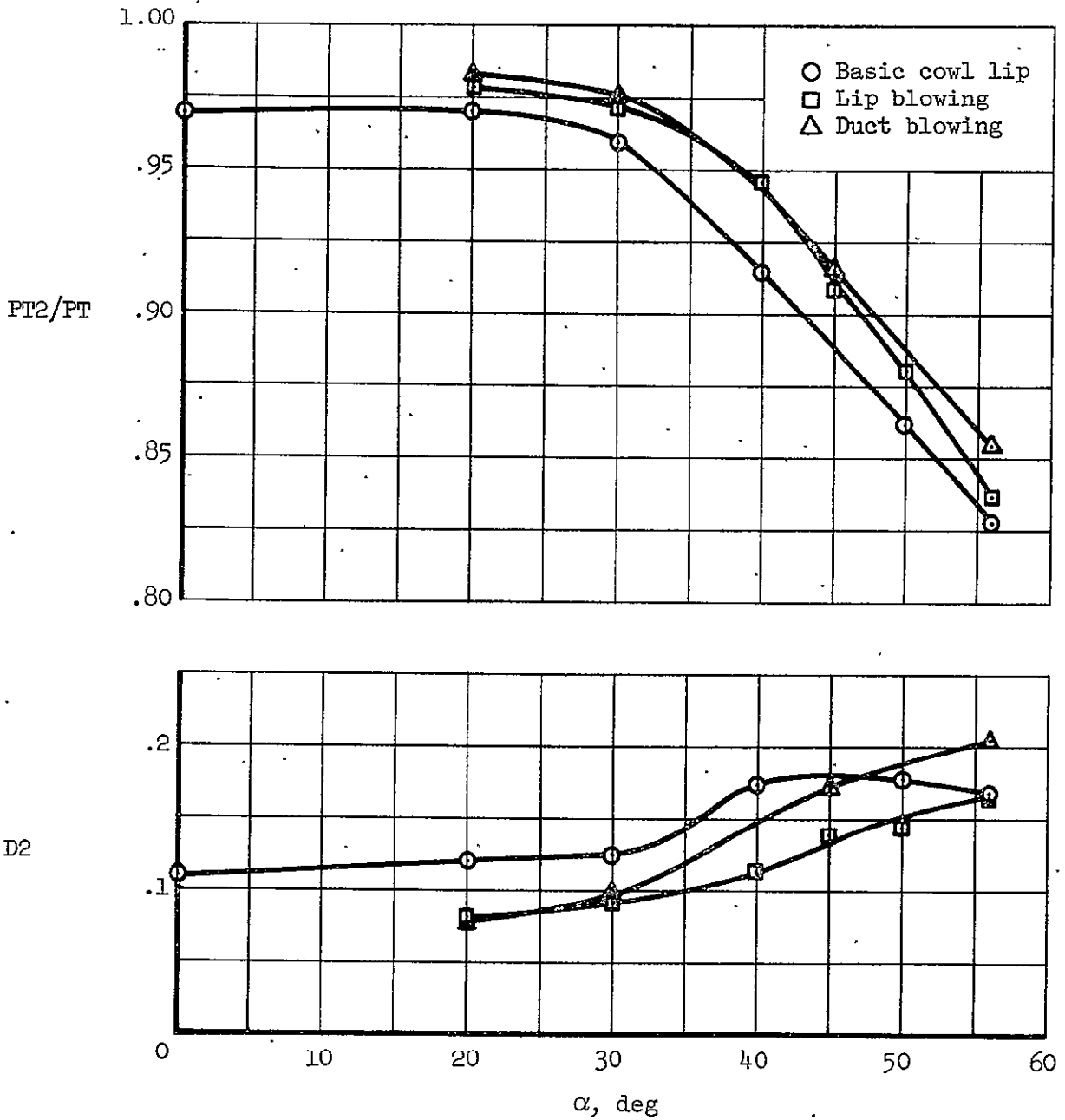
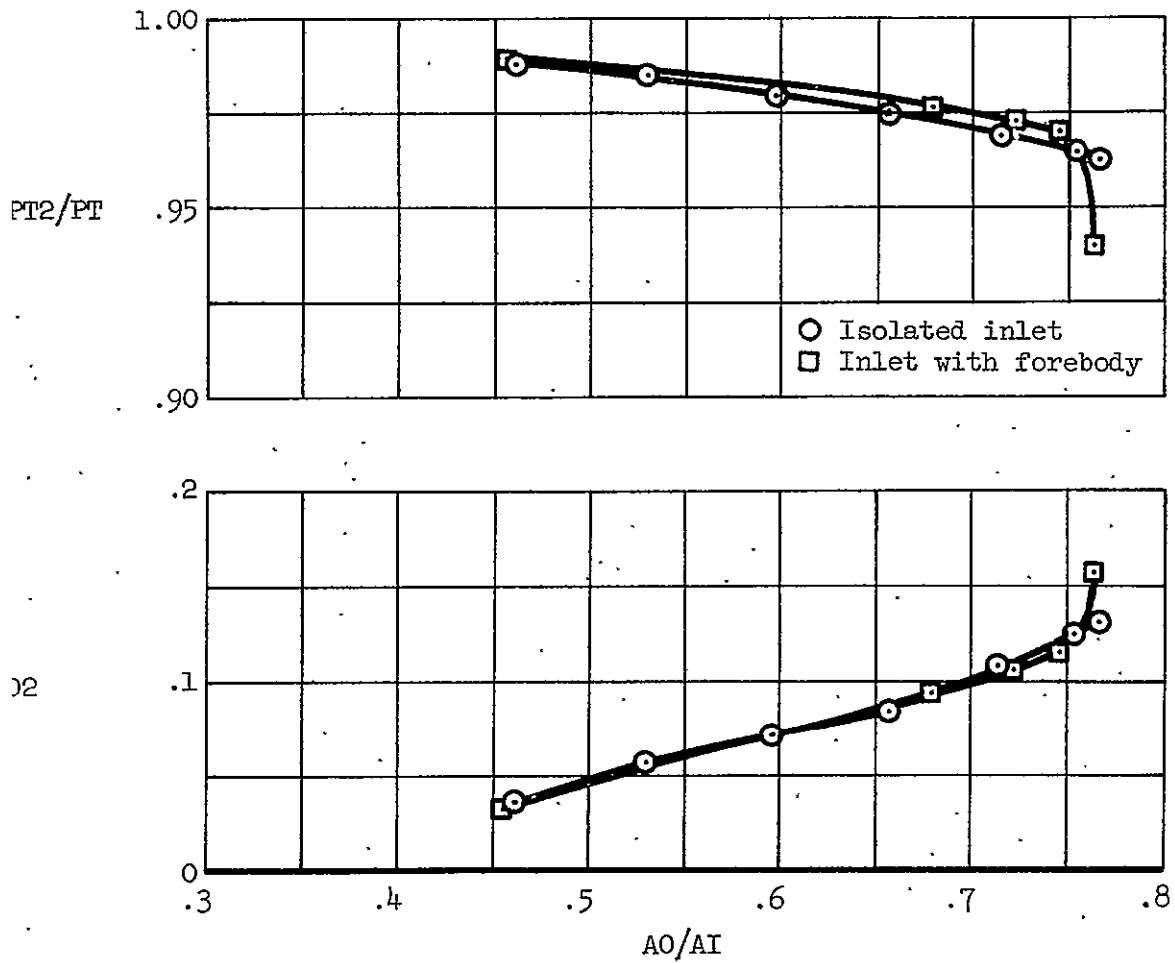


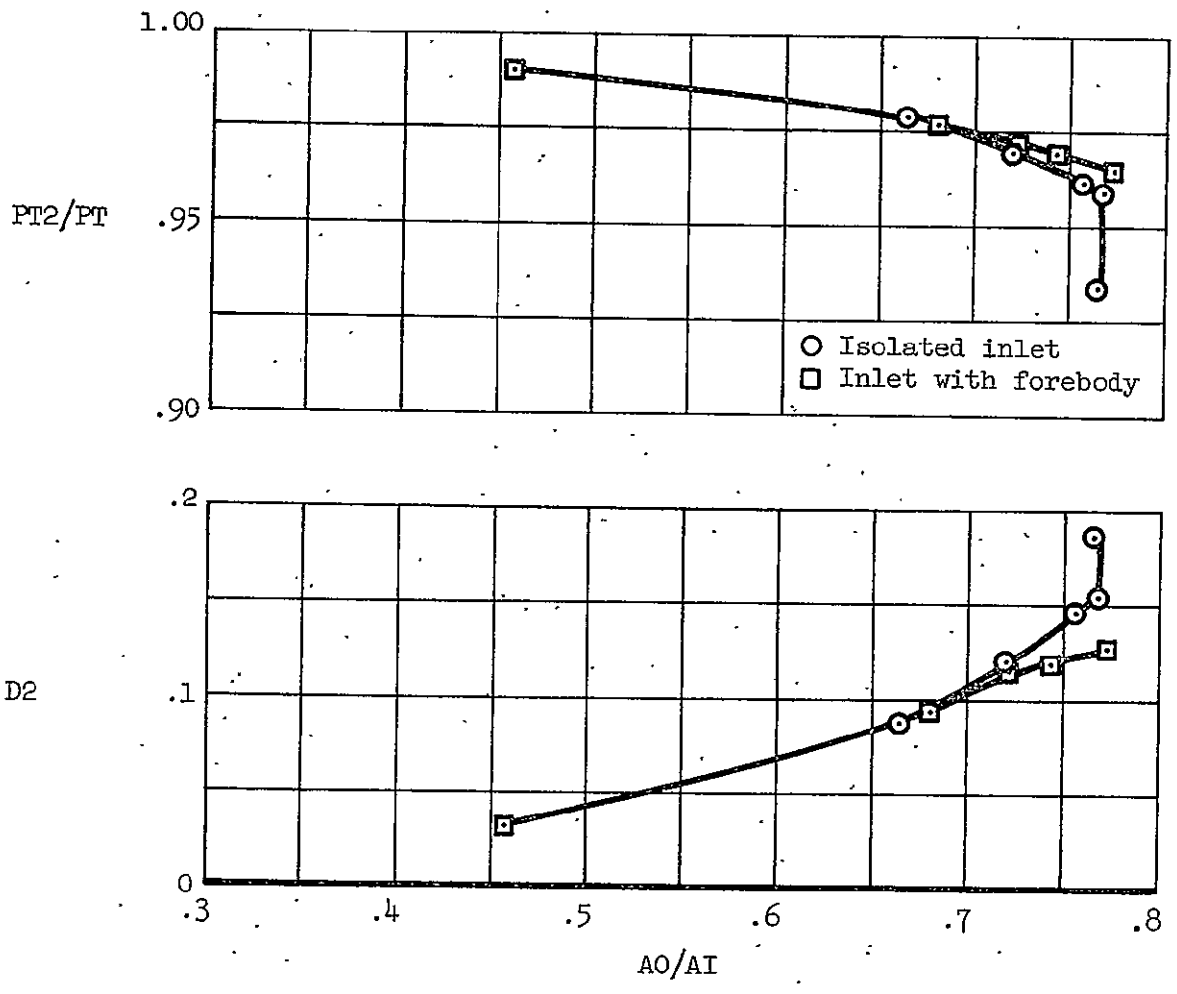
Figure 15.- Performance of isolated inlet with tangential blowing cowl slot and diffuser blowing;  $M = 0.9$ ,  $\beta = 0^\circ$ .





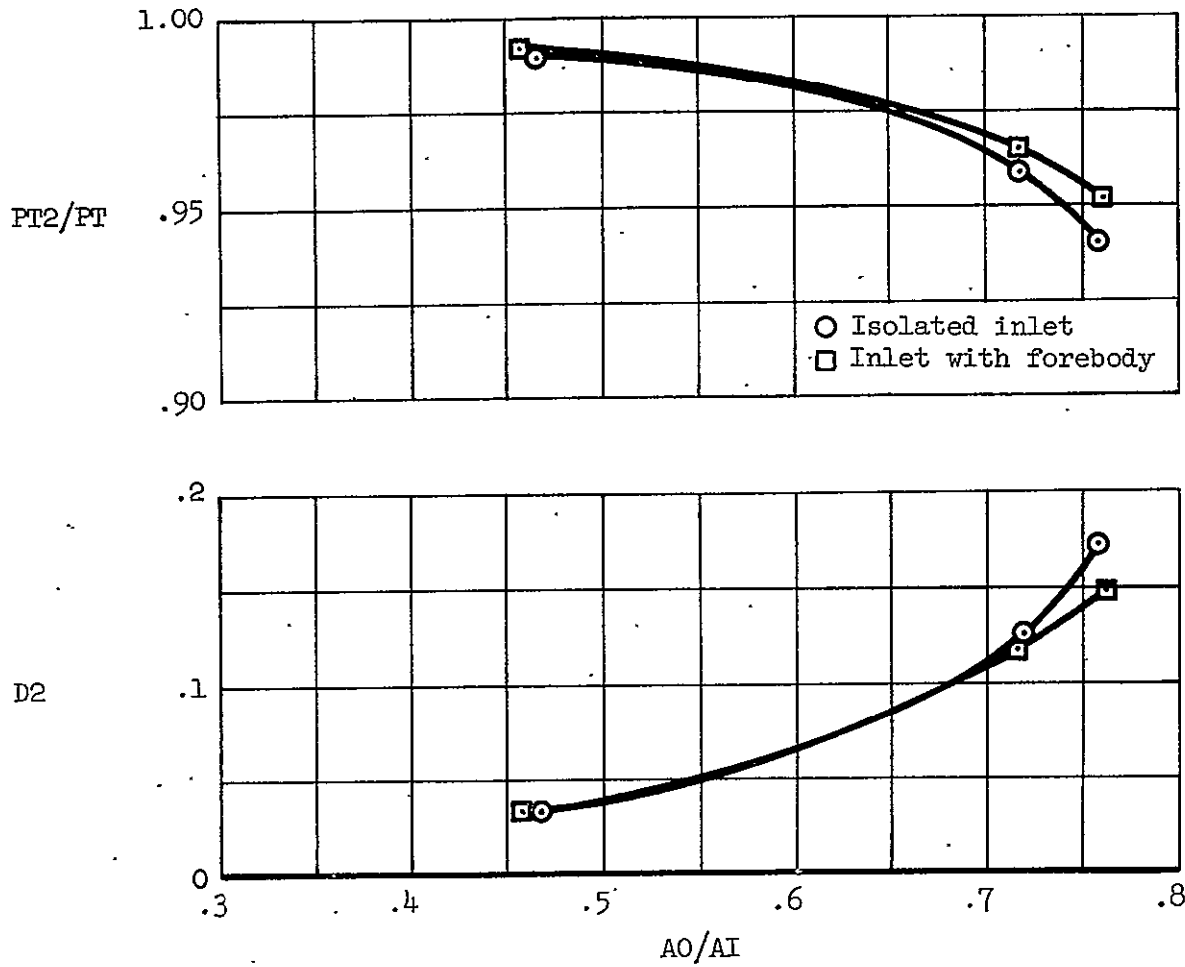
(a)  $\alpha = 0^\circ$

Figure 16.- Performance of inlet with basic cowl lip and forebody;  $M = 0.9$ ,  $\beta = 0^\circ$ .



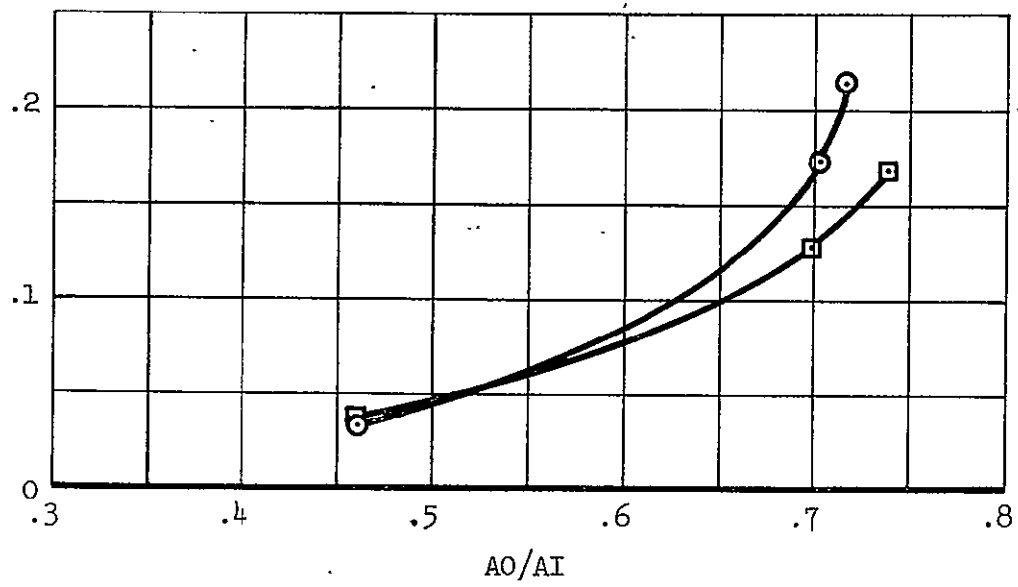
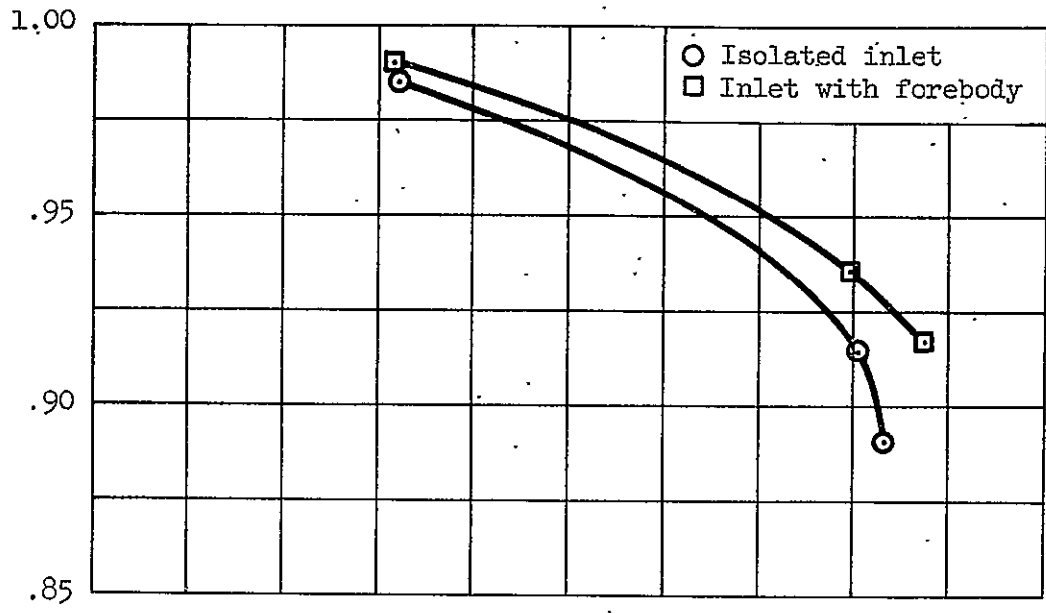
(b)  $\alpha = 20^\circ$

Figure 16.- Continued.



(c)  $\alpha = 30^\circ$

Figure 16.- Continued.



(d)  $\alpha = 40^\circ$

Figure 16.- Concluded.

APPENDIX  
SAMPLE OF TABULATED DATA

TST-161 PH-1 TN-14 17:93

IO-PRESSOUT1

03 MAY 76@18:56

RUN:SEQ  
17:93

CONF	MACH	Q	PT	P	TTR	TR	RN/FT	ALPHA	BETA	PREF	WC2	PT2/PT	AO/AI	D2	PTRMS	MTH	FLAP/SLAT
1	0.901	712.7	2125	1255	574.8	494.6	4.031	0.28	0.11	1418	244.0	0.9629	0.7660	0.1305	0.0000	0.856	0

GX1	DX1	DX2	KA2	KC2	KRA2	PERCENT	WC2	QI/PT2	KTHETA	DS	KTHETAS
0.0000	0.2735	0.0520	0.1914	0.0765	0.1893	112.4	0.1884	0.0517	36.48	0.0517	

(AN/NSQRPT)MAX	RING1	RING2	RING3	RING4	RING5	THETA	RING1	RING2	RING3	RING4	RING5
	0.0039	0.0097	0.0141	0.0113	0.0125		82.83	99.89	87.51	121.6	108.8

ID	IDCMAX	IDRMAX	IDC1	IDC2	IDC3	IDC4	IDC5	IDCHUB	IDCTIP	IDR1	IDR2	IDR3	IDR4	IDR5
0.8216	0.0391	0.0603	0.0131	0.0191	0.0262	0.0458	0.0323	0.0161	0.0391	0.0354	0.0261	0.0129	0.0141	0.0603

PA1/P	PA1/PDX	WA1/W2	CMU10	CMU11	VIA10	VIA11	PA2/P	PA2/PDY	WA2/W2	CMU20	CMU21	VIA20	VIA21	(WA1+WA2)/W2	CMU0	CMU1
0.0000	0.0000	0.0000	0.0000	0.0000	0.0000	0.0000	0.0000	0.0000	0.0000	0.0000	0.0000	0.0000	0.0000	0.0000	0.0000	0.0000

(PT2R/PT2)BASE	RING1	RING2	RING3	RING4	RING5	(PT2R/PT2)MEAS	RING1	RING2	RING3	RING4	RING5
	1.075	1.054	1.036	0.9373	0.8978		1.035	1.026	1.013	0.9859	0.9397

A MINUS SIGN INDICATES A BAD COMPRESSOR FACE PRESSURE

CF101	CF102	CF103	CF104	CF105	CF106	CF107	CF108	CF201	CF202	CF203	CF204	CF205	CF206	CF207	CF208
0.9989	0.9992	0.9844	0.9974	0.9994	0.9989	0.9988	0.9990	0.9936	0.9982	0.9896	0.9883	0.9915	0.9753	0.9695	0.9977
CF301	CF302	CF303	CF304	CF305	CF306	CF307	CF308	CF401	CF402	CF403	CF404	CF405	CF406	CF407	CF408
0.9898	0.9780	0.9615	0.9824	0.9501	0.9646	0.9891	0.9868	0.9514	0.9325	0.9666	0.9541	0.9051	0.9425	0.9952	0.9464
CF501	CF502	CF503	CF504	CF505	CF506	CF507	CF508	PT1	SPF1	SPF2	SPF3	SPF4			
0.9151	0.8956	0.9305	0.8953	0.8737	0.8898	0.9377	0.9010								

R101	R102	R103	R104	R105	R106	R201	R202	R203	R204	R205	R206	R207	R208	
0.9993	0.9993	0.9993	0.9994	0.9983	0.9993	0.9954	0.9993	0.9995	0.9991	0.9985	0.9985	0.9985	0.9988	
R301	R302	R303	R304	R305	R306	R307	R308	R309	R310	R401	R402	R403	R404	R405
0.8866	0.9254	0.9248	0.9935	0.9991	0.9991	0.9992	0.9994	0.9988	0.9992	0.9202	0.9990	0.9976	0.9986	0.9985
R406	R407	R408	R409	R410	R501	R502	R503	R504	R505	R506	R507	R508	R509	R510
0.9992	0.9993	0.9996	0.9991	0.9992	0.8420	0.8646	0.9027	0.9435	0.9786	0.9986	0.9991	0.9986		0.9993

P301	P302	P303	P304	P305	P306	P307	P308	P3/PT2	PD101	PD102	PD103	PD104	PD105	PD106	PD107	
0.5701	0.5774	0.5809	0.5703	0.5678	0.5411	0.5567	0.5800	0.5899	0.6815	0.6745	0.6097	0.5706	0.6147	0.6883	0.7232	
PD108	PD109	PD110	PD111	PD201	PD202	PD203	PD204	PD205	PD206	PD207	PD208	PD209	PD210	PD211	PD212	PD213
0.7446	0.7686	0.8138	0.8219	0.7200	0.6621	0.6797	0.6540	0.6932	0.7248	0.6799	0.7185	0.7240	0.7394	0.7456	0.7840	0.8121

TST-161 PH-1 TN-14 17:94

ID-PRESSOUT1

03 MAY 76@18:56

RUN:SEQ  
17:94

CONF	MACH	Q	PT	P	TTR	TR	RN/FT	ALPHA	BETA	PREF	WC2	PT2/PT	AO/AI	D2	PT RMS	MTH	FLAP/SLAT
1	0.901	713.1	2125	1255	574.7	494.5	4.032	0.28	0.13	1418	226.0	0.9689	0.7138	0.1086	0.0000	0.723	0

GX1	DX1	DX2	KA2	KC2	KRA2	PERCENT	WC2	QI/PT2	KTHETA	DS	KTHETAS
0.0000	0.6551	0.0222	0.5316	0.0326	0.2441	104.1	0.1611	0.0343	28.38	0.0305	

(AN/NSQRPT)MAX	RING1	RING2	RING3	RING4	RING5	THETA	RING1	RING2	RING3	RING4	RING5
	0.0033	0.0044	0.0076	0.0074	0.0061		86.35	168.4	101.6	0.0000	0.0000

ID	IDCMAX	IDRMAX	IDC1	IDC2	IDC3	IDC4	IDC5	IDCHUB	IDCTIP	IDR1	IDR2	IDR3	IDR4	IDR5
0.6522	0.0248	0.0504	0.0098	0.0061	0.0233	0.0230	0.0266	0.0080	0.0248	0.0296	0.0232	0.0112	0.0137	0.0504

PA1/P	PA1/PDX	WA1/W2	CMU10	CMU11	VIA10	VIA11	PA2/P	PA2/PDY	WA2/W2	CMU20	CMU21	VIA20	VIA21	(WA1+WA2)/W2	CMU0	CMUL
0.0000	0.0000	0.0000	0.0000	0.0000	0.0000	0.0000	0.0000	0.0000	0.0000	0.0000	0.0000	0.0000	0.0000	0.0000	0.0000	0.0000

(PT2R/PT2)BASE	RING1	RING2	RING3	RING4	RING5	(PT2R/PT2)MEAS	RING1	RING2	RING3	RING4	RING5
	1.074	1.054	1.036	0.9385	0.8980		1.030	1.023	1.011	0.9863	0.9496

A MINUS SIGN INDICATES A BAD COMPRESSOR FACE PRESSURE

CF101	CF102	CF103	CF104	CF105	CF106	CF107	CF108	CF201	CF202	CF203	CF204	CF205	CF206	CF207	CF208
0.9996	0.9993	0.9880	0.9970	0.9987	0.9992	0.9995	0.9993	-0.9861	0.9977	0.9981	-0.9894	0.9911	0.9858	0.9855	0.9977
CF301	CF302	CF303	CF304	CF305	CF306	CF307	CF308	CF401	CF402	CF403	CF404	CF405	CF406	CF407	CF408
0.9762	0.9815	0.9906	0.9841	0.9571	0.9731	0.9851	0.9903	0.9334	0.9426	0.9762	0.9648	0.9231	0.9537	0.9960	0.9556
CF501	CF502	CF503	CF504	CF505	CF506	CF507	CF508	PT1	SPF1	SPF2	SPF3	SPF4			
0.9084	0.9100	0.9519	0.9126	0.8944	0.9145	0.9481	0.9211								

R101	R102	R103	R104	R105	R106	R201	R202	R203	R204	R205	R206	R207	R208
0.9992	0.9994	0.9993	0.9996	0.9988	0.9992	0.9964	0.9993	0.9998	0.9993	0.9987	0.9996	0.9992	0.9987
R301	R302	R303	R304	R305	R306	R307	R308	R309	R310	R401	R402	R403	R404
0.9225	0.9504	0.9556	0.9976	0.9992	0.9994	0.9992	0.9998	0.9991	0.9990	0.9728	0.9994	0.9985	0.9993
R406	R407	R408	R409	R410	R501	R502	R503	R504	R505	R506	R507	R508	R509
0.9995	0.9995	0.9997	0.9993	0.9995	0.8716	0.8897	0.9206	0.9582	0.9888	0.9992	0.9992	0.9986	0.9995

P301	P302	P303	P304	P305	P306	P307	P308	P3/PT2	PD101	PD102	PD103	PD104	PD105	PD106	PD107
0.5870	0.6054	0.6094	0.5950	0.5946	0.5658	0.5857	0.6067	0.6127	0.6918	0.7182	0.6838	0.6688	0.6940	0.7455	0.7719
PD108	PD109	PD110	PD111	PD201	PD202	PD203	PD204	PD205	PD206	PD207	PD208	PD209	PD210	PD211	PD212
0.7891	0.8064	0.8435	0.8488	0.7772	0.7359	0.7460	0.7334	0.7540	0.7808	0.7490	0.7713	0.7735	0.7831	0.7872	0.8194
															0.8413

TST-161 PH-1 TN-14 17:95

ID-PRESSOUT1

03 MAY 76a18:56

RUN:SEQ  
17:95

CONF	MACH	Q	PT	P	TTR	TR	RN/FT	ALPHA	BETA	PREF	WC2	PT2/PT	AO/AI	D2	PTRMS	MTH	FLAP/SLAT				
1	0.901	712.7	2125	1255	576.2	495.8	4.018	0.25	0.14	1417	206.4	0.9751	0.6563	0.0843	0.0000	0.617	0				
GX1	DX1	DX2	KA2	KC2	KRA2	PERCENT	WC2	QI/PT2	KTHETA	DS	KTHETAS										
0.0000	0.1419	0.6175	0.1919	0.0257	0.0777	95.13	0.1324	0.0287	27.60	0.0218											
(AN/NSQRPT)MAX	RING1		RING2		RING3		RING4		RING5		THETA	RING1		RING2		RING3		RING4		RING5	
	0.0024		0.0020		0.0045		0.0061		0.0055			83.18		152.3		90.63		0.0000		0.0000	
ID	IDCMAX	IDRMAX	IDC1	IDC2	IDC3	IDC4	IDC5	IDCHUB	IDCTIP	IDR1	IDR2	IDR3	IDR4	IDR5							
0.5373	0.0234	0.0402	0.0078	0.0102	0.0195	0.0275	0.0192	0.0090	0.0234	0.0235	0.0187	0.0085	0.0104	0.0402							
PA1/P	PA1/PDX	WA1/W2	CMU10	CMU11	VIA10	VIA11	PA2/P	PA2/PDY	WA2/W2	CMU20	CMU21	VIA20	VIA21	(WA1+WA2)/W2	CMU0	CMUL					
0.0000	0.0000	0.0000	0.0000	0.0000	0.0000	0.0000	0.0000	0.0000	0.0000	0.0000	0.0000	0.0000	0.0000	0.0000	0.0000	0.0000					
(PT2R/PT2)BASE	RING1		RING2		RING3		RING4		RING5		(PT2R/PT2)MEAS	RING1		RING2		RING3		RING4		RING5	
	1.027		1.029		1.022		0.9738		0.9463			1.023		1.019		1.008		0.9896		0.9598	

A MINUS SIGN INDICATES A BAD COMPRESSOR FACE PRESSURE

CF101	CF102	CF103	CF104	CF105	CF106	CF107	CF108	CF201	CF202	CF203	CF204	CF205	CF206	CF207	CF208	
0.9993	0.9993	0.9905	0.9982	0.9992	0.9992	0.9993	0.9993	-0.9834	0.9986	0.9986	-0.9925	0.9926	0.9897	0.9929	0.9983	
CF301	CF302	CF303	CF304	CF305	CF306	CF307	CF308	CF401	CF402	CF403	CF404	CF405	CF406	CF407	CF408	
0.9716	0.9890	0.9911	0.9886	0.9644	0.9810	0.9868	0.9946	0.9382	0.9599	0.9801	0.9723	0.9421	0.9621	0.9966	0.9689	
CF501	CF502	CF503	CF504	CF505	CF506	CF507	CF508	PT1	SPF1	SPF2	SPF3	SPF4				
0.9190	0.9293	0.9618	0.9303	0.9172	0.9299	0.9617	0.9380									
R101	R102	R103	R104	R105	R106	R201	R202	R203	R204	R205	R206	R207	R208			
0.9993	0.9995	0.9994	0.9994	0.9984	0.9997	0.9979	0.9994	0.9993	0.9992	0.9990	0.9992	0.9988	0.9996			
R301	R302	R303	R304	R305	R306	R307	R308	R309	R310	R401	R402	R403	R404	R405		
0.9425	0.9668	0.9738	0.9989	0.9996	0.9996	0.9995	0.9994	0.9988	0.9993	0.9850	0.9994	0.9992	0.9990	0.9987		
R406	R407	R408	R409	R410	R501	R502	R503	R504	R505	R506	R507	R508	R509	R510		
0.9996	0.9996	0.9997	0.9991	0.9998	0.9035	0.9196	0.9465	0.9705	0.9935	0.9991	0.9988	0.9988		0.9993		
P301	P302	P303	P304	P305	P306	P307	P308	P3/PT2	PD101	PD102	PD103	PD104	PD105	PD106	PD107	
0.6068	0.6313	0.6382	0.6201	0.6226	0.5934	0.6126	0.6328	0.6355	0.7095	0.7624	0.7489	0.7442	0.7625	0.7994	0.8184	
PD108	PD109	PD110	PD111	PD201	PD202	PD203	PD204	PD205	PD206	PD207	PD208	PD209	PD210	PD211	PD212	PD213
0.8316	0.8450	0.8732	0.8766	0.8300	0.7975	0.8019	0.7934	0.8088	0.8291	0.8059	0.8206	0.8206	0.8268	0.8293	0.8531	0.8721





TST-161 PH-1 TN-14 17:97

ID-PRESSOUT1

03 MAY 76 218:56

RUN:SEQ  
17:97

CONF	MACH	Q	PT	P	TTR	TR	RN/FT	ALPHA	BETA	PREF	WC2	PT2/PT	AO/AI	D2	PT RMS	MTH	FLAP/SLAT
1	0.898	710.2	2124	1259	575.1	495.3	4.022	0.27	0.14	1418	164.7	0.9846	0.5291	0.0575	0.0000	0.449	0
GX1	DX1	DX2	KAZ	KC2	KRA2	PERCENT	WC2	QI/PT2	KTHETA	DS	KTHETAS						
0.0000	0.2622	0.0552	1.8948	0.0812	0.2276	75.91	0.0804	0.0432	26.05	0.0378							
(AN/NSQRPT)MAX - RING1 RING2 RING3 RING4 RING5 THETA- - RING1 RING2 RING3 RING4 RING5																	
0.0014 0.0038 0.0046 0.0049 0.0039 83.76 74.47 71.31 0.0000 0.0000																	
ID	IDCMAX	IDRMAX	IDC1	IDC2	IDC3	IDC4	IDC5	IDCHUB	IDCTIP	IDR1	IDR2	IDR3	IDR4	IDR5			
0.3399	0.0245	0.0215	0.0042	0.0207	0.0334	0.0361	0.0128	0.0124	0.0245-0.0147-0.0095-0.0024	0.0051	0.0215						
PA1/P	PA1/PDX	WA1/W2	CMU10	CMU11	VIA10	VIA11	PA2/P	PA2/PDY	WA2/W2	CMU20	CMU21	VIA20	VIA21	{WA1+WA2}/W2	CMU0	CMUL	
0.0000	0.0000	0.0000	0.0000	0.0000	0.0000	0.0000	0.0000	0.0000	0.0000	0.0000	0.0000	0.0000	0.0000	0.0000	0.0000	0.0000	
(PT2R/PT2)BASE - RING1 RING2 RING3 RING4 RING5 (PT2R/PT2)MEAS - RING1 RING2 RING3 RING4 RING5																	
0.9863 0.9960 1.009 1.009 1.002 1.015 1.010 1.002 0.9949 0.9785																	

57

A MINUS SIGN INDICATES A BAD COMPRESSOR FACE PRESSURE

CF101	CF102	CF103	CF104	CF105	CF106	CF107	CF108	CF201	CF202	CF203	CF204	CF205	CF206	CF207	CF208	
0.9994	0.9995	0.9949	0.9993	0.9996	0.9999	1.0000	0.9997-0.9736	0.9996	0.9992-0.9954	0.9946	0.9939	0.9971	0.9985			
CF301	CF302	CF303	CF304	CF305	CF306	CF307	CF308	CF401	CF402	CF403	CF404	CF405	CF406	CF407	CF408	
0.9541	0.9978	0.9943	0.9929	0.9795	0.9893	0.9918	0.9960	0.9440	0.9861	0.9893	0.9857	0.9651	0.9790	0.9976	0.9898	
CF501	CF502	CF503	CF504	CF505	CF506	CF507	CF508	PT1	SPF1	SPF2	SPF3	SPF4				
0.9433	0.9670	0.9787	0.9587	0.9508	0.9591	0.9775	0.9723									
R101	R102	R103	R104	R105	R106	R201	R202	R203	R204	P205	R206	R207	R208			
0.9997	0.9998	0.9999	0.9998	0.9993	0.9997	0.9990	0.9999	0.9999	0.9997	0.9996	0.9996	0.9994	0.9994			
K301	R302	R303	R304	R305	R306	R307	R308	R309	R310	R401	R402	R403	R404	R405		
0.9701	0.9842	0.9894	0.9993	0.9995	0.9995	0.9998	0.9993	0.9997	0.9996	0.9935	0.9999	0.9993	0.9996	0.9988		
R406	R407	R408	R409	R410	R501	R502	R503	R504	R505	R506	R507	R508	R509	R510		
0.9999	0.9996	0.9998	1.000	0.9997	0.9476	0.9596	0.9779	0.9879	0.9980	0.9993	0.9998	0.9989				
P301	P302	P303	P304	P305	P306	P307	P308	P3/PT2	PD101	PD102	PD103	PD104	PD105	PD106	PD107	
0.6471	0.6804	0.6885	0.6708	0.6730	0.6424	0.6645	0.6843	0.6793	0.7482	0.8428	0.8503	0.8556	0.8674	0.8867	0.8964	
PD108	PD109	PD110	PD111	PD201	PD202	PD203	PD204	PD205	PD206	PD207	PD208	PD209	PD210	PD211	PD212	PD213
0.9032	0.9094	0.9243	0.9265	0.9142	0.8911	0.8894	0.8884	0.8941	0.9063	0.8925	0.8992	0.8974	0.9001	0.9017	0.9126	0.9241

TST-161 PH-1 TN-14 17:98

ID-PRESSOUT1

03 MAY 76 18:56

RUN:SEQ  
17:98

CONF	MACH	Q	PT	P	TTR	TR	RN/FT	ALPHA	BETA	PREF	WC2	PT2/PT	AO/AI	D2	PTRMS	MTH	FLAP	SLAT
1	0.900	712.3	2125	1256	577.1	496.6	4.009	0.29	0.15	1417	142.7	0.9883	0.4598	0.0355	0.0000	0.377	0	

GX1	DX1	DX2	KA2	KC2	KRA2	PERCENT	WC2	QI/PT2	KTHETA	DS	KTHETAS
0.0000	0.6951	0.1013	5.8106	0.1489	0.2919	65.76	0.0588	0.0718	25.20	0.0805	

(AN/NSQRPT)MAX	RING1	RING2	RING3	RING4	RING5	THETA	RING1	RING2	RING3	RING4	RING5
0.0037	0.0061	0.0037	0.0028	0.0044	91.96	97.34	0.0000	0.0000	0.0000	0.0000	

ID	IDCMAX	IDRMAX	IDC1	IDC2	IDC3	IDC4	IDC5	IDCHUB	IDCTIP	IDR1	IDR2	IDR3	IDR4	IDR5
0.2025	0.0123	0.0138	0.0088	0.0157	0.0206	0.0120	0.0104	0.0123	0.0112	0.0088	0.0051	0.0015	0.0017	0.0138

PA1/P	PA1/PDX	WA1/W2	CMU10	CMU11	VIA10	VIA11	PA2/P	PA2/PDY	WA2/W2	CMU20	CMU21	VIA20	VIA21	(WA1+WA2)/W2	CMU0	CMU1
0.0000	0.0000	0.0000	0.0000	0.0000	0.0000	0.0000	0.0000	0.0000	0.0000	0.0000	0.0000	0.0000	0.0000	0.0000	0.0000	0.0000

(PT2R/PT2)BASE	RING1	RING2	RING3	RING4	RING5	(PT2R/PT2)MEAS	RING1	RING2	RING3	RING4	RING5
0.9824	0.9924	1.011	1.010	1.006	1.009	1.005	1.002	0.9983	0.9862		

A MINUS SIGN INDICATES A BAD COMPRESSOR FACE PRESSURE

CF101	CF102	CF103	CF104	CF105	CF106	CF107	CF108	CF201	CF202	CF203	CF204	CF205	CF206	CF207	CF208
0.9882	0.9979	0.9969	0.9993	0.9993	0.9991	0.9994	0.9955	-0.9778	0.9955	0.9987	-0.9961	0.9959	0.9961	0.9976	0.9889
0.9694	0.9970	0.9945	0.9940	0.9850	0.9925	0.9936	0.9920	0.9700	0.9925	0.9919	0.9890	0.9747	0.9839	0.9976	0.9931
0.9677	0.9783	0.9837	0.9692	0.9644	0.9691	0.9848	0.9800	PT1	SPF1	SPF2	SPF3	SPF4			

R101	R102	R103	R104	R105	R106	R201	R202	R203	R204	R205	R206	R207	R208
0.9991	0.9989	0.9996	0.9991	0.9988	0.9992	0.9986	0.9992	0.9993	0.9991	0.9994	0.9993	0.9990	0.9988
0.9785	0.9884	0.9907	0.9996	0.9987	0.9996	0.9995	0.9994	0.9993	0.9991	0.9957	0.9996	0.9995	0.9992
0.9986	0.9993	0.9991	0.9992	0.9993	0.9641	0.9731	0.9859	0.9914	0.9988	1.0000	0.9989	0.9987	0.9992

P301	P302	P303	P304	P305	P306	P307	P308	P3/PT2	PD101	PD102	PD103	PD104	PD105	PD106	PD107
0.6687	0.7049	0.7139	0.6959	0.6963	0.6664	0.6879	0.7080	0.7010	0.7689	0.8758	0.8886	0.8958	0.9054	0.9188	0.9249
0.9295	0.9337	0.9438	0.9468	0.9431	0.9239	0.9217	0.9206	0.9244	0.9329	0.9225	0.9272	0.9257	0.9270	0.9280	0.9359
															0.9447

58

IST-161 PH-1 TN-14 17:99

ID-PRESSOUT1

03 MAY 76 18:56

RUN:SEQ

17:59

CONF	MACH	Q	PT	P	TTR	TR	RN/FT	ALPHA	BETA	PREF	WC2	PT2/PT	AO/AI	D2	PTMS	MTH	FLAP/SLAT
1	0.902	713.8	2124	1253	576.9	496.1	4.013	0.27	0.14	1417	239.5	0.9650	0.7532	0.1248	0.0000	0.817	0
GX1	DX1	DX2	KA2	KC2	KRA2	PERCENT	WC2	Q1/PT2	KTHETA	DS	KTHETAS						
0.0000	0.2753	0.0426	0.1927	0.0627	0.2008	110.4	0.1817	0.0445	32.28	0.0413							
(AN/NSQRPT)MAX - RING1 RING2 RING3 RING4 RING5 THETA - RING1 RING2 RING3 RING4 RING5																	
0.0037 0.0080 0.0111 0.0086 0.0112 84.92 93.99 93.18 118.7 0.0000																	
ID	IDCMAX	IDRMAX	IDC1	IDC2	IDC3	IDC4	IDC5	IDCHUB	IDCTIP	IDR1	IDR2	IDR3	IDR4	IDR5			
0.7768	0.0367	0.0571	0.0116	0.0162	0.0241	0.0418	0.0316	0.0139	0.0367	0.0338	0.0258	0.0128	0.0153	0.0571			
PA1/P	PA1/PDX	WA1/W2	CMU10	CMU11	VIA10	VIA11	PA2/P	PA2/PDY	WA2/W2	CMU20	CMU21	VIA20	VIA21	(WA1+WA2)/W2	CMU0	CMU1	
0.0000	0.0000	0.0000	0.0000	0.0000	0.0000	0.0000	0.0000	0.0000	0.0000	0.0000	0.0000	0.0000	0.0000	0.0000	0.0000	0.0000	
(PT2R/PT2)BASE - RING1 RING2 RING3 RING4 RING5 (PT2R/PT2)MEAS - RING1 RING2 RING3 RING4 RING5																	
1.075 1.054 1.036 0.9373 0.8978 1.034 1.026 1.013 0.9847 0.9429																	

A MINUS SIGN INDICATES A BAD COMPRESSOR FACE PRESSURE

CF101	CF102	CF103	CF104	CF105	CF106	CF107	CF108	CF201	CF202	CF203	CF204	CF205	CF206	CF207	CF208	
0.9993	0.9999	0.9865	0.9971	0.9995	0.9996	0.9996	0.9998	0.9916	0.9980	0.9953	0.9883	0.9927	0.9808	0.9743	0.9982	
CF301	CF302	CF303	CF304	CF305	CF306	CF307	CF308	CF401	CF402	CF403	CF404	CF405	CF406	CF407	CF408	
0.9860	0.9790	0.9732	0.9821	0.9540	0.9690	0.9877	0.9877	0.9446	0.9335	0.9686	0.9571	0.9099	0.9450	0.9952	0.9477	
CF501	CF502	CF503	CF504	CF505	CF506	CF507	CF508	PT1	SPF1	SPF2	SPF3	SPF4				
0.9135	0.8987	0.9388	0.9004	0.8795	0.8954	0.9420	0.9111									
R101	R102	R103	R104	R105	R106	R201	R202	R203	R204	R205	R206	R207	R208			
0.9996	0.9994	0.9997	0.9996	0.9986	0.9997	0.9969	0.9998	0.9994	0.9998	0.9989	0.9992	0.9987	0.9992			
R301	R302	R303	R304	R305	R306	R307	R308	R309	R310	R401	R402	R403	R404	R405		
0.8979	0.9332	0.9342	0.9945	0.9994	0.9992	0.9992	0.9994	0.9995	0.9992	0.9305	0.9989	0.9985	0.9993	0.9986		
R406	R407	R408	R409	R410	R501	R502	R503	R504	R505	R506	R507	R508	R509	R510		
0.9997	0.9989	0.9991	0.9996	0.9991	0.8611	0.8709	0.9048	0.9726	0.9827	0.9992	0.9996	0.9990		0.9991		
P301	P302	P303	P304	P305	P306	P307	P308	P3/PT2	PD101	PD102	PD103	PD104	PD105	PD106	PD107	
0.5737	0.5849	0.5884	0.5766	0.5753	0.5479	0.5647	0.5868	0.5956	0.6835	0.6851	0.6307	0.6010	0.6374	0.7043	0.7359	
PD108	PD109	PD110	PD111	PD201	PD202	PD203	PD204	PD205	PD206	PD207	PD208	PD209	PD210	PD211	PD212	PD213
0.7572	0.7782	0.8214	0.8291	0.7345	0.6826	0.6982	0.6781	0.7097	0.7401	0.7000	0.7330	0.7375	0.7519	0.7566	0.7939	0.8193